

**Enhanced skin permeation of small
molecules via retention of
enhancer substances in matrix-type
transdermal patches**

Dissertation

zur Erlangung des Doktorgrades (Dr. rer. nat.)

der

Mathematisch-Naturwissenschaftlichen Fakultät

der

Rheinischen Friedrich-Wilhelms-Universität Bonn

vorgelegt von

Anna Otterbach

aus

Freudenberg

Bonn, 2022

Angefertigt mit Genehmigung der Mathematisch-Naturwissenschaftlichen
Fakultät der Rheinischen Friedrich-Wilhelms-Universität Bonn

Gutachter: Prof. Dr. Alf Lamprecht

Gutachter: Prof. Dr. Yann Pellequer

Tag der Promotion: 26. August 2022

Erscheinungsjahr: 2022

Abstract

A long-standing approach to improve the transdermal drug permeation is to use chemical penetration enhancers. Those substances reduce the barrier properties of the skin, especially of the stratum corneum, and facilitate the transdermal permeation of drug substances. The incorporation of enhancer substances in transdermal patches would be highly desirable; however, due to the volatility of certain compounds this is extremely challenging.

This work is focussed on the feasibility of transdermal systems containing volatile penetration enhancers (dimethyl sulfoxide and Transcutol®). Different drug substances (Estradiol, Ibuprofen, Scopolamine, and Rotigotine) were used as model compounds to evaluate the release from the prepared systems and the transdermal permeation. Enhancers and drug substances were incorporated in matrix-type patches where the excipients are embedded in a self-adhesive matrix. The prepared patches contained various enhancer concentrations due to different drying temperatures and times that allowed a complete polymer solvents removal while retaining significant amounts of enhancer. The resulting patches were analysed for enhancer content, drug and enhancer release, drug and enhancer permeation through excised porcine skin, stability, and physicochemical properties.

The skin permeation for Estradiol and Scopolamine was significantly increased by dimethyl sulfoxide (DMSO), Transcutol® improved the permeation of Estradiol as well. The effects of the enhancer substances on the permeation behaviour of the different drugs were examined. The investigation revealed that the interaction between drug, enhancer and matrix polymer had a crucial influence on drug release and on drug permeation. For instance, the presence of DMSO had no influence on the release and permeation of Ibuprofen and Rotigotine but improved the drug delivery of the other drugs. Regarding stability, the presence of enhancer substance had the beneficial effect of inhibiting the drug recrystallization at even lowest concentrations. Storage stability was limited to six months and stabilizing attempts with silica particles did not improve the stability.

Although the technical feasibility range is relatively narrow, such enhancer-containing matrix-type patches are able to significantly enhance drug permeation through the skin while ameliorating the product stability against recrystallization.

Danksagung

Meinem Doktorvater, Herrn Professor Dr. Alf Lamprecht, danke ich für die freundliche Überlassung dieses interessanten Themas und die Bereitstellung des Arbeitsplatzes. Darüber hinaus hat sein Ideenreichtum, die fachlichen Diskussionen, aber auch die mir gewährten Freiräume in meiner Arbeitsweise wesentlich zum Gelingen dieser Arbeit beigetragen.

Herrn Professor Dr. Yann Pellequer danke ich für die Anfertigung des Zweitgutachtens. Bei Herrn Professor Dr. Gerd Bendas und Frau Professor Dr. Ulrike Endesfelder möchte ich mich für Ihre Bereitschaft danken, der Prüfungskommission beizuwohnen.

Ich möchte mich ebenfalls bei der LTS Lohmann Therapie-Systeme AG, insbesondere bei Herrn Dr. Emgenbroich, für die Bereitstellung des umfangreichen Informationsmaterials bedanken.

Meinen Kollegen aus der pharmazeutischen Technologie danke ich für die schöne Zeit und das produktive Arbeitsklima. Der gemeinsame Austausch hat immer wieder zu neuen Ideen geführt und viele Probleme gelöst. Meinen Bürokollegen Dr. Ehab Ali, Markus Ries und Dominic Lucas danke ich für die tolle Büroatmosphäre und die vielen lustigen Momente, die während der Arbeit nie zu kurz kamen. Für die professionelle Einführung in die vielfältigen analytischen Methoden bedanke ich mich ganz herzlich bei Herrn Dr. Daris Grizic. Er hat jederzeit mit großem Engagement dabei geholfen, analytische Probleme zu lösen und stand immer für konstruktive Diskussionen zu Verfügung. Katharina Dauer möchte ich für die vielen Gespräche abseits vom Institutsalltag und ihren wertvollen wissenschaftlichen Input danken. Mein besonderer Dank gilt Martina Gerlitz für ihre Hilfsbereitschaft und ihre unverzichtbare Unterstützung.

Nun zu den wichtigsten Menschen in meinem Leben: mein ausdrücklicher Dank gilt meinen Freunden, deren stetige Motivation zur Entstehung dieser Arbeit beigetragen hat. Ich möchte mich außerdem von ganzem Herzen bei meiner Familie bedanken: ich kann mich immer auf euch verlassen und danke euch für die Geduld, euer Interesse und die liebevolle Unterstützung in jeder Hinsicht. Ich danke ganz besonders Robin für den bedingungslosen Rückhalt, den er mir in der ganzen Zeit geboten hat und die Fähigkeit, mich in jeder Situation zum Lächeln zu bringen.

TABLE OF CONTENTS

1. Introduction and theoretical background	3
1.1. Physiology of the skin	4
1.2. Drug delivery via the skin	5
1.3. Classification and composition of transdermal patches	7
1.4. Overcoming stability issues	9
1.5. Preparation of DIA	11
1.5.1. Lab-scale production	11
1.5.2. Commercial manufacturing	12
1.6. Commercial transdermal drug products	15
1.7. Enhancement of drug permeation	15
1.7.1. Active permeation mechanisms	15
1.7.2. Chemical penetration enhancers	17
1.7.3. Passive enhancement techniques	19
2. Aims and scope	21
3. Material and methods	25
3.1. Material	26
3.2. Preparation and evaluation of DIA	29
3.3. In-vitro drug release	30
3.4. Mathematical models describing drug release	31
3.4.1. Higuchi Equation	31
3.4.2. Korsmeier-Peppas Model	32
3.4.3. Weibull Model	32
3.4.4. Fractional rate control	33
3.5. In-vitro skin permeation studies	33

II

TABLE OF CONTENTS

3.6. High-performance liquid chromatography (HPLC)	35
3.6.1. Estradiol	35
3.6.2. Ibuprofen	35
3.6.3. Scopolamine	35
3.6.4. Rotigotine	36
3.7. Gas Chromatography (GC)	36
3.8. X-ray diffraction (XRD)	38
3.9. Differential Scanning Calorimetry (DSC)	38
3.10. Polarized-light microscopy (PLM)	38
3.11. Probe-tack test	39
3.12. Determination of drug solubility	40
3.13. Stability evaluation	40
3.14. Preliminary excipient evaluation	41
3.15. Statistics	41
4. Results & Discussion	43
4.1. Enhanced skin permeation of Estradiol by dimethyl sulfoxide containing transdermal patches	44
4.1.1. Patch preparation and characterization	44
4.1.2. Drug release and permeation behavior	46
4.1.3. Storage stability	52
4.2. Dimethyl sulfoxide in matrix-type transdermal patches: proof of concept and therapeutical implications of the enhancing effect	55
4.2.1. Patch characterization	55
4.2.2. Drug release	60
4.2.3. Permeation behavior	64
4.3. Investigation of stabilization issues in DMSO-containing transdermal patches	69
4.3.1. Preliminary excipient evaluation	72
4.3.2. Patch preparation and characterization	75
4.3.3. Permeation studies & stability evaluation	76

III
TABLE OF CONTENTS

4.4.	Development and process optimization of a transdermal patch containing diethylene glycol monoethyl ether (Transcutol®) to enhance drug permeation and increase patch stability	83
4.4.1.	Patch preparation and characterization	83
4.4.2.	Release and permeation experiments	86
4.4.3.	Stability evaluation	90
5.	General conclusion and outlook	93
6.	References	97
7.	Appendix	109
7.1.	Publications	110
7.2.	List of abbreviations	111
7.3.	List of figures	113
7.4.	List of tables	118

- 1. Introduction and theoretical background**

1. Introduction and theoretical background

1.1. Physiology of the skin

The skin is the largest and one of the most versatile organs of the human body. It covers the underlying organs, tissues, and bones, and protects the body from external influences. It provides hereby an efficient barrier against ultraviolet radiation, chemicals, allergens, microorganisms, the loss of body moisture and nutrients. It furthermore plays a vital role in homeostatic processes, namely regulating body temperature and blood pressure. The skin is also an important sensory organ that allows the body to sense temperature, pressure, and pain [1].

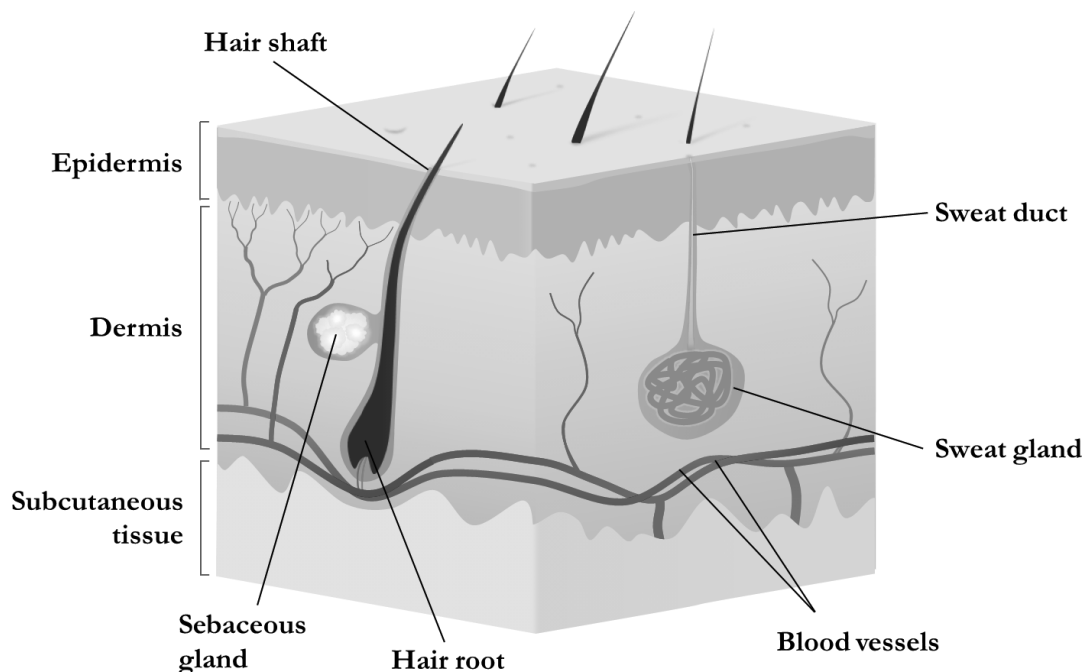


Figure 1. Schematic structure of the skin.

Figure 1 displays the structure of the skin and the three main layers epidermis, dermis, and subcutaneous tissue. The epidermis is divided into several layers which are formed through mitosis at the innermost basal cell layer. Those cells go through many morphological changes during their lifecycle and migrate towards the surface, where after a transit time of approximately four weeks the outermost skin cells are desquamated [2]. This epidermal differentiation allows the formation of the viable cell layers stratum spinosum, stratum granulosum, and stratum lucidum. The outermost layer of the epidermis, the stratum corneum (SC), plays the major role in providing the semi-permeable barrier function of the skin. It consists of 15-20 rows (thickness: 10-20 μm) of nonviable, flattened

1. Introduction and theoretical background

cells filled with keratin (corneocytes), which are connected via desmosomes, and intercellular lipids [1], [3].

The dermis is located beneath the epidermis and provides nutritional epidermal support, elasticity, and flexibility to the skin, and immune response for the whole body. Contained within the dermis are nerve fibres responsible for sensing pressure, pain and temperature, as well as hair follicles, sebaceous glands and sweat glands [4]. The primary functions of the subcutaneous tissue are thermal isolation, energy storage and cushioning of the body. Therefore, it mainly consists of fat cells. It furthermore attaches the skin to the underlying tissues and provides the required vascular and neural structures [1].

1.2. Drug delivery via the skin

Dermally applied drug products comprise topical and systemic drug delivery. Topical effects are typically obtained with semi-solid or liquid dosage forms which act within the skin or locally on the skin surface to treat skin diseases. However, the delivery of a drug substance into the systemic circulation is obtained with transdermal formulations. Transdermal systems represent an attractive and non-invasive method of systemic drug delivery, with the main advantage of avoiding the hepatic first-pass metabolism [5].

The vehicle is usually a transdermal therapeutic patch (TTP), but there are also other dosage forms such as sprays and gels for transdermal administration [6]. TTP offer constant plasma peaks and provide sustained and controlled drug delivery through the skin up for to one week. Due to the increased systemic bioavailability, they represent a suitable vehicle for drugs that cannot be administered orally due to a high first-pass effect. Additionally, lower daily administered drug doses and the simplified self-administration lead to reduced side effects and increased the patient compliance [7]. Disadvantages of TTPs can be, especially after a prolonged skin contact, the induction of mild adverse skin reactions like skin irritation and sensitization. In rare cases, these side effects can cause a therapy discontinuation by the patients. Patients should further avoid external heat sources (sauna, warming blankets, sunbathing) while applying transdermal patches because this factor can significantly increase plasma drug concentrations [8].

1. Introduction and theoretical background

Depending on the site of application, the skin penetration can be different. The thickest horny layer can be found under the soles, thus the amounts of permeated substances for this body part is ten times less than for abdominal skin. On the contrary, the skin permeability of the forehead or the scrotum shows the highest values [9]. Some body parts show a comparable permeability, which allows applying a patch on, e.g., different sites of the trunk or the upper arm by obtaining similar plasma concentrations. Therefore, the buttock, thighs, abdomen, and upper arm are relevant anatomical sites. Those parts have to be generally without large scars, few hairs, and the clothing-induced rubbing should be avoided [10] – [13].

Despite the outstanding barrier properties of the skin, it is still a well-known and common target for drug administration. There are different routes by which applied substances can enter the skin: transappendageal (via hair follicles and sweat ducts) or transepidermal, across the stratum corneum [14]. The relative area of skin appendices represents less than 1% of the total skin surface, thus the transepidermal route is generally considered as the predominant route. Permeation of substances via the SC occurs either transcellular, alternating through corneocytes and intercellular lipids, or intercellular within the intercellular lipid bilayers. The transcellular route is the shortest, but it offers a greater permeation resistance, because the molecules have to pass both, lipophilic and hydrophilic structures directly. Once the permeant passes the SC, it gets into deeper tissues, where it can be taken up into the systemic circulation. [4]. Since transdermal administration is not suitable for all drugs or therapeutic indications, it requires a detailed study of the physicochemical and biological properties of the drugs in question. A successful drug molecule for passive transdermal delivery is preferentially non-ionic, lipophilic, effective at low doses (< 10 mg/day), and has a low molecular weight (< 500 Da) [7], [42].

The driving force for the diffusion of a permeating substance is the concentration gradient across the skin barrier. During the steady-state diffusion, which is described by Fick's first law, the rate of the permeating substance can be expressed with the so-called Flux J_{ss} (Eq. 1).

$$J_{ss} = \frac{\Delta Q}{\Delta t * F} = \frac{D * V_K}{d} * \Delta c \quad \left[\frac{\mu g}{h * cm^2} \right] \quad (1)$$

1. Introduction and theoretical background

The amount of permeated drug ΔQ through a homogenous membrane of the area F per time t depends on the thickness of the SC d , the diffusion coefficient in the stratum corneum D , the partitioning coefficient V_k and the concentration gradient Δc of the permeant between vehicle and skin. Thus, permeation can be increased by reducing the thickness of the SC, altering the diffusion properties and the partitioning of the drug into the skin, and by increasing the concentration gradient [15].

1.3. Classification and composition of transdermal patches

Transdermal patches are flexible, single-dose preparations that contain drug substances incorporated into an adhesive, drug-containing polymer matrix (drug-in-adhesive, DIA) or a reservoir combined with a rate-controlling membrane. Reservoir-type patches employ drug(s) and excipients dissolved in a semi-solid or liquid reservoir. The drug release from the reservoir is controlled by a semi-permeable membrane. Those systems require an additional adhesive layer to stick onto the skin. The production of reservoir-type patches is more demanding than matrix-type patches, especially because more components of various physical conditions can be involved. Those formulations are used when the drug is not sufficiently soluble in polymers, or sufficient adhesion properties of a DIA-system cannot be guaranteed [16]. A severe disadvantage of those patches must be assessed: the risk of leakage and drug overdosages as a possible result. In the early 2000s, fentanyl patches were recalled due to the leaking reservoir. The reservoir contained an ethanolic fentanyl-gel and due to the leakage increased drug doses might have been absorbed [17].

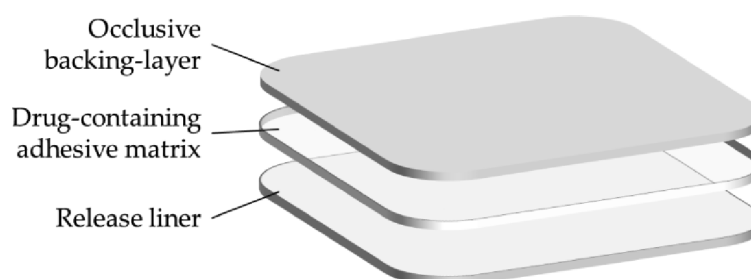


Figure 2. Layers of a monolithic DIA. The release liner is part of the drug product, although it has to be removed before usage.

1. Introduction and theoretical background

Commercially available TTP are often matrix-type patches [8]. The embedding of drugs in self-adhesive matrices offers the advantage that no further fixing due to the adhesive properties of the patch itself is required. This leads to more flexibility and a decreased thickness. Therefore, wearing comfort and the cosmetic acceptance are increased, resulting in enhanced patient convenience. The simple structure of DIA is divided into three main layers; the so-called backing covers the adhesive drug-containing matrix layer(s) on the dorsal site and is generally impermeable to the drug and water (**Figure 2**). The so-called release liner covers the proximal site of the patch. It protects the drug-containing layer during transport and storage, prior to application of the patch it has to be removed by peeling it off. The backing ensures occlusive properties during patch application, favouring drug permeation due to enhanced skin hydration [18].

The polymers necessary to form the drug-containing matrix should comprise controlled drug-release and adhesion. They are known as pressure-sensitive adhesives (PSAs) and can be divided into four main groups: polyacrylate copolymers, polyisobutylenes (PIB), polysiloxanes, and hot-melt PSA. They are biologically and chemically inert, non-sensitizing, non-irritating, and they do not cause any type of systemic toxicity [19]. The choice of PSA is an essential step in the development of a matrix-type patch and, the selection depends on various factors, including drug solubility, compatibility of drug and polymer, adhesive properties, and drug-polymer interactions. Those interactions can significantly impact the drug release prior to percutaneous absorption and thus the process of transdermal drug administration. Therefore, it is very crucial to know the diffusion properties of a drug within the polymer for the development of transdermal systems. This work is focused on acrylic PSA because of the broad experience, especially in the development of commercial products and their versatile and individual properties. The functional groups of acrylic PSA, such as carboxylic groups, interact with secondary amid groups of drug molecules, which reduces their diffusion coefficient within the matrix and inhibits the skin permeation of basic drugs [20], [21]. On the contrary, the interaction between those PSA and drugs with carboxylic or ester groups are clearly lower [22]. The matrix may further contain additives to increase drug permeation, inhibit crystal growth, or in a broader sense, stabilizing excipients.

1. Introduction and theoretical background

1.4. Overcoming stability issues

When formulated as a transdermal patch, passive diffusion is the driving force to promote the transition of the drug from a transdermal patch into and through the skin [23]. Accordingly, the drug is typically formulated in a saturated to supersaturated state within the transdermal patches to create maximal concentration gradients. Such systems, however, are thermodynamically unstable because the driving force is always towards the lower energy crystalline form. The urge for the transformation into the more ordered state is the reason for the high risk of recrystallization of drugs, especially during storage, which often occurs with drugs with limited solubility in the matrix of the carrier system [24], [25]. The problem with drug recrystallization is, that it affects drug release and permeation, namely reducing drug solubility and flux values [26]. It further leads to changes in the viscoelastic properties; the adhesive properties of matrix-type patches were significantly decreased with an increasing amount of crystals [27]. Those factors affect the success of the therapy and, of course, storage stability. Thus, transformation into the crystalline form can lead to the failure of a product.

To solve this problem, various formulation approaches have been tested, typically based on the use of crystallization inhibiting excipients or by maintaining the amorphous state of the drug to stabilize the supersaturated condition in transdermal patch formulation [25]. Among them, mainly polymers have been examined, such as polyvinylpyrrolidones (PVP) [26], [28], or methacrylic acid copolymers [29]. In general, the viscosity of PSAs is relatively high, which leads to relatively low drug diffusion coefficients within the matrices, and thus their recrystallization occurs slowly within storage, not immediately after production. The formation of crystals starts with the formation of a so-called embryo due to the collision of single molecules. The embryo might be redissolved within the matrix, but the agglomeration of further drug molecules forms nuclei. The continuous accumulation of molecules promotes crystal growth until the system is in a saturated state again. Excipients with crystal-growth inhibiting properties interact with drug molecules and prevent the formation of nuclei [28].

The interaction between excipients and PSA can increase the glass transition temperature (T_g) of the matrix polymer which reduces the mobility of the drug molecules and therefore slows down the transformation from amorphous to crystalline (antiplasticizing effect) [30]. Kim et al. investigated the effect of various crystal-growth inhibitors on the permeation of Ketoprofen. Drug

1. Introduction and theoretical background

recrystallization in a PIB-matrix was successfully delayed with PVP, Tween, Poloxamer and Labrasol, but the flux values decreased proportionally to the increasing amount of additive. PVP was found to be the most effective growth inhibitor, but the flux values of Ketoprofen were reduced to a quarter in comparison with the PVP-free matrices [26]. A further, successful approach to maintain the supersaturated state was performed by Tahir et al. by incorporating the drug into nanocarriers. The obtained amorphous nanoscale dispersion was distributed into a hydrophilic matrix-polymer (hydroxypropyl methylcellulose), providing additional antinucleant properties. In comparison with the nanoparticle-free control patches, the resulting flux values were, as well as the stability after four weeks, significantly increased [31]. Liu et al. recently reported on the successful inhibition of Rotigotine recrystallization by forming eutectic liquid co-crystals consisting of drug and organic acids. The combination of Rotigotine and lactic acid was found to interact with the PSA, which inhibited drug recrystallization. Additionally, the transdermal permeation of the eutectic mixture was significantly improved in comparison to the pure drug [32].

1. Introduction and theoretical background

1.5. Preparation of DIA

Starting with solvent-based adhesives, the production of DIA requires organic solvents to create a liquid and castable drug-adhesive mass. The properties of specific polymer-solvent-mixtures as a basic product facilitate easy processing and the possibility to cast the viscous mass to a desired thickness [33]. However, by the end of the production cycle, those solvents must be eliminated to enable the curing of the drug-containing adhesive mix. Insufficient solvent evaporation would inhibit the formation of the solid DIA structure on the one hand and create toxicological or skin-irritating issues on the other. For this purpose, it is necessary to control the final drug product and the intermediates. The monitoring of the relevant processes enables the identification of critical process parameters that could crucially affect the quality of the product [34]. The produced drug product must meet the requirements of the authorized regulatory agency (e.g., European Medicines Agency, U.S. Food & Drug Administration) in terms of quality, safety, and stability. Relevant issues are drug content uniformity, homogeneity, patch size and thickness, residual solvents, impurities, lacking adhesive properties, drug recrystallization, container closure system, and storage stability, which could alter the approved release and/ or permeation properties [35].

1.5.1. Lab-scale production

The preparation of transdermal patches in lab-scale offers many possibilities regarding equipment, production process and final dosage form. Especially scientific lab-scale research aims to examine a specific scientific issue, e.g., enhancing the permeation of a drug or investigating the influence of excipients on the permeation process. The practical work for those purposes is highly variable and flexible because regulatory limits are quite low compared to commercial development studies. Here, the development is performed in lab-scale or pilot-scale and the goal is to develop a production process and drug product that complies with regulatory specifications. Simultaneously, it must be manufacturable on dedicated commercial equipment.

In general, the first production step is the homogenization of the drug-in-adhesive components, namely polymer, solvents, drug, and excipients in a g – kg scale. Many types of mixers can be used (stirrer bars, stirrers, drum hoop mixers) and several properties need to be considered: the purpose of this step is to create a homogenous and uniform mass with a minimum amount of trapped air bubbles. If the energy input is too high, air may be incorporated to a large extent. Those air bubbles

1. Introduction and theoretical background

must be removed from the liquid mixture prior to the following casting process. The required resting times would increase the production time to an unnecessary extend. Further, the mixing step needs to be performed in a closed container to avoid the evaporation of organic solvents for safety reasons.

Afterwards, the liquid mass is spread onto a release or backing liner. This procedure may be performed using Petri dishes or small-scale coating machines. The advantages of coating machines are an adjustable film-thickness, adjustable coating speeds, and a larger coating area. However, the usage of Petri dishes offers a quick and easy casting process because the mixture has just to be poured into the Petri dish. It is therefore preferable for preliminary studies where no high priority is placed on an accurate thickness of the layer. The wet laminates have to be dried subsequently to remove the organic solvents. Drying can be performed in a drying cabinet, on a bench top at normal room conditions, or in a vacuum drying oven. It is essential to remove the organic solvents from the adhesive, to ensure the quality and harmlessness of the final drug product. Finally, the dried laminate is covered with a backing or release liner (depending on the already used liner), cut into small pieces with a hollow punch or scissors, and packed in sealed pouches.

1.5.2. Commercial manufacturing

The commercial manufacturing of matrix-type patches is typically designed as a combination of both, batch and continuous processes [8]. Process steps are liquid blending of drug(s) and excipients, followed by a combined coating, drying and laminating process. The final steps are cutting of the patches and pouching them into the primary package.

The process begins as previously described with the mixing of drugs and excipients, but the volume of the mixing vessel is big enough to prepare a batch size of several hundred kilograms of adhesive solution. Afterwards, the manufacturing proceeds with the combined process steps coating, drying, and lamination as displayed in **Figure 3**. The process flow starts on the left side with the drug-containing mass that is applied on the release layer at the “coating head”. Here, the distance between the rollers determines the thickness of the applied adhesive layer. The coated but wet backing liner is automatically transported into the drying channel, where air nozzles and heat ensure solvent evaporation from the drug-containing mass. After this step, the adhesive side is covered with

1. Introduction and theoretical background

a backing liner in the lamination station, resulting in the first intermediate of the manufacturing process, the laminated master roll.

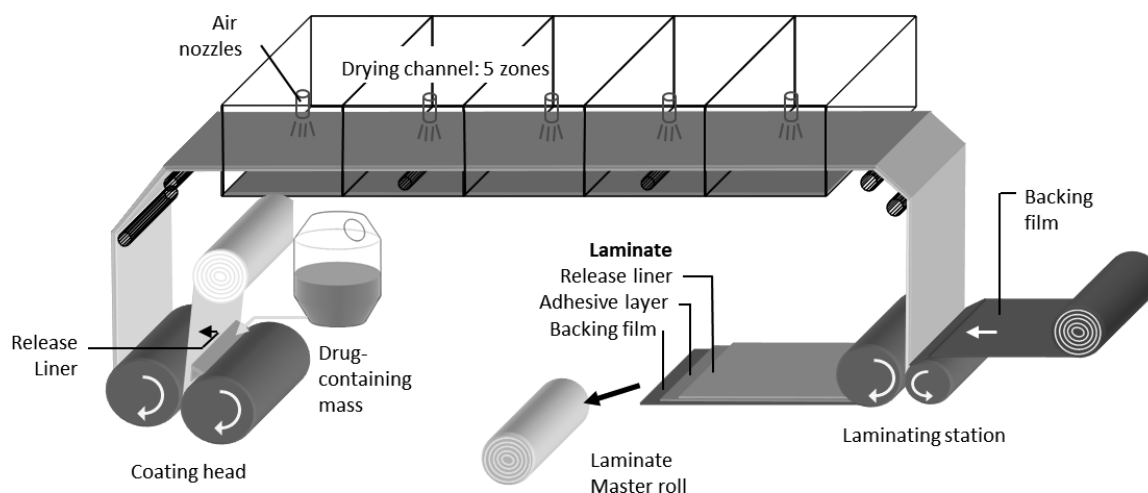


Figure 3. Process steps for manufacturing of DIA: Overview of coating, drying and lamination. Image by courtesy of LTS Lohmann Therapie-Systeme AG.

The master roll is cut in the following step: a slitting apparatus as displayed in **Figure 4A** is used to unwind the big roll and knives cut the roll lengthwise. The resulting narrow strips are rolled up again (**Figure 4B**). The next step of the manufacturing is the die-cutting and packaging. Here, the narrow rolls are transferred to a cutting and pouching machine. The whole process is displayed in **Figure 4C** (process direction: from right to left): initially, the rolls are unrolled again to enable the continuous die-cutting of the patches. Subsequently, the remaining trellis is separated from the patches. Within the following steps, the patches are laminated with the pouching foil from above and below, and each patch is sealed gas-tight into the pouch material in a sealing station (primary packaging). Finally, the sealed patches are cut and packed (secondary packaging).

1. Introduction and theoretical background

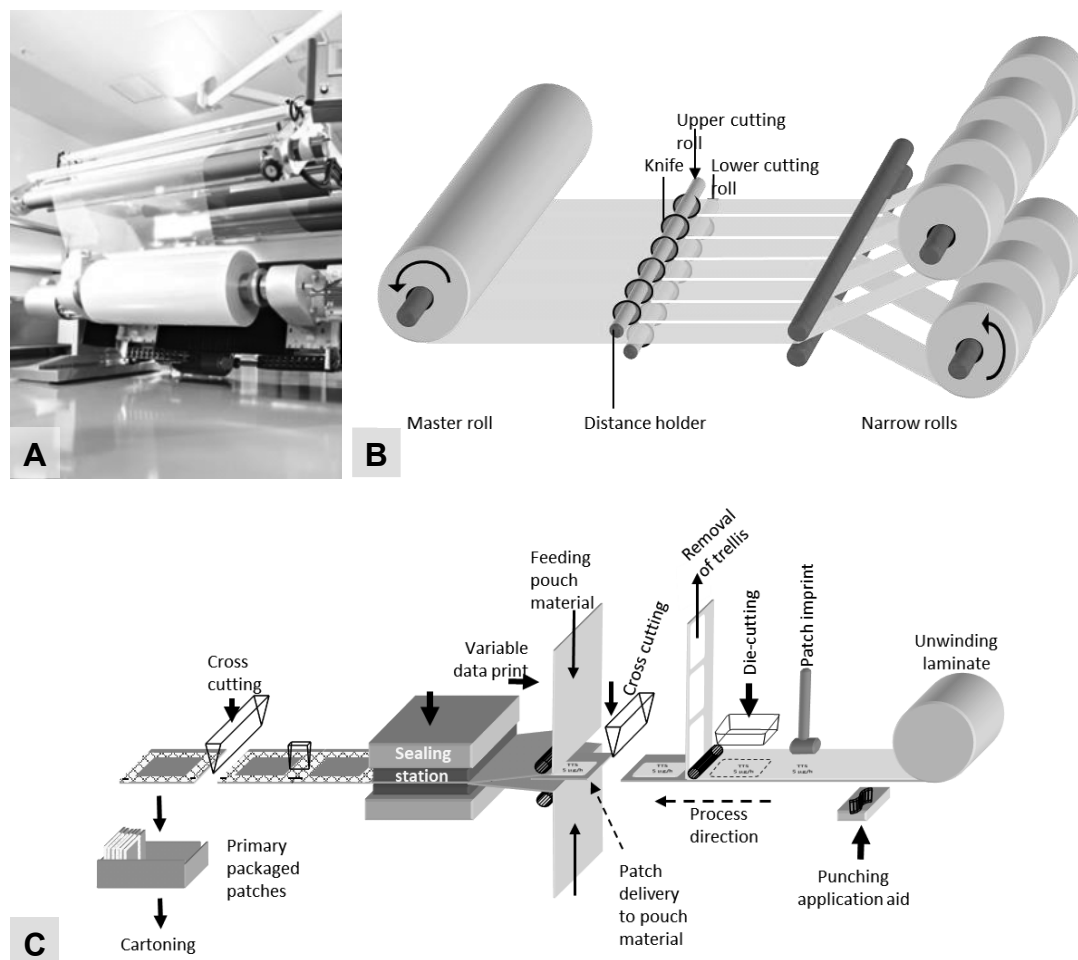


Figure 4. Process steps for manufacturing of DIA: (A) Slitting apparatus, (B) overview of slitting, (C) overview of pouching. Image by courtesy of LTS Lohmann Therapie-Systeme AG.

1. Introduction and theoretical background

1.6. Commercial transdermal drug products

Over the past decades, the given advantages led to a significantly increased approval of transdermal drug products. The various advances in transdermal drug delivery and polymer research facilitated this development, the integration of novel approaches to enhance drug transport via the skin will support the market expansion in the future. Yewale et. al reported a worldwide market share of \$12.7 billion in 2005, \$37.8 billion in 2018 and an expected growth up to \$ 49.4 billion by 2024 [19]. Fehler! Verweisquelle konnte nicht gefunden werden. gives an overview of registered transdermal drug products and their indications in the European Union (EU), source: Gelbe Liste Pharmindex database [36].

1.7. Enhancement of drug permeation

1.7.1. Active permeation mechanisms

The skin is a well-suited application site for drug administration, but due to the stratum corneum it is still a major obstacle for the permeating substance. As a consequence, many enhancement approaches have been developed in the past. Active mechanisms facilitate drug permeation due to the disruption and/or reducing the thickness of the SC. This approaches include microneedle-based systems, which penetrate the epidermis with needles of 25 - 2000 μm length, ensuring minimally invasive and pain-free drug delivery by creating micro-scale pathways into the skin [37]. There is no commercial patch using microneedles available yet, but the clinical trials for an “Adhesive Dermally-Applied Microarray (ADAM)” for the intracutaneous delivery of Zolmitriptan as migraine treatment are still ongoing [38].

Another approach is the needleless injection, by which the drug gets pushed into the skin at supersonic speeds with special devices. The application of ultrasound on the skin forms gaseous cavities within the lipids of the SC and therefore leads to a reversible disruption [39]. Transdermal delivery can further be increased by the application of a constant low-voltage current, which is called iontophoresis. The electrical force boosts the drug transport across the stratum corneum of tiny, charged molecules and some macromolecules. Likewise leads the so-called electroporation to a reversible barrier disruption by applying short, high-voltage pulses. Further techniques are thermal ablation, by which the skin surface is transiently heated to hundreds of degrees for split seconds,

1. Introduction and theoretical background

and the microdermabrasion, which describes the complete removing of the stratum corneum prior to drug application [40]. A significant advantage of those systems is to enable the transdermal administration of macromolecules with a molecule size larger than 500 Da or hydrophilic biopharmaceuticals. However, the development and production of those systems, except micro-needle systems, is yet still challenging, often expensive and slightly patient-friendly.

1. Introduction and theoretical background

1.7.2. Chemical penetration enhancers

On the contrary, there are conventional and passive enhancement approaches like chemical penetration enhancers (CPE). These substances improve the partitioning of an administered drug substance into the skin and/or enhance the diffusion through the skin. The drug permeation is hereby increased due to reversible interactions of CPE with components of the SC, resulting in temporarily reduced barrier properties [41]. CPE has various substance classes, including alcohols, esters, ether alcohols, sulphoxides, pyrrolidones, surfactants, amides, fatty acids, and terpenes. According to Equation 1, J_{ss} can be improved by increasing the diffusion coefficient of the drug, e.g., by CPE-induced disruption of the SC-lipid organisation. A further mechanism is to enhance the partitioning of the drug into the SC by acting as a co-solvent in the skin. In General, the main mechanisms of action of CPE mainly comprise the interaction with SC-lipids, resulting in a disturbed and better permeable structure and protein modifications. Interactions with the keratin in the corneocytes can cause conformation modifications and allow the formation of vacuoles [42].

Within an extremely wide choice of chemically completely differing compounds, organic solvents were found to enhance the skin permeability nearly half a century ago [43]. Among them, dimethyl sulfoxide (DMSO) has become somewhat a first choice, as an organic solvent that exhibits significant permeation enhancing potential, combined with its versatile solvent properties and the relatively low vapor pressure. Besides, its toxicity is relatively limited compared to other solvents with this potential [15], [44]. The molecule consists of a hydrophilic sulfoxide group and two hydrophobic methyl groups, which provides an amphiphilic character. Due to its structural features, DMSO interacts with cell membranes, resulting in an enhanced permeation of hydrophilic, and hydrophobic drugs. The effect on cell membranes depends on the concentration of DMSO, from an increased bilayer-fluidity at lower concentrations, through to the formation of water pores and the extraction of lipid molecules at higher concentrations [45], [46]. Although the permeation enhancing effect of DMSO was proven in countless experiments, a commercial transdermal product containing the substance does not exist. However, at this time it is rather used in topical formulations [47].

On the long list of permeation modifying excipients, which has emerged from decades of research, the highly purified form of diethylene glycol monoethyl ether (Transcutol[®], TC) represents an efficient and safe CPE as well [48]. In addition, TC is an excellent solubilizer for many poorly soluble compounds. Due to this property, the drug diffusion through the skin is enhanced because

1. Introduction and theoretical background

drug diffusion depends on good solubilization in both, vehicle and enhancer substance [49], [50]. Diethylene glycol monoethyl ether is a small and hydrophilic molecule and at room temperature a hygroscopic, clear liquid. It readily infiltrates and saturates the SC, where it forms an intracutaneous depot. In particular, the substance strongly interacts with intercellular water in the SC, causing a modified mobility of intercellular lipid domains. Thus, the solubility of the drug in the skin increases and the skin barrier function decreases. Hereby, TC does not alter the skin structures, which is beneficial regarding skin irritancy. The FDA (Food and Drug Administration) has approved products for topical use with concentrations up to almost 50 % and for transdermal use up to 5 % in the USA. [51]. It is used in Anturol®, a gel for transdermal application of Oxybutynin, and Elestrin® gel to enhance the permeation of Estradiol [15].

A major hurdle of incorporating organic solvents such as DMSO and TC as penetration enhancer is the risk of evaporation during manufacturing, storage and application. Due to the volatile nature of organic solvents, especially the process temperatures and pressures during production have to be adjusted accordingly. One might assume that this is the most probable reason why especially Transcutol® is exclusively used for transdermal gels so far.

Lipophilic enhancers with long-chain fatty acids, such as oleic acid, modify the lipid domains of the SC and increase both drug diffusivity and drug partitioning. The combination of oleic acid with terpenes (D-Limonene) further increased the permeation of lipophilic and amphiphilic molecules [52]. Oleyl oleate, for example, is an ingredient of BuTrans®, a transdermal patch indicated for the management of pain containing Buprenorphine. Ethanol is also used as penetration enhancer, but due to the required high concentration between 40 and 80 % it is rather used for topical formulations as in Oestrogel® to promote the transdermal permeation of Estradiol. Ethanol in lower concentrations is commonly used in combination with other permeation enhancing agents like propylene glycol (Sandrena®), isopropyl palmitate (Estraderm® MX) or oleic acid, 2-propanol, and propylene glycol (Fortesta®) [15].

1. Introduction and theoretical background

1.7.3. Passive enhancement techniques

The permeation rate of a drug depends on its thermodynamic activity in the vehicle, because the driving force out of the formulation and thus the transdermal delivery is enhanced to its maximum [24]. In order to improve drug permeation physically, transdermal patches are usually supersaturated systems, comprising a high thermodynamic potential and a large concentration gradient Δc (Eq. 1). Davis et al. investigated the relation between supersaturation and drug transport and found out that the degree of supersaturation proportionally increases the drug transport via the skin [53]. Supersaturated systems can be easily obtained by solvent evaporation or, in the case of hot-melt adhesives, by melting the compounds and subsequently supercooling of the melt. The resulting solutions are in an amorphous and solid-state.

A further, long-standing, and well-known approach is to enhance the hydration of the skin. The skin plays a major role in regulating the body temperature, mainly controlled by perspiration through eccrine sweat glands. The secreted water evaporates from the skin surface, resulting in a cooling effect. If this transepidermal water loss is blocked by occluding the skin with an impermeable layer, the water content in the SC increases. The hydration status of the SC is usually significantly lower than in the underlying, viable layers, but it is very hygroscopic and can absorb up to 500 % of its dry weight [54]. Thus, occluding the skin leads to an enhanced hydration status of the SC, which induces the swelling of corneocytes and the expansion of intercellular spaces, leading to the formation of pores in the SC. The result is a decreased diffusional resistance, facilitating the increased permeation of both, lipophilic and hydrophilic substances [55].

2. Aims and scope

2. Aims and scope

Especially transdermal therapeutic systems (TTS) focus on the beforementioned advantages of the delivery through the skin and can provide a relatively constant plasma level of the active over a longer period. β -Estradiol (E2) is a drug candidate commonly administered via the skin because this kind of application ensures the required therapeutic regimen for E2 by a continuous uniform systemic drug delivery up to one week [56]. The substance is used for menopausal hormone replacement therapy to prevent osteoporotic fractures and to reduce the breast cancer incidence [57]. In this therapeutic context, constant plasma levels of E2 are most desirable, while peaks and troughs, as they typically occur during an oral administration, should be avoided. According to these properties, E2 was used as model drug in chapter four to evaluate the basic feasibility of this study. Although toxicity after permeation is a general issue with organic solvents, they are missing on the list of penetration enhancers due to their high volatility, which essentially risks their premature elimination by evaporation during the production steps. Accordingly, it is a major challenge to incorporate a volatile penetration enhancer that could increase the permeated drug amount and simultaneously stabilize the supersaturated patch matrix from drug recrystallization while evaporating the matrix polymer solvents to solidify the patch.

The successful development of a novel transdermal patch containing DMSO as permeation enhancer and β -Estradiol as a model compound is addressed in chapter 4.1. Dimethyl sulfoxide is a well-known and widely used dermal penetration enhancer. Thus, its incorporation in transdermal patches would be highly desirable. However, due to its volatility this is extremely challenging. The development and optimization of the production parameters was a demanding procedure that finally resulted in a manufacturing process with high efficiency and repeatability. The difficulty was hereby to identify the amount of DMSO necessary to increase drug permeation significantly and simultaneously not to exceed the critical amount of enhancer that resulted in wet and unusable patches. Transdermal patches were prepared from an acrylate polymer (Duro-Tak® 387-2510) containing various DMSO concentrations due to different drying temperatures and times. The resulting patches were analysed for DMSO content, E2 and DMSO release, E2 and DMSO permeation through excised porcine skin, and recrystallization during stability testing. The stability samples were further examined for their DMSO content and drug permeation as well.

2. Aims and scope

Due to the different properties of each molecule, the formulation development of transdermal patches is a challenging process for every new drug candidate. This circumstance further aggravates the implementation of novel permeation enhancement techniques. The effect and applicability of those techniques have to be examined case by case for each drug candidate, as well as each drug product. Hence, chapter 4.2 evaluates the applicability of the formulation approach described in chapter 4.1. Three drug candidates (Ibuprofen, Scopolamine, Rotigotine), which are commonly administered via the skin, were chosen as model drugs. Patches with each drug candidate were prepared with and without DMSO. The formulations were analysed regarding tackiness, appearance, drug permeation through excised porcine skin and drug release. The used drug substances offered different physicochemical properties; therefore, the release behaviour was examined more precisely to discover possible differences between the candidates.

Chapter 4.3 reports on the attempt of DMSO-retention in transdermal patches by using different kinds of silica particles. Various excipients with different properties (particle size, surface area, chemical modifications) were tested concerning their ability to retain and stabilize DMSO successfully during production and storage. Incorporating silica particles with a large surface area were thought to adsorb and thus, entrap the volatile solvent within the adhesive matrix, whereas small particles (< 100 nm) could form a solid barrier surrounding the solvent. Preliminary evaporation experiments with suspensions of the chosen excipients in DMSO revealed good processible properties for Aerosil® 300. Thus, patches containing DMSO and different amounts of Aerosil® were prepared to evaluate the maximum amount of excipient that could be incorporated to retain and stabilize the desired solvent concentration. Afterwards, the most promising formulation was tested over a period of three months regarding appearance, DMSO content and drug permeation.

2. Aims and scope

A further development approach is mentioned in chapter 4.4: exchanging the penetration enhancer DMSO. The alternative substance should possess similar solvent properties or may be less volatile and of course, be a penetration enhancer as well. Due to a distinct lower vapor pressure and the well-reported permeation enhancing features, Transcutol® (TC) was chosen. TC is also known as diethylene glycol monoethyl ether and offers a fully established safety profile. Further, it is used as an enhancer substance in commercially available drug products for transdermal usage. E2 was used as a model drug to compare the resulting drug release and permeation with those obtained for the DMSO-patches. Chapter 4.4 describes the development and optimization of patch production, drug release and permeation studies, and the stability results. Additionally, the permeation enhancing effect and mechanism of action of Transcutol® was evaluated and compared with DMSO.

3. Material and methods

3. Material and methods

3.1. Material

β -Estradiol (E2) was obtained from TCI Chemicals (Eschborn, Germany). Scopolamine hydrobromide (SCO) and Ibuprofen (IBU) were purchased from Caelo (Hilden, Germany). Rotigotine (ROT) was purchased from Acros Organics (Fair Lawn, NJ, USA). All active substances were of analytical grade. The structural formulae of the drug substances are displayed in Figure 5; the properties are summarized in Table 1.

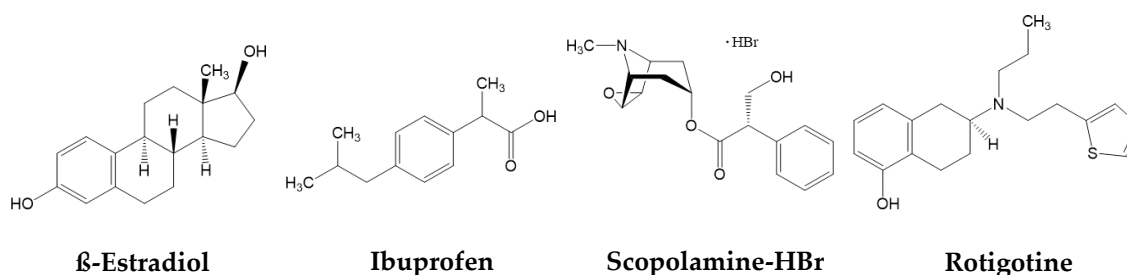


Figure 5. Structural formulae of the used model drugs.

Table 1. Indication and physicochemical properties of the used APIs. Substance information were obtained from (1) the European chemicals agency (ECHA), (2) PubChem, (3) S. K. Chandrasekaran et al. or McAfee et al. [57] – [60], (4) predicted using advanced chemistry development (ACD/Labs) software V11.02.

Drug	Indication	Polar surface area [\AA^2]	MV [cm^3]	log P	Solubility in water [mg/mL]	Melting Point [$^{\circ}\text{C}$]
β -Estradiol	Hormone-replacement therapy	40.5 ²	232.6 ⁴	3.9 ¹	0.002 ¹	170 ¹
Ibuprofen	Treatment of pain, fever and inflammation	37.3 ²	200.3 ⁴	3.9 ¹	0.011 ¹	75-77 ¹
Scopolamine-HBr	Motion sickness, postoperative nausea	62.3 ²	230.9 ⁴	1.4 ²	520 ³	195 ²
Rotigotine	Parkinson's disease, restless legs syndrome	51.7 ²	273.3 ⁴	4.0 ⁴	0.037 ²	77 ⁴

3. Material and methods

DMSO was supplied by VWR (Darmstadt, Germany). TC (Transcutol® P, pharmaceutical grade) was received as a gift from Gattefossé (Saint-Priest, France). 1,3-dimethyl-2-imidazolidinone and γ -Cyclodextrin were obtained by TCI Chemicals (Eschborn, Germany). Ethyl acetate (EA), acetonitrile, sodium lauryl sulphate (SLS), methanol and acetone were purchased from Merck (Darmstadt, Germany). Backing liner (3M™ Scotchpak™) and release liner (3M™ Scotchpak™) were obtained as a gift from 3M™. All chemicals were at least of analytical grade.

In this work an acrylate polymer, Duro-Tak® 387-2510 (DT), was used as adhesive matrix for the DIA. DT is supplied as a viscous and transparent solution, consisting of a non-crosslinked acrylate copolymer with hydroxylic groups dissolved in ethyl acetate (91 %) and hexane (9 %). The solid content of the viscous gel is 41.5 %, as obtained from the supplier, and it was a gift from Henkel (Waalwijk, Netherlands). In comparison to polymers without functional groups, with amide or carboxylic groups, OH-groups led in previous studies to an increased drug permeation and enhanced drug-polymer miscibility without altering drug release, especially with Duro-Tak® 387-2510 [20], [21], [58], [59].

Florite® PS-10 is a fine-grained Calcium-Silicate powder with an average particle size of 10 μm . Florite® PS-200 is a fine-grained Calcium-Silicate granulate with larger average particle size of 150 μm . Both were obtained as a gift from Tomita Pharmaceutical (Tokyo, Japan) [60].

FujiSil™ is a spray-dried granular amorphous silica powder with an average particle size of ~ 80 μm and a specific surface area of 400 m^2/g [61]. The fine and ultra-light magnesium-aluminometasilicate Neusilin® US2 offers a specific surface area of 300 m^2/g and an average particle size of 60 – 120 μm [62]. FujiSil™ and Neusilin® were gifts from Fuji Chemical Industries USA (Burlington, NJ, USA).

Parteck SLC 500 is a mesoporous silica powder with an average median particle size of 17 – 25 μm and a specific surface area of 500 m^2/g [63]. It was a gift from Merck (Darmstadt, Germany).

Syloid® 244 FP and Syloid® Al-1 FP are synthetic, amorphous silica particles. They offer a specific surface area of 300 m^2/g and 600 m^2/g , mean particle sizes are 3.5 μm and 10 μm , respectively [64], [65]. The powders were gifts from Grace (Worms, Germany).

3. Material and methods

Aerosil® 300 is a hydrophilic fumed silica with a specific surface area of ~ 300 m²/g and an average particle size of 7 nm. Aeropearl® 300 is a granulated colloidal silicon dioxide with a similar specific surface area of ~ 300 m²/g and an average particle size of 30 µm [66]. Both were kindly donated by Evonik (Hanau-Wolfgang, Germany). Product information were obtained from the supplier.

Pig ears were obtained from a local abattoir immediately post-sacrifice and prior to steam cleaning (Bonn, Germany).

3. Material and methods

3.2. Preparation and evaluation of DIA

Patches were prepared by solvent evaporation technique. **Figure 6A** illustrates the consecutive process steps. Initially, drug and excipients were blended in glass vials and stirred until a transparent and homogeneous mixture without air bubbles was obtained. Subsequently, the viscous solution was cast on a drug-impermeable and occlusive backing liner, using a film applicator (Multicator 411, Erichsen, Hemer, Germany) and spread to a thickness of 460 μm . Afterwards the laminates were transferred onto a forced convection oven and dried under varying conditions (different times and temperatures). The dried laminates were covered with a removable fluoropolymer coated release liner to protect the pressure-sensitive surface of the adhesive (**Figure 6B**) and cut into circular DIA using a punch die with a diameter of 1.5 cm (**Figure 6C**). Prior to storage, the patches were wrapped and sealed airtight into aluminium-composite pouches.

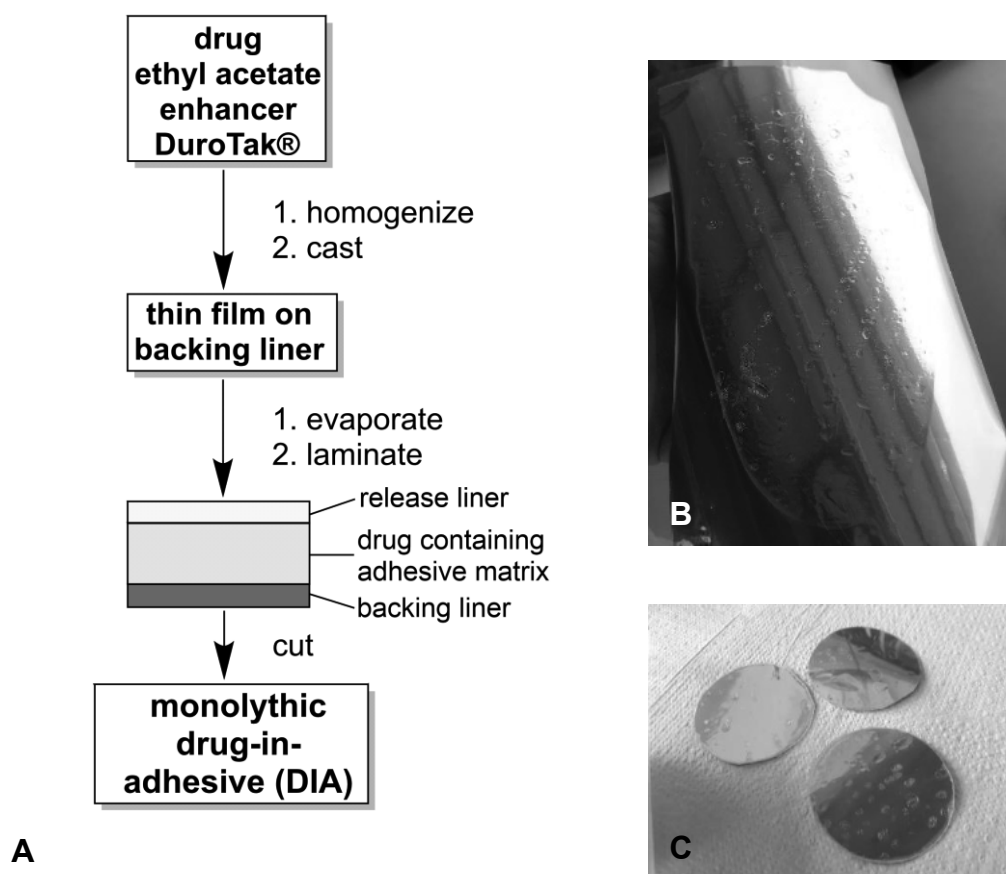


Figure 6. (A) Schematic overview of the patch production process, (B) dried and covered adhesive laminate and (C) final dosage form: circular drug-in-adhesive patches.

3. Material and methods

The drying process or rather the different amounts of residual volatile compounds after varying drying conditions were monitored via gas chromatography (GC) to evaluate the kinetics and the ideal conditions of the process. Drug load of the patches was determined by dissolving each patch (before or after permeation experiments) in 5 mL acetone and adding 10 mL of a 2.5 g/L SLS solution to precipitate the polymer that could clog the high-performance liquid chromatography (HPLC) apparatus or the column. The mixture was centrifuged at 15,000 rpm at 20°C (RCF = 21,380), subsequently the polymer-free supernatant was assayed by the HPLC methods described below. The residue was completely dried and weighed to determine the polymer mass.

3.3. In-vitro drug release

The drug release from DIA was analysed with a modified franz diffusion cell apparatus equipped with jacketed franz cells and a heater/circulator-system as displayed in **Figure 7A** (SES Analysensysteme, Bechenheim, Germany). Initially the release liner was removed from the DIA, afterwards the patch was placed and fixed over the circular orifice as displayed in **Figure 7B**, adhesive-side facing towards receiver compartment to ensure the absence of air bubbles between patch and receptor fluid.

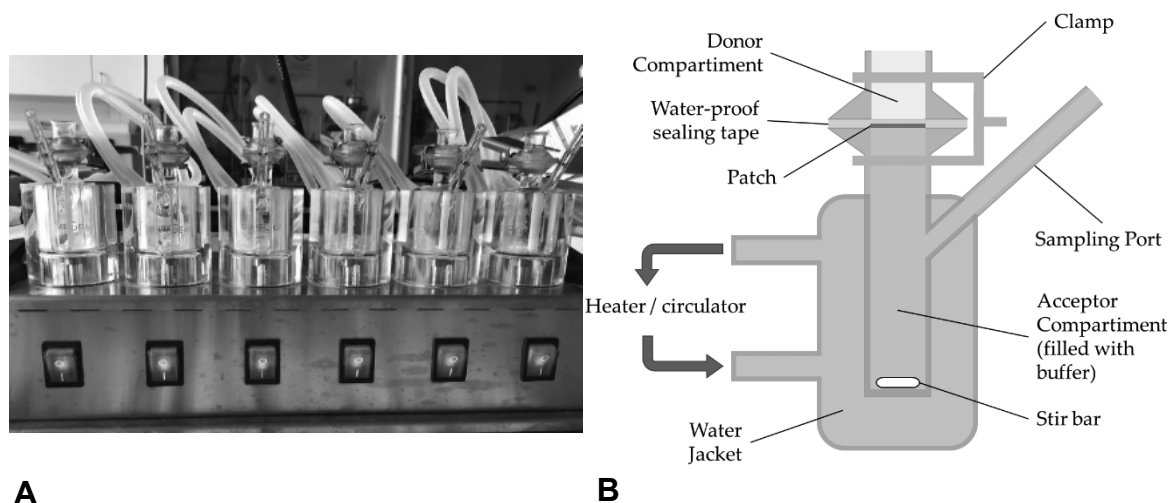


Figure 7. (A) Franz diffusion cell stirrer system: six franz cells are installed next to each other and connected to a heater/circulator system. The six cells can be used simultaneously. (B) Franz-diffusion cell scheme of the experimental set up for drug release experiments.

3. Material and methods

The acceptor compartment was filled with a solution of 0.5% γ -cyclodextrin in PBS (phosphate-buffered saline, pH 7.4). γ -cyclodextrin was added to increase the drug solubility in the acceptor phase [67]. The acceptor solution was continuously stirred and kept at 32°C, and samples were withdrawn at predetermined time points, replaced with fresh acceptor solution, and analysed by HPLC. Experiments were performed in triplicate.

3.4. Mathematical models describing drug release

In order to analyse the drug-release mechanism, release kinetics were obtained by fitting the obtained in-vitro release data with linear and non-linear regression analysis of various models (Higuchi, Weibull, and Korsmeyer-Peppas). The model parameters were calculated using the DDSolver (China Pharmaceutical University, Nanjing, China), the correlation coefficient (R^2) was used as an indicator for the best fitting [68], [69]. For all models, M_t/M_∞ is the fraction (%) of drug released per time t .

3.4.1. Higuchi Equation

$$\frac{M_t}{M_\infty} = k_H * t^{0.5} \quad (2)$$

This simple equation describes the release of drugs from matrix systems, where k_H is a constant reflecting the design of the system. In this model, the fraction of drug released is proportional to the square root of time. The applicability of the model is limited to systems, in which the drug is very fine distributed or suspended and where, if applicable, particles have a much smaller diameter than the thickness of the system. Further swelling or dissolution of the matrix system has to be negligible, the drug diffusion must be constant and the dominating release-mechanism, and the system should maintain sink conditions [70]–[72].

3. Material and methods

3.4.2. Korsmeier-Peppas Model

$$\frac{M_t}{M_\infty} = k_{KP} * t^n \quad (3)$$

The equation describes the drug release from polymeric systems, but is in contrast to Eq. 2 more comprehensive, because swelling of the matrix and a further release-mechanism (case-II-transport) have been incorporated. The constant k_{KP} incorporates structural and geometric characteristics of the vehicle, and n is the release exponent, that indicates the mechanism of drug release. For thin films, $n = 0.5$ indicates Fickian diffusion, values between 0.5 and 1.0 imply a release based on both, diffusion and swelling (anomalous transport) and for $n = 1$, the drug release rate is time-independent (Zero-order kinetic) and primarily controlled by the swelling of the polymer-system. The determination of n is limited to the first 60 % of drug release [69], [72]–[74].

3.4.3. Weibull Model

$$\frac{M_t}{M_\infty} = \frac{M_{max}}{M_\infty} * \left(1 - e^{-\frac{t^\beta}{\alpha}}\right) \quad (4)$$

M_{max}/M_∞ is the maximum fraction of the drug released at infinite time. β is the dimensionless shape parameter of the dissolution curve, and α is the scale parameter, defining the release rate of the process. The constant indicates the time t , at which 63.2 % of the drug has been released; therefore, $1/\alpha$ represents the rate constant. If $\beta = 1$, the shape of the release curve is exponential, $\beta > 1$ indicates a sigmoidal curve and in the case of $\beta < 1$, the initial slope of the curve is steeper than exponential. The model can only describe, but not suitable characterize release kinetics, because it is an empiric model, lacking an adequate kinetic fundament [69], [75]–[77].

3.4.4. Fractional rate control

$$F_D = \frac{M_{total}}{M_{device}} \quad (5)$$

Guy and Hadcraft addressed in this equation whether the rate control resides in the release process (by the device) or in the skin. M_{total} represents the amount of drug permeated when the device was placed in contact with the skin and M_{device} the amount released from the delivery system into an aqueous sink. $F_D = 1$ indicates an entirely device-controlled delivery, when $F_D < 1$ the skin controls the process [78].

3.5. In-vitro skin permeation studies

In order to evaluate the transdermal drug permeation, pig skin was used because the permeability was found to be similar to human skin [79]. Pig ears were gently cleaned and excised upon reception. Afterwards the skin was separated from the porcine ear by carefully removing the connecting tissues with a surgical scalpel. After removing most of the subcutaneous fat, the skin was placed between two even plates clamped together and cooled to $-20\text{ }^{\circ}\text{C}$ in a freezer. The frozen skin was removed from the freezer and the plate covering the stratum corneum was taken off. A dermatome was used to cut skin strips with a thickness of 1 mm, and the obtained strips were cut to circular disks using a die punch [80], [81]. Subsequently, the integrity of the samples was assessed by visual inspection and by checking the tightness of the skins mounted onto jacketed franz diffusion cells. The diffusion cell system is displayed in **Figure 7A**.

The prepared skin was placed between the donor and acceptor compartment of the cells, and a pinch clamp secured both parts of the cells as shown in **Figure 8** [82]. The acceptor compartment was entirely filled with PBS containing 0.5 % γ -cyclodextrin. Initially, 2 ml of the acceptor solution were placed on top of the skin. The system was maintained at $32 \pm 0.5\text{ }^{\circ}\text{C}$ and continuously stirred with a magnetic bead for 1 h to equilibrate the skin [81]. Stirring was performed to maintain a constant hydrodynamic flow of the acceptor solution. After equilibration, the top side of the skin was dried carefully, and a DIA was placed upon the skin surface. After 1, 2, 4, 6, 9, 24, and 28 h, 2 mL of acceptor fluid were withdrawn through the sampling port and replaced with fresh acceptor solution, avoiding any air bubbles under the skin.

3. Material and methods

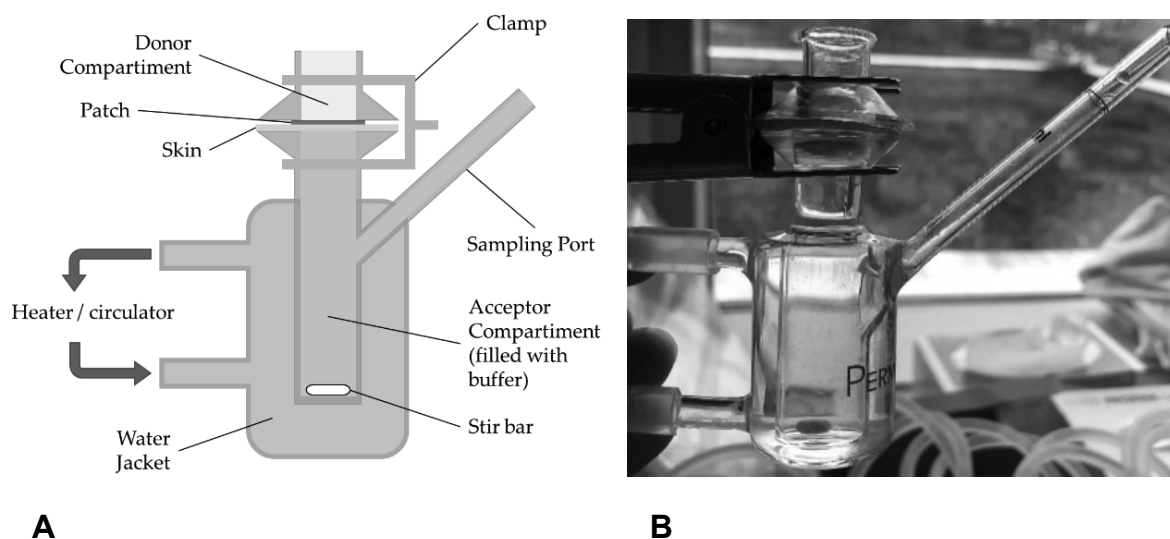


Figure 8. Franz diffusion cell **(A)** scheme of the experimental set up for permeation experiments, **(B)** Franz-diffusion cell – experimental set up in lab scale.

Experiments were performed in triplicate and drug concentrations were determined by HPLC. Flux J_{ss} [$\mu\text{g}/\text{h}\cdot\text{cm}^2$] is constant within the steady-state period and was calculated by linear regression analysis from the slope of the plot of cumulative drug permeated per cm^2 of skin against the time. The lag-time is the intercept of J_{ss} with the x-axis.

Following the permeation experiments, skin samples were cut into thin horizontal slices with a cryo-microtome (SLEE medical, Mainz, Germany). Acetone and methanol were added to the collected slices to extract the penetrated drug amount, which remained in the skin. The mixture was homogenized with an ultra turrax (IKA, Staufen, Germany) at room temperature. Subsequently, the suspension was centrifuged at 15,000 rpm for 30 min at 25°C. The supernatant was assayed via High-performance liquid chromatography and, if applicable, via gas chromatography.

3. Material and methods

3.6. High-performance liquid chromatography (HPLC)

A Shimadzu (Duisburg, Germany) LC-2050C-3D separations module combined with a Photodiode Array Detector was used. Analysis was performed with a reversed-phase C18 column (LiChrospher 100 RP 18-5 μ ; 250 mm length; 4.6 mm inner diameter, 5 μ m particle size).

3.6.1. Estradiol

The analysis of E2 was performed using a modified method from Ph. Eur 9.0 [83]. The mobile phase consisted of water and Acetonitrile (60/40, v/v) running isocratic at 1 mL/min, and the column temperature was kept at 25 °C. Detection was performed at 220 nm (injection volume = 20 μ L, LOQ = 0.10 μ g/mL, LOD = 0.05 μ g/mL). HPLC method was calibrated in the range of 0.10 - 120.00 μ g/mL.

3.6.2. Ibuprofen

Ibuprofen was analysed according to a modified method developed and validated by Farrar et al [84]. Acetonitrile and water (adjusted to pH 2.5 with H₃PO₄) in a ratio of 60/40 (v/v) was used as a mobile phase with an isocratic flow of 1 mL/min, and the column temperature was kept at 30 °C. After injecting a sample volume of 20 μ L, the detection was performed at 220 nm (LOQ = 0.10 μ g/mL, LOD = 0.70 μ g/mL). HPLC method was calibrated in the range of 0.10 - 217.00 μ g/mL.

3.6.3. Scopolamine

Scopolamine was assayed according to a modified method from Ph. Eur. 9.0 [85]. The mobile phase consisted of 23 % acetonitrile, 47 % Na-dodecylsulfate solution (2.5 g/L), which was previously adjusted to pH 2.5 with H₃PO₄, and 30 % methanol (v/v). Analysis was performed isocratic at 1.4 mL/min, and the column temperature was kept at 30 °C. The injection volume was 20 μ L and Scopolamine was detected at a wavelength of 210 nm (LOQ = 0.12 μ g/mL, LOD = 0.90 μ g/mL). HPLC method was calibrated in the range of 0.12 - 116.00 μ g/mL.

3. Material and methods

3.6.4. Rotigotine

The analysis of Rotigotine was performed according to a modified method from Ph. Eur. 9.0 [86]. The mobile phase consisted of 70 % acetonitrile and 30 % water, adjusted to pH 2.5 with trifluoroacetic acid, running isocratic with a flow of 1.4 mL/min at 30 °C column temperature. After injecting a sample volume of 20 µL, the detection was performed at 224 nm (LOQ = 0.10 µg/mL, LOD = 0.80 µg/mL). HPLC method was calibrated in the range of 0.10 - 101.00 µg/mL.

3.7. Gas Chromatography (GC)

Residual solvent analyses were performed using a modified static-headspace method according to Ph. Eur 9.0 [87]. The amount of Hexane, EA, DMSO and Transcutol® was determined with a Focus GC Gas Chromatograph, equipped with a flame ionization detector (FID) and TriPlus RHS Autosampler (ThermoFisher Scientific, Dreieich, Germany).

For the monitoring of the drying process, the initial adhesive mass, respectively dried DIA, were transferred into closed glass vials and dissolved in 1 mL 1,3-Dimethyl-2-imidazolidinone (DMI). The headspace oven and the syringe were maintained at 100 °C, and the sample was heated and agitated for 25 min. Afterwards, a headspace volume of 1 mL was withdrawn from the sample and injected. Analytical separation was performed on a FS-CS-624 column (30 m length, 0.32 mm ID, Chromatography Service, Langerwehe, Germany). N₂ was used as carrier gas with a flow of 2.0 ml/min and the FID kept at 240 °C. The oven program for residual solvent analysis of the patches started at 70 °C heating up to 130 °C at 30 °C/min. The final heating phase (60 °C/min) resulted in a temperature of 220 °C, which was kept constant for 1.5 min. The limits of quantification were 4.5 ng/mL for EA (LOD: 2.0 ng/mL), 3.3 ng/mL for hexane (LOD: 1.0 ng/mL), and 5.5 µg/mL for DMSO (LOD: 2.0 µg/mL). An exemplary chromatogram including all compounds is displayed in **Figure 9**.

3. Material and methods

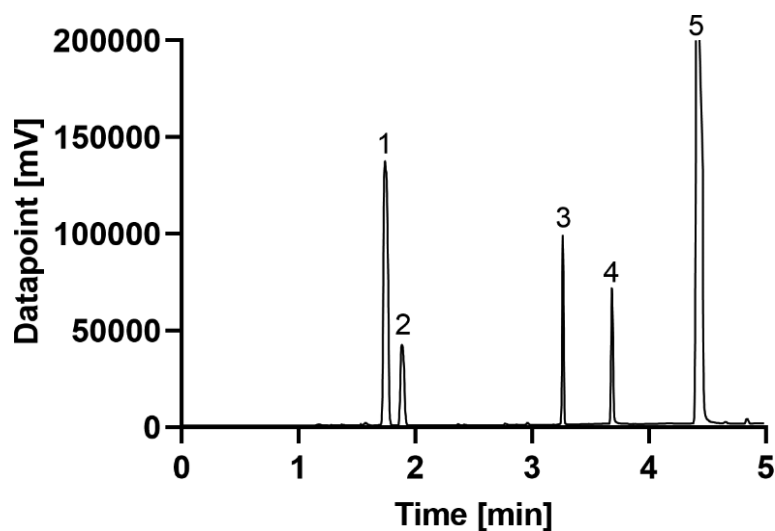


Figure 9. Chromatogram obtained from a mixture of 0.50 $\mu\text{L}/\text{mL}$ n-hexan, 0.05 $\mu\text{L}/\text{mL}$ EA, 5.00 $\mu\text{L}/\text{mL}$ DMSO and 5.00 $\mu\text{L}/\text{mL}$ TC dissolved in DMI and analysed via headspace-GC. 1 = n-hexane ($t_{\text{R}} = 1.73$), 2 = ethyl acetate ($t_{\text{R}} = 1.89$), 3 = dimethylsulfoxide ($t_{\text{R}} = 3.26$), 4 = Transcutol® ($t_{\text{R}} = 6.38$), 5 = DMI ($t_{\text{R}} = 4.42$).

Aqueous samples received from permeation experiments were diluted with methanol (1:1) and analysed via liquid injection of 1 μL diluted sample. An AS-JXR column (15 m length, Altmann Analytik, München, Germany) was used. The oven program started at 80 $^{\circ}\text{C}$, followed by heating up to 140 $^{\circ}\text{C}$ at 50 $^{\circ}\text{C}/\text{min}$. The final temperature of 220 $^{\circ}\text{C}$ (90 $^{\circ}\text{C}/\text{min}$) was kept constant for 1 min. GC method was calibrated in the range of 0.02 - 0.50 $\mu\text{L}/\text{mL}$ for DMSO (LOQ = 0.02 $\mu\text{L}/\text{mL}$, LOD = 0.01 $\mu\text{L}/\text{mL}$).

3. Material and methods

3.8. X-ray diffraction (XRD)

Pure drug powder and the prepared patches were assessed for crystallinity using X-ray diffraction. XRD measurements were performed in reflection mode (X'Pert MRD Pro, PANalytical, Almelo, Netherlands) with an X'Celerator detector and nickel filtered CuK α 1 radiation ($\lambda = 1.54 \text{ \AA}$) at 45 kV and 40 mA in the angular scan range from 4° to $45^\circ 2\theta$ at a scan speed of $0.017^\circ/\text{sec}$. Patches were mounted on sample holders (15 mm) without the release liner, matrix-site facing upwards. Data evaluation was performed with X'Pert High Score version 2.2.

3.9. Differential Scanning Calorimetry (DSC)

DSC experiments were performed using on a Mettler-Toledo DSC 2 (Mettler-Toledo, Gießen, Germany) equipped with a nitrogen cooling system (30 mL/min). Glass transition temperatures (T_g) and melting temperatures (T_m) of the DT, APIs, and adhesive matrices were analysed via heating-cooling-heating cycles at 10 K/min. Analysis of the matrices were limited to DMSO- and solvent-free specimens. A sample amount of approximately 10 mg was weighed into aluminium pans and sealed with a pierced lid. T_m and T_g values were determined as the onset of the inflection in the DSC thermogram.

3.10. Polarized-light microscopy (PLM)

Patches were investigated for the presence of drug crystals using a polarized light microscope (Leica DM 2700 M, Leica microsystems, Wetzlar, Germany) equipped with a camera (MicroPublisher 5.0 RTV, Teledyne Photometrics, Tucson, AZ, USA). DIA were mounted onto a microscopic slide, and the entire surface of the patches was scanned in reflection. Linear polarization equipment was combined with a λ -plate was applied to distinguish crystalline structures from the patch matrix. All microscopic experiments were conducted at ambient temperature.

The average diameter of occurring droplets and standard deviations were calculated by measuring the particles over an area of 1.2 mm^2 of the pictures taken from the PLM using ImageJ software (National Institutes of Health, NIH, Bethesda, MD, USA).

3.11. Probe-tack test

The ability of a pressure-sensitive adhesive to bond under conditions of light contact pressure and a short contact time is called tack. The adhesive properties of the prepared DIA were determined via probe-tack measurements and performed with a texture analyser (TA-HDi, Stable Micro Systems, Godalming, United Kingdom) according to [88]. Initially, the release liner was removed, and the specimens were clamped in the texture analyser, adhesive side facing towards the downwards moving probe. Samples were restricted from moving by clamping them under a stainless-steel plate with an orifice for the probe. A cylindrical stainless-steel probe (diameter: 6 mm) was brought into contact with the matrices (applied force: 1 N) and removed after a contact time of 5.0 s with a rate of 5 mm/s, while the required tensile force was recorded. PSA were tested at room temperature (22 °C), and the probe was cleaned with acetone after each test. The maximum of the tensile stress curve (σ_{\max}) as displayed in **Figure 10** was selected as response.

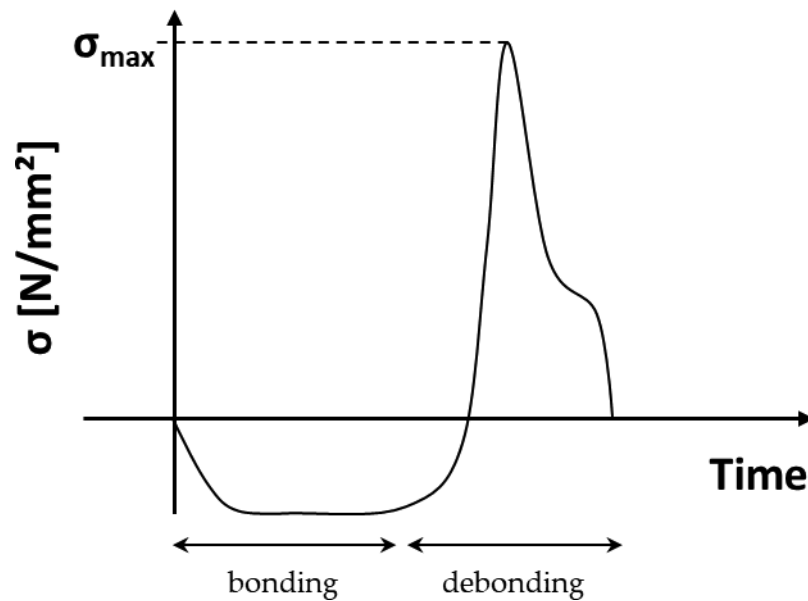


Figure 10. Exemplary stress-time curve of the probe-tack test. The bonding phase describes the contact of the probe with the specimen. During the debonding phase, the probe was retracted at a defined speed.

3. Material and methods

3.12. Determination of drug solubility

An excess amount of drug was placed into a screw-cap glass filled with 1 mL of the franz cell acceptor medium (PBS containing 0.5% γ -cyclodextrin). The glass was closed, sealed with Teflon tape, and weighed. Experiments were performed at 32 °C in a shaker bath for 28 h. The pH and weight of the glasses were checked at the end of the experiment. After removing the samples from the shaker bath, the solutions were filtered and analysed via HPLC to determine the drug concentration in the filtrate. Experiments were performed in triplicate; results are shown in **Table 2**. The drug concentrations in the acceptor medium were constantly below these values during release and permeation experiments.

Table 2. Equilibrium drug solubility in the acceptor medium of release and permeation experiments after 28 hours at 32 °C.

	β -Estradiol	Ibuprofen	Scopolamine-Hbr	Rotigotine
Solubility [mg/mL]	0.194 \pm 0.002	1.644 \pm 0.027	> 300	0.027 \pm 0.001

3.13. Stability evaluation

For the patches containing DMSO and E2, stability studies were performed over six months at different conditions (fridge: 2 - 8 °C, climate chamber: 25 °C/60% RH). Sealed (PET-AL-composite foil, Medewo, Germany) samples were stored at both conditions. Additionally, unsealed samples were stored at 25 °C/60% RH. After one, two, three, and six months, stability samples were tested for the residual amount of DMSO. After three and six months, samples were additionally tested for in-vitro permeation and XRPD measurements were performed.

For chapter 4.24.3 "Investigation of stabilization issues in DMSO-containing transdermal patches", three different storage conditions were necessary: long-term (25 °C/60 % RH), accelerated (40 °C/75 % RH) and stress test (50 °C/75 % RH) conditions according to the applicable ICH guideline [89]. Samples were stored in sealed containers for three months and tested after one, two, and three months for transdermal permeation, appearance, and DMSO-content.

The stability evaluation for chapter 4.4 was carried out at accelerated conditions (40 °C/75 % RH) for three months and in sealed containers.

3.14. Preliminary excipient evaluation

Initially, it was important to evaluate the miscibility of the excipients with DMSO. Therefore, increasing excipient amounts were blended with DMSO and stirred at 35 °C. The resulting suspensions were assessed regarding consistency and appearance. If a suitable and fluid mixture of excipient and DMSO was obtained, the solvent evaporation in a drying cabinet without air circulation at 40 °C was monitored gravimetrically. The evaporation of the DMSO-excipient-blends were compared to the evaporation of pure DMSO. Mixtures that decelerated the evaporation of DMSO were chosen for further experiments.

The next step was to examine the ability of the candidates to retain DMSO successfully within the patch matrix. For this purpose, relevant excipients were blended with DMSO, EA, and DT. The mixtures were stirred until homogeneous and bubble-free masses were obtained. The mixtures were cast on the backing liner and placed in a forced convection oven at 40 °C. The drying of the laminates was monitored via GC and compared to the DMSO-evaporation rate of excipient-free mixtures.

3.15. Statistics

All results were expressed as mean values \pm SD, measurements were performed in triplicate. Statistical analysis was performed by GraphPad software (San Diego, CA, USA) using analysis of variance test (ANOVA), followed by significance analysis with Sidaks's multiple comparison test. Differences were considered significant at levels of * $p < 0.05$, ** $p < 0.01$, and *** $p < 0.001$. Surface plots have been generated using OriginPro 8G (OriginLab Corporation, Northampton, MA, USA).

4. Results & Discussion

4. Results & Discussion

4.1. Enhanced skin permeation of Estradiol by dimethyl sulfoxide containing transdermal patches

4.1.1. Patch preparation and characterization

To eliminate the organic solvents ethyl acetate and n-hexane to a level of unquantifiable amounts, a minimum drying temperature of 30 °C combined with a minimum duration of 4 h was found necessary. Accordingly, an attempt of drying at 20 °C for 4 h led to significant residual ethyl acetate content. Generally, it was found relatively difficult to retain DMSO in the patches being a total solvent, and simultaneously DMSO evaporation was observed at drying conditions that were relatively similar, i.e., after 2 h of drying at 50 °C, after 4 h at 40 °C and after 16 h at 30 °C. Exemplary compositions are shown in **Table 3**.

Figure 11 illustrates the drying conditions and the subsequent DMSO content per patch, while threshold values of around 10 mg of DMSO/patch were the maximum of DMSO, which could be incorporated before the formulations turned into a wet and unusable gel mass. However, patches with drying conditions at 35 °C (3 h and 4 h) and 40 °C (2 h and 3 h) had sufficiently high energy input during drying to obtain solid patch formulations.

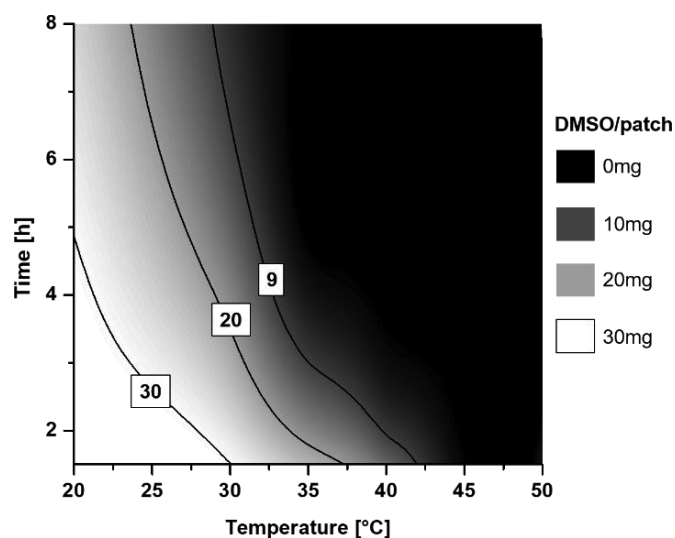


Figure 11. Contour plot of the effect of drying time and temperature on the residual amount of DMSO/patch. The line with the value 9 displays the maximum amount of DMSO (9 mg) which can be incorporated to produce a suitable transdermal patch.

4. Results & Discussion

Table 3. Exemplary compositions of the adhesive mass at different production times. From an initially ($t = 0$ h) viscous and liquid mixture to a homogeneous drug-in-adhesive layer (per DIA). Control was prepared without dimethyl sulfoxide (DMSO) (mean \pm SD; n.d. = not detected).

Drying Conditions	0 h	20 °C 4 h	35 °C 3 h	40 °C 2 h	35 °C 4 h	40 °C 3 h	50 °C 24 h	Control 50 °C 24 h
DMSO [%]	38.4 \pm 2.2	62.9 \pm 11.7	36.4 \pm 3.8	29.5 \pm 3.9	19.7 \pm 1.7	6.9 \pm 1.3	n.d.	-
EA [%]	42.5 \pm 0.9	0.8 \pm 0.0	n.d.	n.d.	n.d.	n.d.	n.d.	n.d.
Hexane [%]	2.1 \pm 0.1	n.d.	n.d.	n.d.	n.d.	n.d.	n.d.	n.d.
Duro-Tak® (solid content) [%]	16.2 \pm 2.7	34.6 \pm 4.3	48.8 \pm 12.3	67.1 \pm 10.1	76.3 \pm 12.4	89.4 \pm 9.4	95.6 \pm 9.4	95.6 \pm 7.1
β -Estradiol [%]	0.8 \pm 0.1	1.6 \pm 0.8	2.4 \pm 0.3	3.4 \pm 0.5	4.0 \pm 0.6	3.8 \pm 0.6	4.4 \pm 0.6	4.4 \pm 0.5
Matrix weight [mg]	102.0 \pm 0.8	57.0 \pm 9.1	23.6 \pm 2.0	20.7 \pm 0.3	17.7 \pm 1.8	15.8 \pm 0.6	17.8 \pm 1.1	18.3 \pm 1.0
Appearance	Viscous liquid	Wet layer	Uniform DIA	Uniform DIA	Uniform DIA	Uniform DIA	Uniform DIA	Uniform DIA

E2 recrystallization was observed only in patches prepared at 50 °C for 24 h, which had DMSO in the initial mixture and in the DMSO-negative controls (**Figure 12**). Peak heights were 3.1 % resp. 4.7 % compared to the reference peak of pure E2 at 18.39 °. All other patterns showed the absence of detectable peaks at 18.4 °.

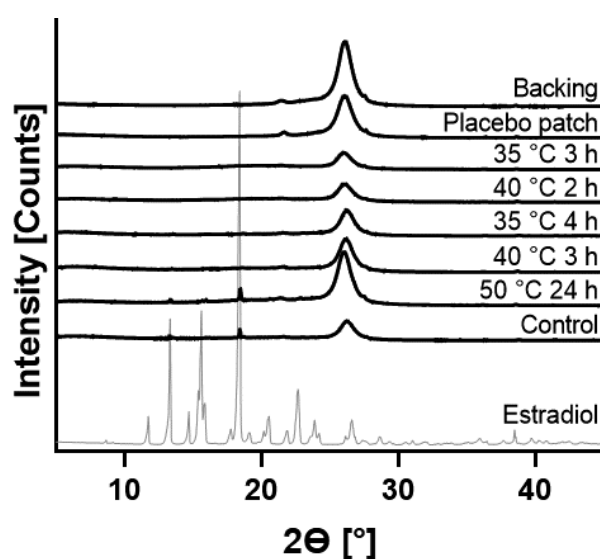


Figure 12. XRD patterns of pure E2 and the prepared patches. The placebo patch was prepared without DMSO and E2 (consisting of DT), and the control patch was prepared without DMSO (consisting of E2 + DT).

4. Results & Discussion

4.1.2. Drug release and permeation behavior

In general, Estradiol-release curves of patches with different amounts of DMSO are comparable (**Figure 13**). The total amount of E2 was released within 32 h from 40 °C, 2 h. The patches prepared at 35 °C, 4 h and 35 °C, 3 h showed 80 % drug release, and for the remaining patches it was 70 % – 75 %. The mathematical expression best-describing drug release was Korsmeyer-Peppas ($R^2 = 0.99$).

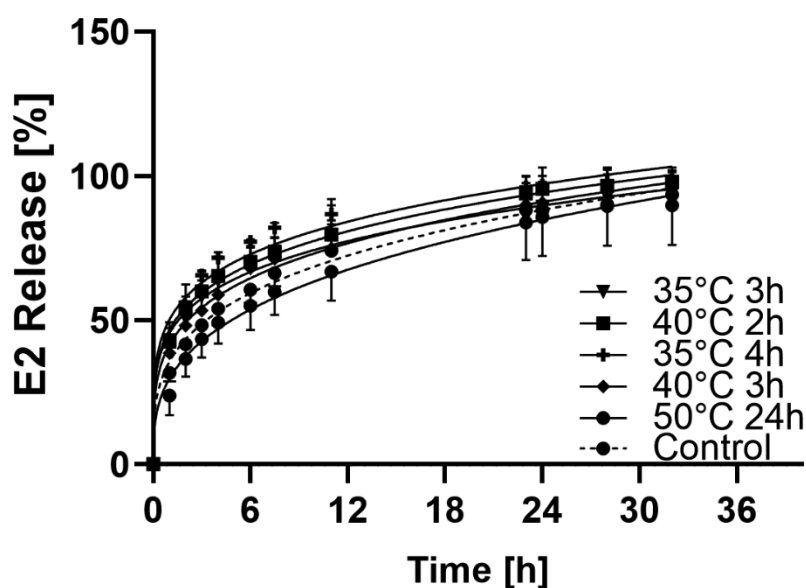


Figure 13. In vitro release profile in phosphate buffered saline (PBS, pH 7.4) at 32 °C.

While release profiles of the different formulations were closely related, E2 skin permeation showed significant differences between the patch types (**Figure 14A**), where the permeated E2 amount correlated to the DMSO amount after preparation. After 28 h, the cumulative drug amount of the formulation containing the highest amount of DMSO (35 °C, 3 h) was four times higher than of 50 °C, 24 h (**Table 4**). The highest mean dose delivered was 82 $\mu\text{g}/24\text{ h}$ (35 °C, 3 h), the lowest for 50 °C, 24 h and control were 26 $\mu\text{g}/24\text{ h}$ and 24 $\mu\text{g}/24\text{ h}$, respectively. Lag times increased with increasing DMSO content of the patches.

4. Results & Discussion

Table 4. Flux values, lag- time, mean delivered dose and kinetic release rate of the prepared patches.

Drying Conditions	35 °C, 3 h	40 °C, 2 h	35 °C, 4 h	40 °C, 3 h	50 °C, 24 h	Control 50 °C, 24 h
Flux J_{ss} E2 [$\mu\text{g}\cdot\text{cm}^{-2}\cdot\text{h}^{-1}$]	4.12 ± 0.3	3.2 ± 0.4	2.3 ± 0.2	1.8 ± 0.1	1.22 ± 0.2	1.1 ± 0.2
Lag-time [h]	5	5	7	6	3	3
Mean permeated dose [$\mu\text{g}/24$ h]	82	63	43	36	26	24
Kinetic release rate K_{KP}	0.40 ± 0.01	0.43 ± 0.07	0.34 ± 0.01	0.39 ± 0.09	0.35 ± 0.04	0.32 ± 0.04

DMSO permeation profiles showed, in contrast to E2, a neglectable lag time (**Figure 14B**) and visibly permeated faster through the skin than the drug. The permeated amount of DMSO from 40 °C, 3 h was not detectable in the current experimental setting. Besides, the permeated DMSO amount reached a slowly increasing plateau after 6 – 9 h with all respective patches. Again, similar to E2, the flux and permeated DMSO amount increased with increasing the initial DMSO content of the patch (**Figure 15B**). Linear correlations were found between DMSO content in the patch and drug flux J_{ss} E2, with lowest flux values ($1.22 \pm 0.24 \mu\text{g}\cdot\text{cm}^{-2}\cdot\text{h}^{-1}$) for the patches containing no DMSO (50 °C, 24 h) (**Figure 15A**). J_{ss} E2 increases proportionally to the amount of penetration enhancer to a maximum of $4.12 \pm 0.25 \mu\text{g}\cdot\text{cm}^{-2}\cdot\text{h}^{-1}$ for 35 °C, 3 h. Based on these data, the presence of DMSO in the patch improved drug permeation nearly 4-fold. Additionally, the drug flux J_{ss} E2 increases proportionally to the flux of DMSO (**Figure 15C**). There was no correlation observed between permeation and release behaviour of E2 (**Figure 15D**).

4. Results & Discussion

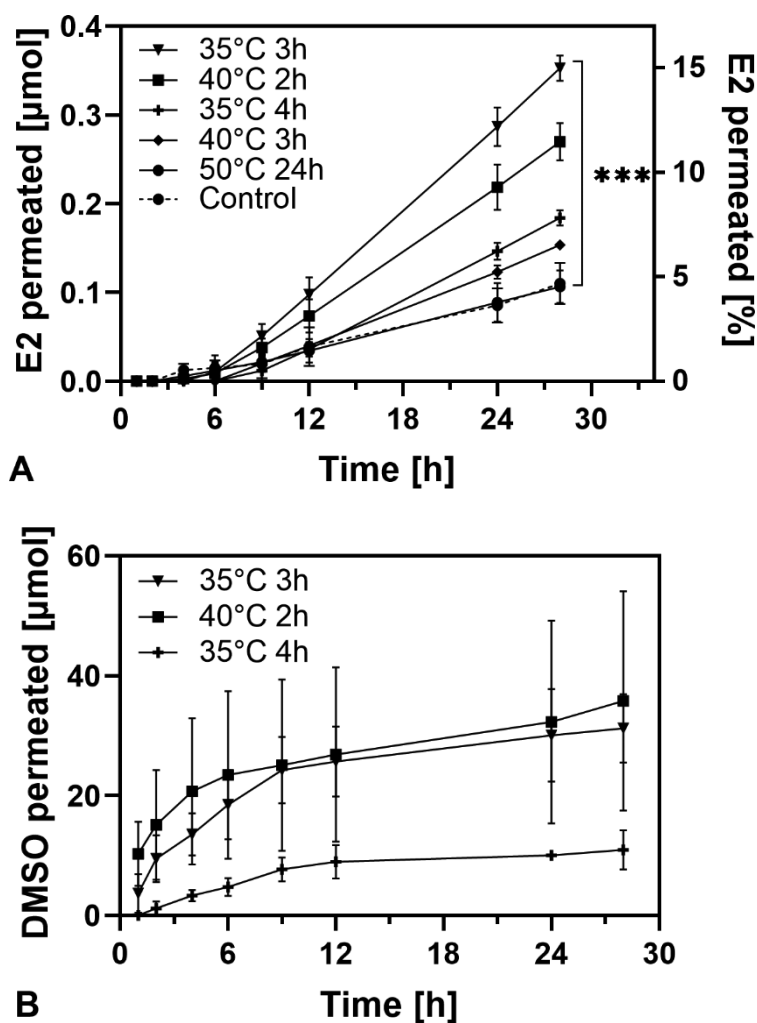


Figure 14. Permeation profiles of E2 (A) and DMSO (B) across pig skin at 32 °C. Percentual permeated amount of DMSO: 35 °C, 4 h: 11.5 ± 0.7 ; 40 °C, 2 h: 21.8 ± 1.9 ; 35 °C, 3 h: 65.4 ± 3.1 (mean \pm SD). *** Indicates significant differences ($p < 0.001$).

Earlier studies tested transdermal permeation of various drugs combined with different permeation enhancing substances, including DMSO, and could not improve drug permeation; this is undoubtedly related to the fact that drying was performed above 50 °C (60/65 °C) [90], [91]. Consequently, the authors explained the lack of permeation enhancement with an insufficient DMSO concentration, quoting an enhancing effect with concentrations above 50 %. However, it was possible to significantly enhance the permeation of Ketorolac with a concentration of five percent DMSO in a transdermal gel system (reservoir-type patch) when heating of the formulation was not involved [92].

4. Results & Discussion

Accordingly, such reservoir-type patches, as well as topical formulations (solutions, gels) containing DMSO showed an enhanced permeation behaviour [44], [92], [93]. The amount of DMSO incorporated in both topical formulations and reservoir-type patches was able to establish its enhancing effect as no heat was applied during production, limiting the risk of DMSO evaporation.

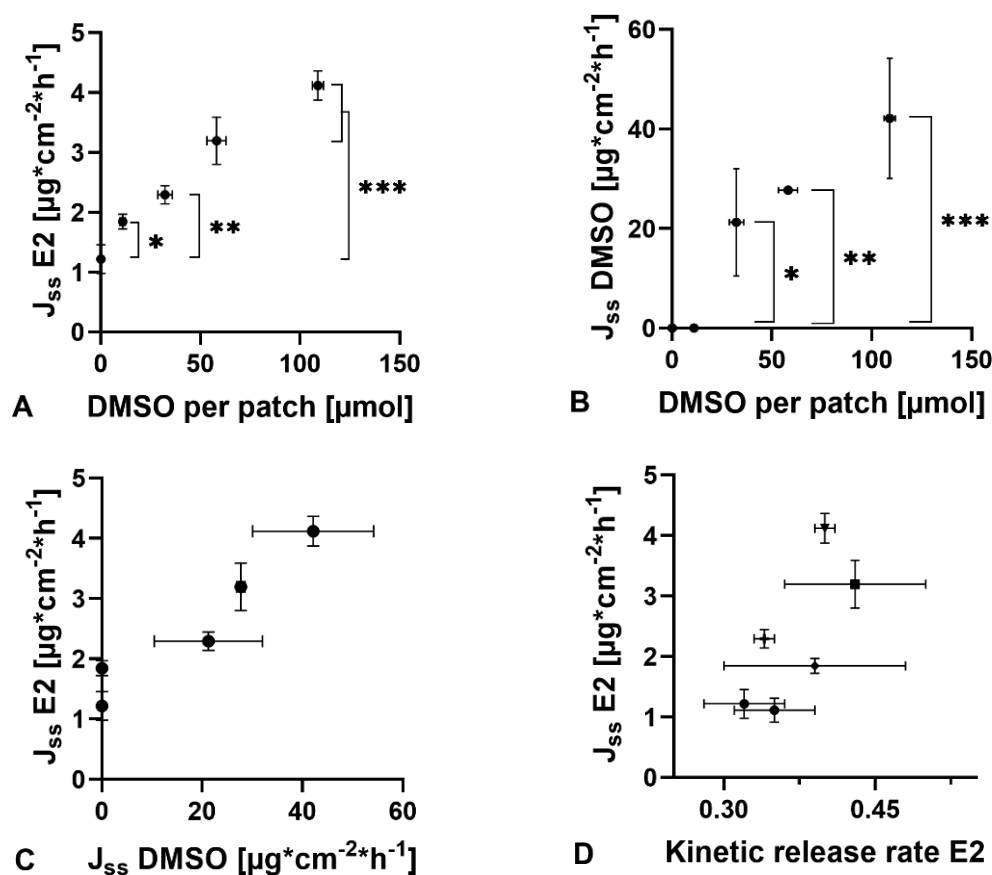


Figure 15. (A) Correlation between steady-state flux ($J_{ss} E2$) of Estradiol and DMSO per patch ($R^2 = 0,972$). (B) Correlation between steady-state flux of DMSO ($J_{ss} DMSO$) and DMSO per patch ($R^2 = 0,924$). (C) Correlation between steady-state flux of Estradiol ($J_{ss} E2$) and steady-state flux of DMSO ($J_{ss} DMSO$) ($R^2 = 0,884$). (D) Correlation between kinetic release rate of Estradiol ($J_{ss} E2$) and steady-state flux of Estradiol ($J_{ss} E2$) ($R^2 \leq 0,5$). * Indicates significant differences ($p < 0,05$), ** indicates significant differences ($p < 0,01$) and *** indicates significant differences ($p < 0,001$).

4. Results & Discussion

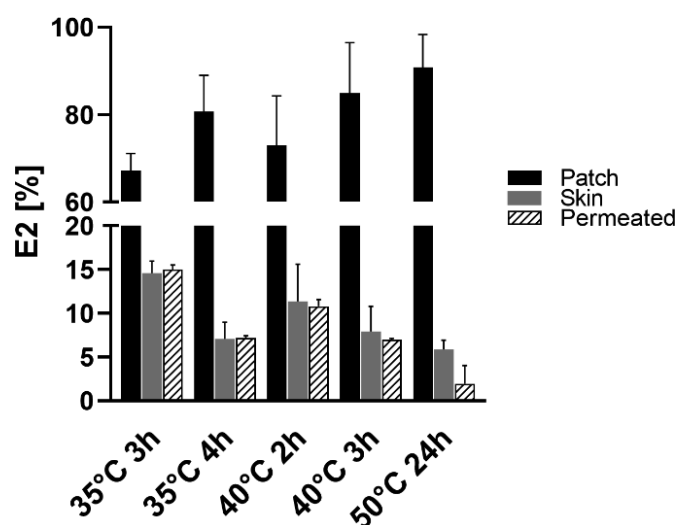


Figure 16. Distribution of E2 after 28 h permeation experiments in skin and patch and through permeation into the acceptor compartment of Franz cells.

The E2 distribution in the patch, skin, and acceptor compartment differed clearly between the formulations (**Figure 16**). An increasing DMSO content per patch was associated with higher E2 amounts recovered from the acceptor phase and mainly extracted from the skin layer (35 °C, 3 h > 40 °C, 2 h > 35 °C, 4 h > 40 °C, 3 h > 50 °C, 24 h). Drug concentrations were at similar levels when comparing skin and acceptor phase, except for the patch containing no DMSO (50 °C, 24 h). Here, the amount of E2 recovered in the skin was twice the permeated amount.

Drug permeation through the skin occurs in different steps. The first step is to release the drug from the patch matrix, followed by partitioning of the drug into the stratum corneum and diffusion through the stratum corneum. Permeating this primary barrier is the major rate-limiting step in the diffusion process of the drug through the skin, there upon the drug enters viable tissues, subsequently entering the systemic circulation. Considering the similar results of release studies and the missing correlation between permeation and release behaviour of E2, it is evident that the enhancement mechanism does not rely on a DMSO-supported faster release of E2 from the patch matrix. However, the flux of E2 increases significantly with the amount and flux of DMSO, indicating a DMSO-dependent intradermal effect that improves the skin permeation.

4. Results & Discussion

Therefore, the increased drug flux is a consequence of improving the second step of drug permeation, i.e., the enhanced stratum corneum partitioning and diffusion. In order to allow simulating the partitioning between the different structures closest to the *in vivo* situation, full-thickness skin was used in these experiments. Patches with a higher DMSO amount led to enhanced drug concentrations in the skin after the permeation experiments. This observation points towards an increased drug permeation due to the enhanced solubility of E2 in the stratum corneum. It has been described earlier that a “push–pull effect” occurs when a faster permeating enhancer substance is added to the donor vehicle [94]. DMSO permeates faster into and through the stratum corneum than E2; in the skin, DMSO increases the drug solubility and a “pull effect” occurs, favouring the diffusion of the drug out of the donor vehicle. The correlation between the flux of DMSO and E2 suggests that the permeation of E2 followed the permeation of DMSO closely. The excess free energy of E2 causes the “push effect” in the donor phase.

DMSO permeation increases quickly at the beginning of the experiments and results in a steady-state plateau. This observation suggests that DMSO can build a reservoir in the skin by providing enhanced skin solubility of E2. However, it was reported that DMSO enhanced drug permeation in the skin by affecting the stratum corneum structure (altering protein structures and interaction with lipids) [95], [96]. Due to the fact that the lag-time of the drug did not shorten with the presence of DMSO; mechanism of increased drug permeation is not related to a faster drug permeation. A more possible mechanism is the co-permeation of DMSO the drug and thus, the formation of an Estradiol-depot within the skin. The increased drug concentration in the skin improves the drug concentration due to an increased concentration gradient between skin and acceptor medium.

Although DMSO is an excellent permeation enhancing agent, it needs to be mentioned that its administration can cause local skin irritations and a garlic-like breath due to its excretion via lungs that has been reported in some cases [44]. Nevertheless, the irritancy potential of a dermal formulation containing 45.5 % of DMSO was clinically investigated and showed no adverse effects in most of the patients, while for the remaining cases mainly dry skin was reported [97]. Another study evaluated the relative irritancy of increasing DMSO concentrations *in vivo* and determined histopathological changes from 50 % upwards [98]. Accordingly, as patches in the current study did not exceed 40 % of DMSO content, one would only expect limited skin irritancy resulting from the new patch formulations.

4. Results & Discussion

The delivered dose rate of the produced patches per day is further comparable to the performance of two approved E2 matrix patches: Climara® and Menorest® (both 50 µg/24 h for 7 days resp. 3 – 4 days of suggested use) [56]. Both patches have a larger size (13 – 15 cm²) and a higher drug load (4 mg) compared to our prepared patches (1.04 cm², 0.7 mg). Since more than 80 % of the drug remains in the patches after 28 h of permeation experiments, a more extended period of administration with constant drug levels is possible.

4.1.3. Storage stability

The absence of recrystallization after six months for all DMSO-based formulations regardless of the storage conditions was confirmed by XRPD (data not shown). In terms of DMSO loss, patches revealed to be stable during the first month under all test conditions as DMSO-content did not differ significantly (**Figure 17**). Besides the significant permeation improvements, this is another advantage of the patches containing DMSO because recrystallization is a common problem with actives such as Estradiol. A higher drug load in the vehicle promotes a higher flux through the skin; therefore, supersaturation of transdermal systems is a widespread method to enhance transdermal performance. The problem is that supersaturated systems are only metastable. The drug is indeed at its highest thermodynamic activity, which enables a flux increased to a multiple; hence it also tends to form crystals, which reduces skin permeation [99]. The patches without DMSO showed crystals already after the production, which indicates a temporary existence of a supersaturated status. The patches with DMSO had the same drug load, but crystals were absent even after six months of storage. DMSO is not miscible with Duro-Tak®; the resulting matrix system of the patches could therefore be imagined as a homogeneous dispersion of DMSO in DT. Based on this assumption, a possible explanation for the stabilization could be the increased matrix solubility of E2 in the presence of DMSO, which inhibits the nucleation of E2 crystals in the matrix.

The benefit of low temperatures was minor as during longer periods; significant DMSO loss occurred of all formulations when stored at 4 °C (sealed, **Figure 18A**). The slightest change in DMSO content was found when patches were stored sealed at 25 °C/60 % RH (**Figure 18B**). Generally, a more distinct reduction of DMSO content in patches was found for those with the initially highest amount (35 °C, 3 h), the lowest loss for those with the lower initial DMSO content. Accordingly, after three months at 25 °C/60 % RH (sealed), 40 °C, 2 h, and 35 °C, 4 h patches still did not show statistically significant DMSO losses. Generally, the DMSO loss during storage translated into lower E2

4. Results & Discussion

permeation through the skin. While 6 months of storage under any storage conditions led to a significant lowering of E2 permeation, E2 permeation did not significantly change in patches 40 °C, 2 h and 35 °C, 4 h after three months (Figure 18C, E).

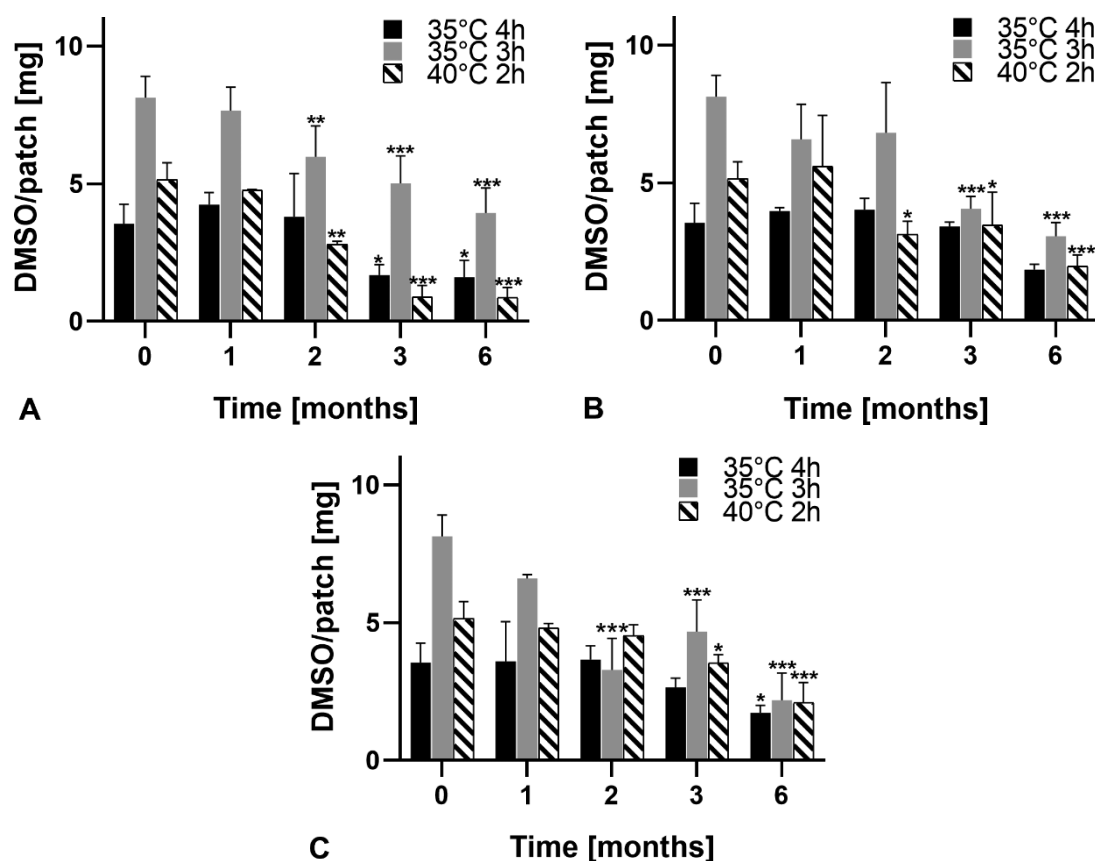


Figure 17. DMSO/patch at different storage conditions over a period of six months. (A) 2–8 °C (sealed), (B) 25 °C/60% RH (sealed), (C) 25 °C/60% RH (unsealed). Residual amounts after one, two, three and six months were compared to the initial amount at $t = 0$. * Indicates significant differences ($p < 0.05$), ** indicates significant differences ($p < 0.01$) and *** indicates significant differences ($p < 0.001$).

Although the volatility of DMSO was undoubtedly the major formulation hurdle, this study nonetheless affirmed the feasibility of producing transdermal patches with sufficiently high amounts of DMSO to increase drug permeation through the skin. Nevertheless, the production process would probably need to be further optimized, especially if scaled up in a continuous production. The formulation could further be improved by creating a matrix, which would sufficiently retain DMSO. This may be achieved by increasing the viscosity of the initial adhesive mass or by changing the polymer type.

4. Results & Discussion

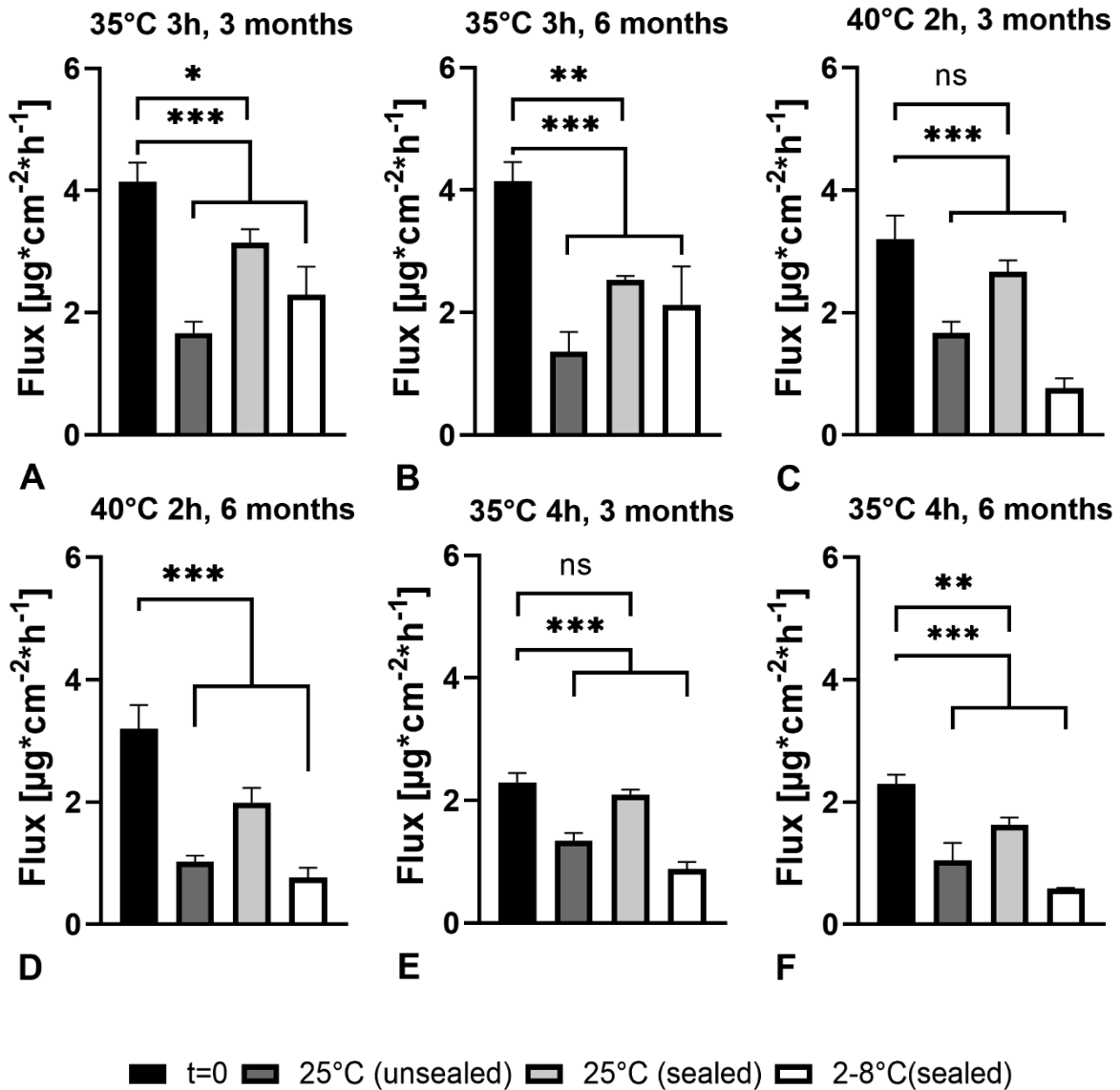


Figure 18. E2 permeation of 35 °C, 3h after three (A) and six months (B), 40 °C, 2h after three (C) and six months (D), and of 35 °C, 4h after three (E) and six months (F) of storage. Flux values after three and six months were compared to the initial value at t=0. * Indicates significant differences ($p < 0.05$), ** indicates significant differences ($p < 0.01$) and *** indicates significant differences ($p < 0.001$).

4.2. Dimethyl sulfoxide in matrix-type transdermal patches: proof of concept and therapeutical implications of the enhancing effect

4.2.1. Patch characterization

Patches containing Ibuprofen (IBU), Scopolamine-HBr (SCO), and Rotigotine (ROT) were prepared with DMSO (test) and without DMSO (control) according to 3.2. DIA were laminated with a release-liner subsequently to the drying process (35 °C, 3 h) and tested for residual solvents, DMSO-amount, and appearance. GC-analysis of the prepared test patches revealed that the targeted amount of DMSO (9 mg/patch, **Figure 19**) was successfully and consistently retained, indicating a robust production process, even if different drug substances were involved. The resulting products were dry and uniform adhesive matrices. The absence of ethyl acetate and hexane was confirmed for all test and control formulations (**Table 5**). The relative drug amount of the control patches (4.0 ± 0.5 %) was generally higher than for the test patches (2.4 ± 0.2 %). This was observed for the E2-formulations in chapter four as well, where drying at 35 °C for 3 hours led to a relative drug amount of 2.4 ± 0.3 %, whereas the DMSO-free formulations contained 4.4 ± 0.5 % drug.

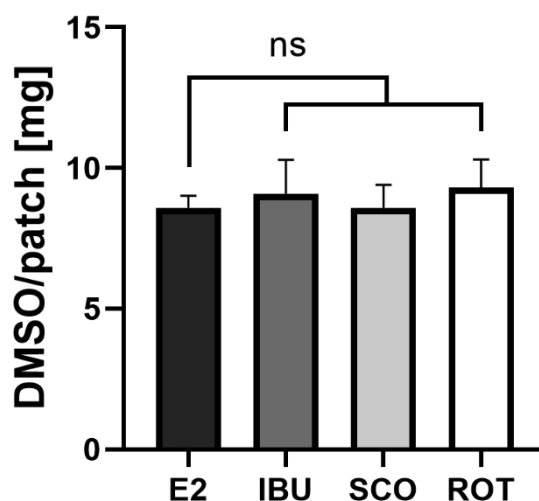


Figure 19. Comparison of DMSO-amount/ patch of test patches with E2-patches, chapter 4 (see 4.1, p. 44). Test formulations (IBU, SCO, ROT) were produced analogous to the beforementioned E2-patches, drying was performed at 35 °C for 3 h. “ns” indicates non-significant differences.

4. Results & Discussion

Table 5. Composition and appearance of the prepared patches dried at 35 °C for three hours. Control patches were prepared without dimethyl sulfoxide (DMSO). Values indicate mean \pm SD; n.d. = not detected.

Drug	Test			Control		
	IBU	SCO	ROT	IBU	SCO	ROT
DMSO [%]	34.5 \pm 2.3	42.5 \pm 0.5	36.4 \pm 3.8	-	-	-
EA [%]	n.d.	n.d.	n.d.	n.d.	n.d.	n.d.
Hexane [%]	n.d.	n.d.	n.d.	n.d.	n.d.	n.d.
Duro-Tak [®] (solid content) [%]	62.9 \pm 4.8	56.3 \pm 3.6	59.3 \pm 2.0	95.4 \pm 0.2	95.7 \pm 0.7	96.6 \pm 0.2
Drug [%]	2.1 \pm 0.7	2.7 \pm 0.2	2.4 \pm 0.0	4.4 \pm 0.1	4.3 \pm 0.7	3.4 \pm 0.2
Matrix weight [mg]	25.4 \pm 4.3	20.3 \pm 0.5	24.3 \pm 1.2	18.8 \pm 0.8	18.9 \pm 0.6	19.9 \pm 1.3
Appearance	Uniform, clear DIA	Uniform, clear DIA	Uniform, clear DIA	Uniform, clear DIA	Uniform, opaque DIA	Uniform, clear DIA

After drying, the visual inspection of the laminated DIA subsequently revealed uniform and transparent, crystal-free matrices, except for the SCO control. The patches were uniform as well but had an opaque, milky look. Therefore, further investigations with PLM and XRD were conducted for the SCO patches. The obtained XRD patterns presented in **Figure 20A** showed the absence of detectable peaks for both, test and control, compared to the reference peak of pure and crystalline Scopolamine-HBr at 21 °. The microscopic investigation of the DMSO-free patches by PLM confirmed the absence of detectable crystals for the SCO control as well (**Figure 20B**).

For the patches containing IBU, the microscopic investigation confirmed the presence of crystals for the DMSO-free patch (**Figure 20D**) and the absence of recrystallization for the test patch (**Figure 20C**). During the drying process, the evaporation of the solvents from the IBU control caused the concentration of IBU until an unstable, supersaturated drug-in-matrix system was built. Consequently, the drug passed over into a lower energetic form; in other words, it recrystallized. The presence of an enhancer in the test patch apparently prevented the recrystallization of IBU in the matrix.

4. Results & Discussion

Thermogravimetric analysis of the used APIs revealed the melting points (T_M) of the crystalline drugs and their glass transition temperatures (T_G). According to **Table 6**, the highest melting point was obtained for SCO (200.1 °C), followed by ROT (96.6 °C) and IBU (76.5 °C). The T_G of the drugs was about 90 – 140 °C lower than the corresponding T_M . The measured melting points complied with the literature references. For pure DT (placebo patch) and the DMSO-free matrices of the control patches, the obtained curves did not differ significantly and showed solely glass-transitions ranging between – 45.4 and – 48.2 °C.

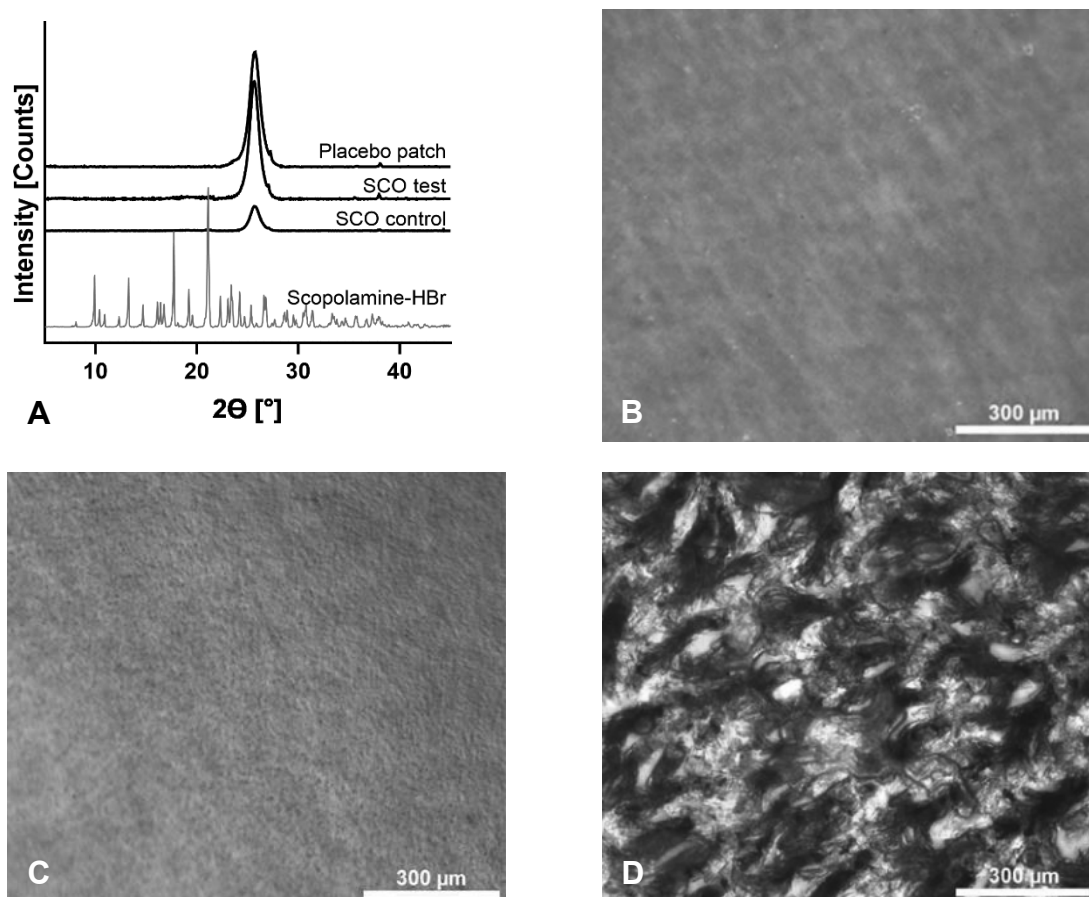


Figure 20. (A) XRD patterns of pure SCO and the prepared patches. The placebo patch was prepared without DMSO and drug-free (consisting of DT). (B) PLM pictures of the DMSO-free SCO control patch, (C) the IBU test patch and (D) the IBU control patch (magnification = 10x).

4. Results & Discussion

Table 6. DSC results of pure APIs, drug-free matrix, and the drug-containing control patches. Mean values \pm standard deviation.

Sample	T _M [°C]	T _G [°C]
IBU	76.5 \pm 0.57	- 44.5 \pm 1.51
SCO	200.1 \pm 0.36	64.0 \pm 0.59
ROT	96.6 \pm 0.07	6.3 \pm 0.02
DT (placebo patch)	-	- 48.2 \pm 1.10
IBU control	-	- 45.4 \pm 2.01
SCO control	-	- 47.0 \pm 0.07
ROT control	-	- 45.7 \pm 1.86

The adhesive properties of the prepared patches were characterized via probe tack testing. The required tensile stress to detach the probe from the adhesive matrices was between 0.08 – 0.27 N/mm². The obtained values were compared with the adhesive properties of a placebo patch, its matrix consisted solely of DT. **Figure 21** displays clear differences between the formulations. ROT test showed, compared to the placebo patch (0.16 N/mm²), a detaching force of 0.08 N/mm² and thus a significantly reduced adhesion. SCO control and IBU control were prepared without DMSO. For both formulations, a higher force (0.23 – 0.27 N/mm²) was necessary to remove the probe from the matrices, indicating a higher bonding strength. The adhesive properties of ROT control, SCO and IBU test (σ_{\max} : 0.19 N/mm², 0.17 N/mm², and 0.17 N/mm², resp.) were comparable to pure DT. In comparison, the control formulations without DMSO showed greater values for σ than the test formulations.

Regarding the adhesive properties of the patches, DMSO somehow exerted a plasticizing effect on the matrix material. For all formulations, the tack values of the controls were higher than the test matrices. The reduction of the adhesiveness was only significant for the patches containing ROT and DMSO. Due to fact, that all patches displayed sufficient adhesion, it was not characterized as a deficiency. Unfortunately, it was not possible to perform DSC measurements of the test matrices due to the evaporation of DMSO. Nevertheless, Song et al. have adequately proven that Duro-Tak® 87-2287 blended with various non-volatile chemical penetration enhancers (Span 80, N-methyl pyrrolidone, Azone and Isopropyl palmitate) resulted in a reduced T_G of the polymer [100]. The used PSA was

4. Results & Discussion

comparable to the currently used kind of DT, because it contained hydroxylic groups and lacked a crosslinker. The glass transition temperature of the mixtures was lowered by 10 -15 °C in comparison to pure PSA and was dependent on the amount of enhancer. Moreover, based on the reduced tackiness, one would expect a reduced T_G for the test formulations. This expectation is confirmed by a correlation between tackiness and T_G that had been investigated by Fujita et al., where the glass transition temperature of PSAs elevated with increasing amounts of tackifier [101]. Thus, the plasticising effect of DMSO led to a decrease in both, tackiness and glass transition temperature.

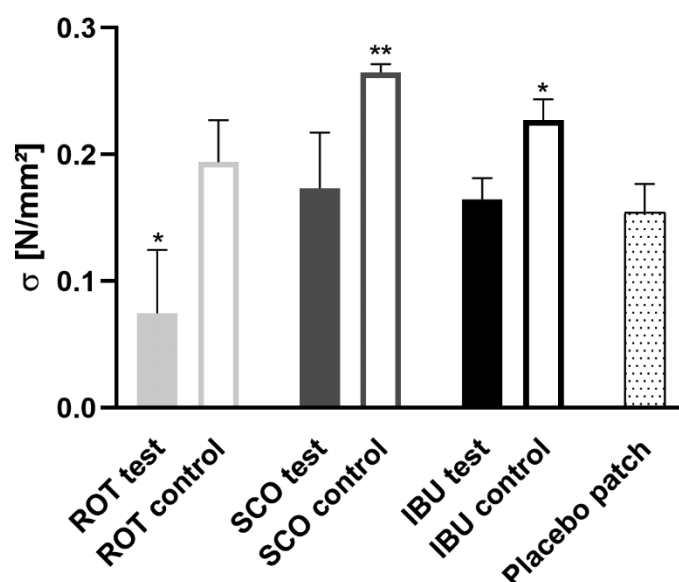


Figure 21. Probe tack results of the prepared DIA (test: with DMSO, control: without DMSO) compared to the adhesive properties of a placebo patch consisting solely of DT. * Indicates significant differences ($p < 0.05$) and ** indicates significant differences ($p < 0.01$) in comparison with the placebo patch.

4. Results & Discussion

4.2.2. Drug release

The release of the different drugs varied widely in released amount and curve shape. The mathematical expressions best-describing drug release were Weibull ($R^2 = 0.968 \pm 0.01$) and Korsmeyer-Peppas ($R^2 = 0.948 \pm 0.03$). Due to the slightly better R^2 -values, release curves were fitted according to Weibull but evaluated according to both.

The total drug amount had only been released for the patches containing IBU, whereas it was a significantly lower proportion for SCO and ROT. The by far highest drug solubility in the acceptor medium was determined for SCO, followed by IBU and ROT. However, the saturation concentrations were still many times higher than the concentrations measured during release and permeation experiments for all drug candidates.

For IBU, drug release in the initial phase was faster for the test patches. After 0.5 hours, 19 % was released from control patches, whereas the corresponding value for the test patches was 32 %. The fitting of the early release phase (< 60 %), according to Korsmeyer-Peppas, confirmed the observation with the corresponding release rates of $K_{KP}(\text{test}) = 0.54$ and $K_{KP}(\text{control}) = 0.35$ provided by **Table 7**.

Differences between test and control converged with proceeding release until after nine hours, when the whole amount was released from both formulations (**Figure 22A**). For IBU and ROT, there were no significant differences between the released drug amount of test and DMSO-free control patches, but doubtless between the SCO-formulations. After 28 hours, 7.3 % of the drug was released from the test patch containing DMSO, while the amount of released drug was for the control was significantly lower (3.6 ± 1.0 %). For SCO and ROT, the initial release was faster and displayed a decreasing slope with increasing time and, thus, a slowing down of drug release (**Figure 22B, C**).

4. Results & Discussion

Table 7. Model fitting parameters of the release profiles. * Due to the limited applicability of Korsmeier-Peppas, the corresponding release profiles were fitted for the initial 60 % of fractional drug release.

	Weibull		Korsmeier-Peppas		
	R ²	β	R ²	K _{KP}	n
IBU					
test	0.954	0.58 ± 0.11	0.972*	0.54 ± 0.07*	0.67 ± 0.08*
control	0.973	0.85 ± 0.17	0.977*	0.35 ± 0.03*	0.75 ± 0.05*
SCO					
test	0.909	0.46 ± 0.14	0.910	0.02 ± 0.01	0.42 ± 0.16
control	0.965	0.44 ± 0.03	0.965	0.01 ± 0.01	0.44 ± 0.03
ROT					
test	0.984	0.61 ± 0.18	0.957	0.06 ± 0.01	0.40 ± 0.11
control	0.984	0.92 ± 0.27	0.911	0.05 ± 0.02	0.58 ± 0.31

An important factor influencing drug release was the molecular volume (MV) of the drugs, as the diffusivity of molecules usually decreased with increasing molecular volume [102]. This may have explained the release results for IBU but not for SCO and ROT. Since the molecular size of ROT was bigger than SCO, it would have been reasonable to expect the lowest values for ROT, but this was not the case. Therefore, it should be further taken into consideration that the interaction between drug and matrix polymer may played an important role in this process, as Yasunori et al. had adequately described [22]. In this context, hydrogen bonds, ionic bonds, and dipole-dipole interactions between functional groups of drug and polymer played an important role as well. Hydrogen bonding was considered the main interaction between drug and PSA because Duro-Tak® 2510 possesses only hydroxylic groups as functional group. Liu et al. recently investigated the effect of different physicochemical properties (log P, pKa, melting point, molecular weight, molecular volume, polar surface area and drug solubility) on drug release for hydroxyl PSA [32]. They found a positive correlation between increased drug release and a low polar surface area, fully confirming the results mentioned above. The polar surface area represents the ability of a compound to form hydrogen bonds [103], therefore SCO and ROT formed more chemical bonds with the functional groups of the PSA than IBU and were stronger retained within the patch.

4. Results & Discussion

The by far highest value for K_{KP} in **Table 7** was obtained for the IBU test (0.54), followed by the distinctly reduced value of IBU control (0.35). The release constants for SCO and ROT were clearly lower and comparable for the corresponding test and control patches. In general, K_{KP} of ROT (0.05 - 0.06) was increased compared to SCO (0.0 - 0.02). The n-values for SCO and ROT were approximately 0.5 and indicated a fickian diffusion, whereas the values for IBU ranged between 0.6 and 0.8, which supports a non-fickian release mechanism. For all formulations, the β -values were below 1. The plot of K_{KP} vs. polar surface area in **Figure 22D** illustrates the dependency of drug release from the polar surface area of the drug molecules. Here, the release constants increased with decreasing polar area, indicating a reciprocal relationship.

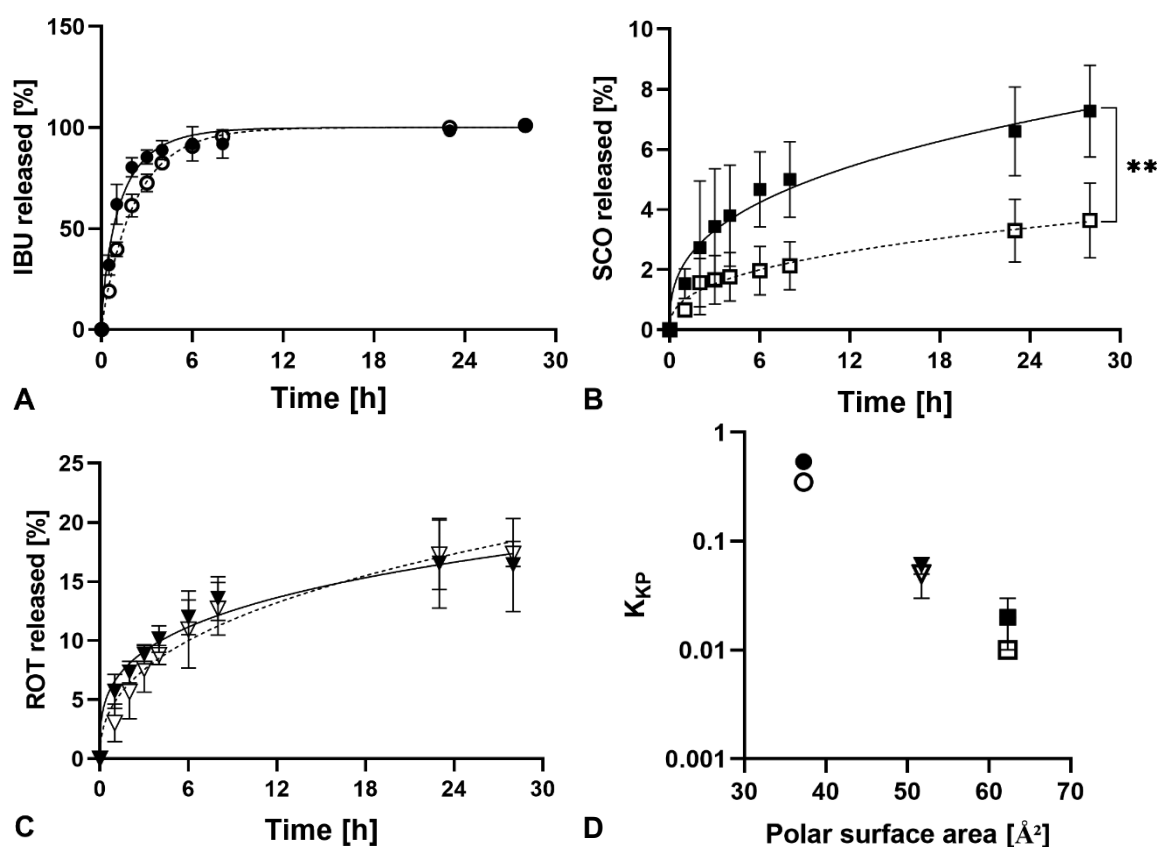


Figure 22. In vitro release profiles of (A) Ibuprofen, (B) Scopolamine and (C) Rotigotine in phosphate buffered saline (PBS, pH 7.4) at 32 °C. (D) Relationship between drug release constant (K_{KP}) and polar surface area ($R^2 > 0.9$). Filled symbols with solid line represent test patches (with DMSO), unfilled symbols with dotted line label control patches (without DMSO). ** indicates significant differences ($p < 0.01$).

4. Results & Discussion

Fitting of the release data according to Korsmeyer-Peppas and Weibull pointed towards a pure fickian release mechanism for SCO and ROT but indicated a non-fickian (anomalous) transport for IBU. While fickian diffusion is controlled by thermodynamic forces, the anomalous transport can rely on complex factors such as swelling, erosion, polymer relaxation processes, and functional interactions between the drug and matrix of the device [104]–[106]. Here, the described electrostatic drug-polymer-interactions should be considered. Presumably, the altered release mechanism of IBU did not rely on the swelling or erosion of the polymer, because Duro-Tak® is a non-swellaable and non-biodegradable polymer. However, it is more likely that the reduced interaction of IBU with the polymer increased the mobility of the drug molecules within the patch and thus facilitated a faster drug release. Nevertheless, to facilitate therapeutically effective skin permeation rates for long-term drug administration, a sufficient and controlled release capacity of the matrix polymer should exist. For drugs with carboxylic groups like Ibuprofen, stronger retention and, thus, controlled release over a longer time period could be achieved with a different and more retaining matrix polymer.

4. Results & Discussion

4.2.3. Permeation behavior

Permeation profiles of the patches containing IBU are shown in **Figure 23A**. There were no significant differences between the IBU test ($J_{ss} = 13 \pm 0.5 \mu\text{g}\cdot\text{cm}^{-2}\cdot\text{h}^{-1}$) and IBU control ($J_{ss} = 14 \pm 1.5 \mu\text{g}\cdot\text{cm}^{-2}\cdot\text{h}^{-1}$) regarding flux or permeated amount of drug. Within 24 hours, the mean permeated dose for the test formulation was $266 \pm 15 \mu\text{g}$ and $285 \pm 30 \mu\text{g}$ for the DMSO-free patches. The lag time was for both formulations 2 hours. In general, the resulting permeation profiles revealed no significant differences between test and control.

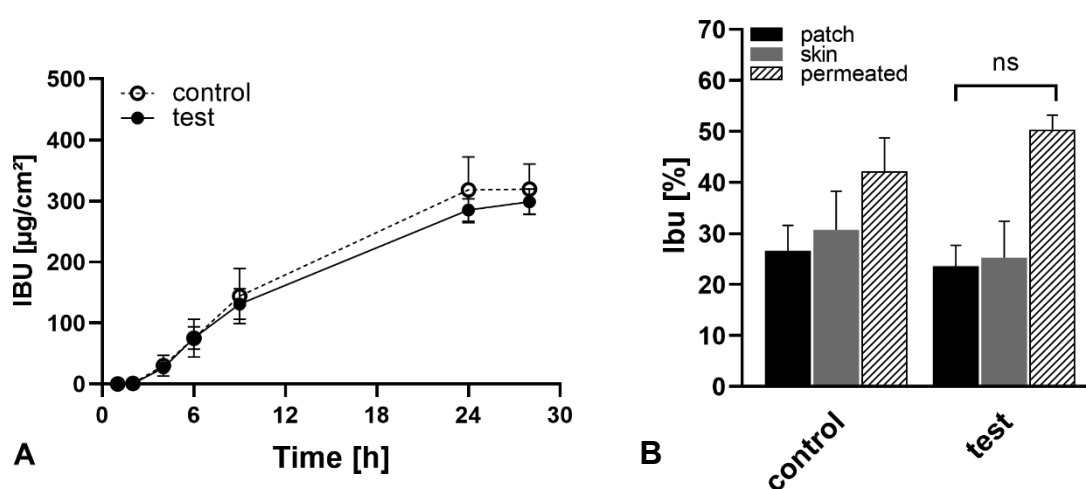


Figure 23. (A) Permeation of Ibuprofen from patches containing IBU prepared without DMSO (control) and with DMSO (test). (B) Distribution of Ibuprofen after 28 h permeation experiments in skin and patch and through permeation into the acceptor compartment of Franz cells. “ns” indicates non-significant differences.

The slope of the curves dropped after 24 hours. This may be an indicator that the constant ‘steady-state’ permeation stopped. Drug partitioning between patch, skin, and acceptor compartment after the permeation experiments is displayed in **Figure 23B**. The distribution was comparable for the test and control, and the recovery rate for all experiments was $99 \pm 2 \%$. Interestingly, a major part of the applied drug was found in the receptor compartment; more specifically, it permeated through the skin. This is the opposite of the drug distribution of SCO (**Figure 24B**), ROT (**Figure 25B**), and E2 (**Figure 16**), where only a small drug fraction permeated and the main part still remained in the patch after the permeation experiment. This observation explains the dropping of the slope after 24 hours: due to the large amount of drug permeated through the skin, the concentration within the patch reduced drastically over time. The concentration in turn is the main driving force for the drug permeation because it is driven by the concentration gradient between the donor and acceptor

4. Results & Discussion

compartment. Therefore, reducing this gradient caused the decreased permeation of IBU towards the end of the permeation experiment.

In contrast to the permeation of IBU test and control, the presence of DMSO caused a significant enhancement for SCO (Figure 24A). The test patches revealed mean flux values of $J_{ss} = 2.56 \pm 0.4 \mu\text{g}\cdot\text{cm}^{-2}\cdot\text{h}^{-1}$, more than 1.5 times higher than the control ($J_{ss} = 1.50 \pm 0.1 \mu\text{g}\cdot\text{cm}^{-2}\cdot\text{h}^{-1}$). For both formulations, the lag time was less than one hour. The mean permeated dose was $37 \pm 3 \mu\text{g}/24 \text{ h}$ for the control and $61 \pm 7 \mu\text{g}/24 \text{ h}$ for the test formulation. The permeated amount of SCO comprised hereby about ~ 20 % of the corresponding permeated amount of IBU test and control. However, the values are roughly similar to the obtained values for the permeation of E2 in chapter 4.1.2. The E2 patch prepared with DMSO (35 °C 3h) provided 82 $\mu\text{g}/24\text{h}$ and the DMSO-free patch (50°C 24 h) 26 $\mu\text{g}/24 \text{ h}$.

Due to the more significant amount of SCO permeated from the test formulations, the resulting proportion of drug left in the test patch after the permeation experiments was lower than for the control patch: the test patch contained 70 % SCO and the control patch 85 % (Figure 24B). The determined amount of drug in the skin was 7.5 % for the test patches and 5.0 % for the control. The

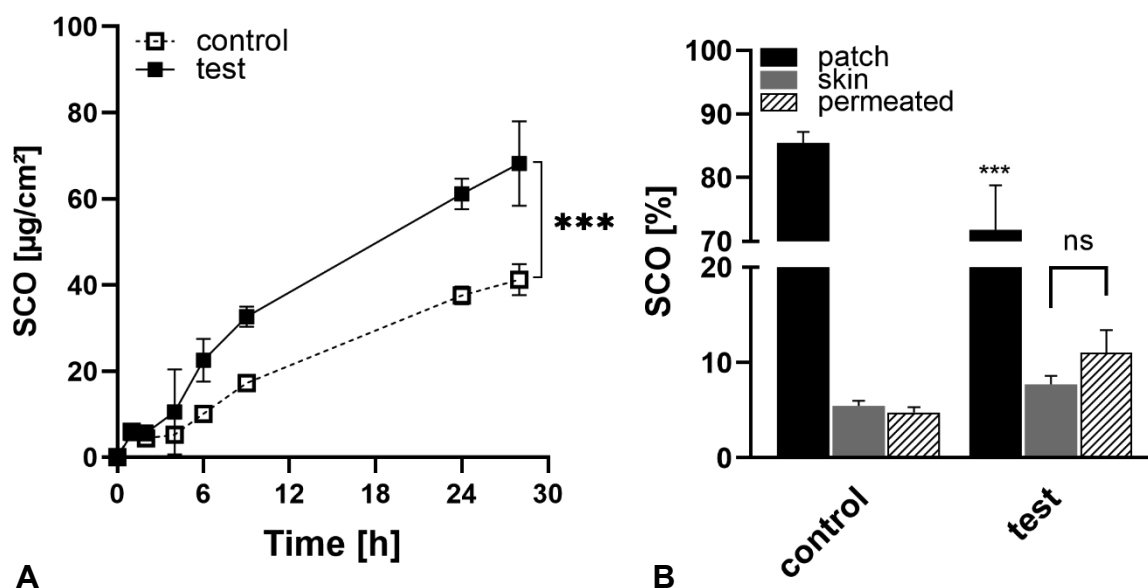


Figure 24. (A) Permeation of SCO from patches prepared without DMSO (control) and with DMSO (test). (B) Distribution of SCO after 28 h permeation experiments in skin and patch and through permeation into the acceptor compartment of Franz cells. *** Indicates significant differences ($p < 0.001$), “ns” indicates non-significant differences.

4. Results & Discussion

percentual amount of SCO found in the skin was only a quarter of the amount of IBU in the skin. After the permeation experiments, the drug recovery rate was $105 \pm 3 \%$ for both, test, and control formulations.

The most remarkable feature of the ROT permeation profiles presented in **Figure 25A** was the large lag time of nine hours for both, control, and test patches. After nine hours, constant drug inflow was detectable in the acceptor compartment. The resulting flux values ($J_{ss}(\text{control}) = 8.9 \pm 1.4 \mu\text{g}\cdot\text{cm}^{-2}\cdot\text{h}^{-1}$, $J_{ss}(\text{test}) = 8.3 \pm 1.8 \mu\text{g}\cdot\text{cm}^{-2}\cdot\text{h}^{-1}$), as well as the mean permeated dose (control: $137 \pm 33 \mu\text{g}/24 \text{ h}$, test: $132 \pm 22 \mu\text{g}/24 \text{ h}$), were comparable. In contrast to IBU, the permeated drug amount and flux values were 4 - 6 times lower. Despite the large lag-time, the permeated amount of ROT was still 5 - 6 times more than SCO.

The partitioning after the permeation experiments was quite similar for test and control. The permeated amount for both formulations was about 20 %, and 60 % remained in the patch. The amount of ROT in the skin was 20 %, which was similar for IBU. The recovery rate for ROT was $103 \pm 2 \%$.

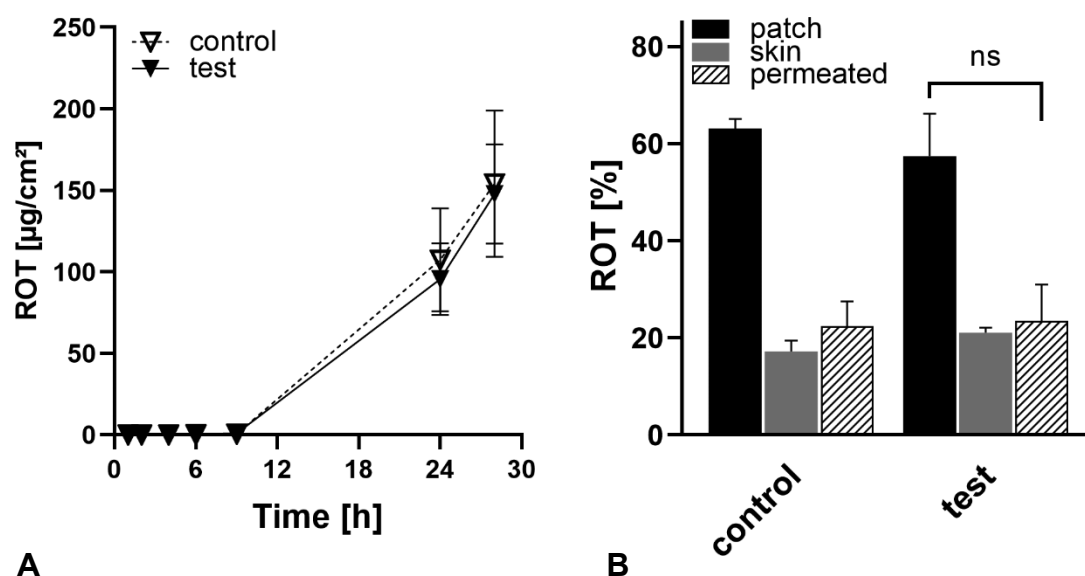


Figure 25. (A) Permeation of ROT from patches prepared without DMSO (control) and with DMSO (test). (B) Distribution of ROT after 28 h permeation experiments in skin and patch and through permeation into the acceptor compartment of franz cells. "ns" indicates non-significant differences.

4. Results & Discussion

Table 8. Flux values, lag- time, mean permeated dose, and fractional rate control of the prepared patches. Values represent mean \pm SD.

	Ibuprofen		Scopolamine		Rotigotine	
	Test	Control	Test	Control	Test	control
J_{ss} [$\mu\text{g}\cdot\text{cm}^{-2}\cdot\text{h}^{-1}$]	12.9 \pm 0.5	14.4 \pm 1.5	2.6 \pm 0.4	1.5 \pm 0.1	8.3 \pm 1.8	9.0 \pm 1.4
Lag-time [h]	1	2	0	0	4	6
Mean permeated dose [$\mu\text{g}/24$ h]	266 \pm 15	285 \pm 30	36.8 \pm 2.6	60.8 \pm 7.1	131.7 \pm 22.1	137.4 \pm 32.7
F_D	0.6	0.4	1.0	1.0	1.0	1.0

The values of the fractional rate control (F_D) displayed in **Table 8** indicated a device-controlled drug delivery ($F_D < 1$), whereas the process was controlled by the skin for both, Scopolamine and Rotigotine ($F_D = 1$). To put it in another way, the amount of permeated Ibuprofen was smaller than the amount of drug released and for both other drugs, the amounts of permeated and released drug were equally large. In combination with the results of the release experiments, it becomes clear that the skin controlled the delivery of IBU, and for SCO and ROT, the process was controlled by the drug release from the patch. DMSO enhanced the permeation of SCO but did not affect the permeation of the other drugs. Since the drug delivery of SCO was exclusively controlled by the release process the, the possibility of DMSO acting as a skin permeation enhancer was ruled out. Moreover, drug partitioning after the permeation experiments did not change in the presence of DMSO. Drug permeation was again inversely proportional to the surface area because the highest amounts of permeated drug were obtained for Ibuprofen, followed by Rotigotine and Scopolamine, resp.

4. Results & Discussion

Interestingly, the presence of DMSO led to an enhanced release of SCO but did not affect the release behaviour of the other drugs. It is conceivable that DMSO interacted with a certain number of the polar functional groups of the PSA by forming hydrogen bonds. Thus, OH-groups of the polymer were occupied and no longer available to interact with the polar groups of the drug molecules. Since Scopolamine offers the largest polar surface area of the tested drugs, the highest number of potential matrix-drug-interactions should be expected here as well. The reduction of the possible binding sites could have therefore sufficiently reduced the interaction of SCO with the polymer and facilitated a faster drug release. A similar behaviour between enhancer substance and acrylic PSA was reported for Span 80 and Duro-Tak® 2287. Span 80 formed hydrogen bonds with the hydroxylic groups of the PSA, and thus, the interaction between drug and adhesive was reduced, which improved the release of Bisoprolol tartrate [100].

4.3. Investigation of stabilization issues in DMSO-containing transdermal patches

The patches described in chapter four were analysed via GC to determine the residual amount of DMSO and via XRPD to confirm the absence of any crystals after different storage times. A further method to investigate the patches was the microscopic examination, which might reveal structural changes within the matrix. Therefore, a batch of patches containing E2 and DMSO was produced according to chapter four (drying conditions: 35 °C, 3h) and stored sealed at accelerated conditions (40 °C ± 2 °C/75% RH) for three months. The pictures were taken subsequently after production revealed transparent and crystal-free matrices (**Figure 26**). After two months, drop-like structures occurred (< 0.5 mm) within the adhesive layer that increased distinctly in size after three months. Partially, drops with a size larger than 1 mm were found. Patches were screened for crystals and their absence was confirmed for all samples. On closer inspection, tiny droplets adhered at the release liner after peeling it off from the DIA, which was stored for three months. In summary, the observed phenomenon indicated the coalescence of finely distributed DMSO-droplets during storage. With progressing time, the built drops merged and supported the continuous formation of bigger drops.

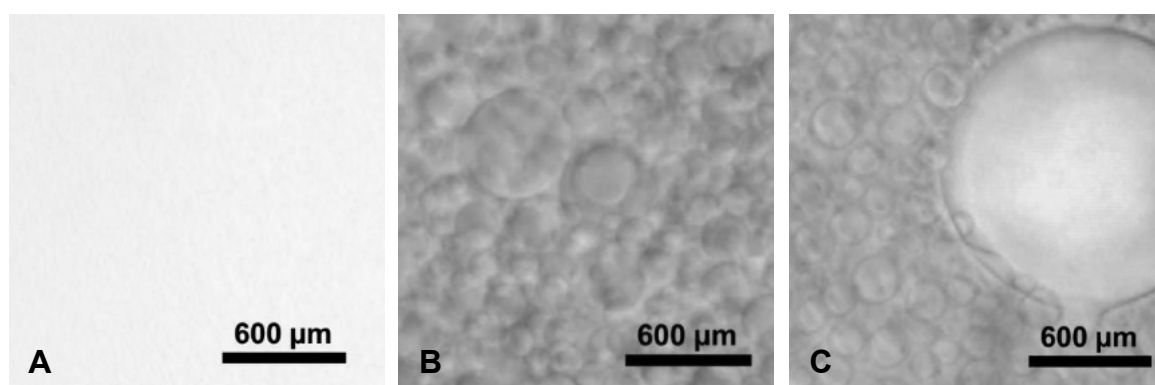


Figure 26. PLM-pictures of the patches containing DMSO (A) subsequently after drying at 35 °C, 3 h (B) after two months and (C) after three months of storage at 40 °C.

4. Results & Discussion

Coalescence is usually a well-known stability issue regarding emulsions. They are dispersed systems consisting of non-miscible liquids. The energy input, which is necessary to homogenize the components, is added to the system in the form of stirring. Emulsions are thermodynamically unstable systems; after homogenisation, the drops of the inner phase tend to merge, and eventually phase separation of the components occurs [107]. The described mechanism is applicable for the patches as well: Duro-Tak® is a hydrophobic polymer and non-miscible with neither water nor the hydrophilic substance DMSO. Therefore, the homogenization of the patch components during the production resulted in a homogeneous dispersion of DMSO in the polymer. After the drying step, DMSO was still liquid, but the polymer on the contrary was in a solid-state due to the evaporation of hexane and ethyl acetate. Hence, DMSO was at that time distributed in a solid, hydrophobic matrix. During storage, the flexibility of Duro-Tak® favoured the molecular mobility of the incorporated substances, DMSO and Estradiol. Additionally, DMSO exerted a plasticizing effect on the polymer, which was confirmed by the results of the probe tack testing in **Figure 21**: for all drugs, the tackiness of the patches containing DMSO was significantly reduced compared to the DMSO-free control patches.

For emulsions, stabilization can be achieved by adding an emulsifier that reduces the interfacial tension between the immiscible, liquid phases and increases the kinetic stability of the system. Nevertheless, in the present case, the use of hazardous surfactants could have caused detrimental effects on the skin due to the direct and long-term application of a transdermal patch.

The main stability problem in the first place was the mobility of DMSO within the matrix. This problem could have been solved by increasing the viscosity of the polymer matrix according to Stokes' law; therefore, the velocity of the dispersed components would have been decreased. Of course, this would have affected the mobility of the drug as well. According to Patel et al., the diffusion within and the release of a drug from a non-degradable polymer depends on the viscosity of the polymer; with increasing viscosity the diffusion coefficient, the release rate constant and the percentage drug release decreased [101]. Thus, increasing the viscosity of the matrix would have had a negative impact on drug release and permeation. Further approaches, according to Stokes', might be the alignment of the density of DMSO and Duro-Tak® and the reduction of the droplet size of the dispersed DMSO. The first approach was found to be not applicable because the density of the dried polymer was neither known nor adjustable. The size of the DMSO droplets could have been further

4. Results & Discussion

decreased by homogenization methods with a higher energy input. But in the following production step, the drying process, the evaporation of the solvents ethyl acetate and hexane caused a shrinking of the adhesive mass; thus, the dispersed droplets of DMSO moved again closer together. Therefore, a solution for the stability problem is to prevent the drop convergence.

Another well-known way to stabilize emulsion is via solid particles; those emulsions are called Pickering emulsions. Here, small solid particles adsorb onto the interface between the immiscible phases and prevent the droplets from coalescing by acting as a flexible but robust colloidal barrier [109]. This approach offers the advantages of maintaining the viscosity of the system, as well as the addition of an indifferent excipient that would not alter the drug permeation. The idea for the coalescing issues was that fine, solid particles could adsorb DMSO and inhibit the coalescence of occurring droplets on the condition that the release of the drug and the enhancer was not altered. Thus, a chemically indifferent substance was required, with a large surface area and a small particle size to ensure a homogeneous distribution within the thin matrix layer. Further, the migration of the stabilizing excipient within the flexible matrix should be low or rather inhibited.

Many authors reported on successfully stabilizing emulsions with silica particles over the past decades [110]–[113]. Those silica-based emulsions offered the advantage of enhanced stability, compared to classical emulsions stabilized by emulsifiers, and the absence of irritating surfactants [114]. Various silica micro- and nanoparticles with different particle sizes, particle geometries and different adsorbing properties were therefore chosen as test candidates for the stabilization of the DMSO-containing patches. Here, the idea was to form a system similar to the beforementioned emulsions with small particles on the one hand and to use the great adsorbing properties of the particles to reduce the bridging between DMSO-drops on the other.

4. Results & Discussion

4.3.1. Preliminary excipient evaluation

Different silica particles with adsorbing attributes were tested for their processability in patch manufacturing and their impact on the adhesive properties of the drug-containing matrix. The first step was to determine the adsorbing properties, more specifically the maximum amount of excipient per 1 g DMSO (c_{\max}) that still led to a fluid mixture. The determined c_{\max} values of the applicable candidates displayed in **Table 9** were between 50 and 500 mg/g DMSO. The maximum concentrations of the silica excipients were limited by total solvent absorption or gel formation. With exceeding the c_{\max} for Aeropearl® 300, Florite® PS-10 and PS-200, FujiSil™, Neusilin®, Parateck® and both grades of Syloid®, DMSO was absorbed. A pasty mass was formed, unsuitable for further processing. For Aerosil®, exceeding the concentration of 50 mg/g DMSO led to the formation of a viscous DMSO-gel. The resulting high viscosity excluded the mixtures with higher concentrations from further experiments. Except for Aerosil® and Neusilin®, the obtained suspensions showed particle deposition and the formation of non-redispersible sediments within five minutes (**Figure 27**). This phenomenon could appear during the casting and/or drying process and therefore affect the required uniformity of the mixture and eventually the drug product. The corresponding excipients were therefore excluded from the list of experiments.

Table 9. Evaluation of the physical mixtures of excipients and DMSO. c_{\max} describes the maximum amount of excipient/1g DMSO that led to a liquid suspension with appropriate fluid properties for further processing. Sedimentation was affirmed when the particles deposited within five minutes.

Excipient	c_{\max} (mg/g DMSO)	Appearance	Sedimentation	Mean particle size ¹
A Aeropearl® 300	100	clear	yes	30 μm
B Aerosil® 300	50	clear	no	7 nm
C Florite® PS-10	100	milky	yes	10 μm
D Florite® PS-200	75	turbid	yes	150 μm
E FujiSil™	100	turbid	yes	80 μm
F Parateck® SLC 500	500	turbid	yes	60 – 120 μm
G Neusilin®	200	clear	no	5 – 20 μm
H Syloid® 244 FP	200	clear	yes	3.5 μm
I Syloid® AI-1FP	400	turbid	yes	10 μm

¹ according to supplier specifications, see chapter 3.1

4. Results & Discussion

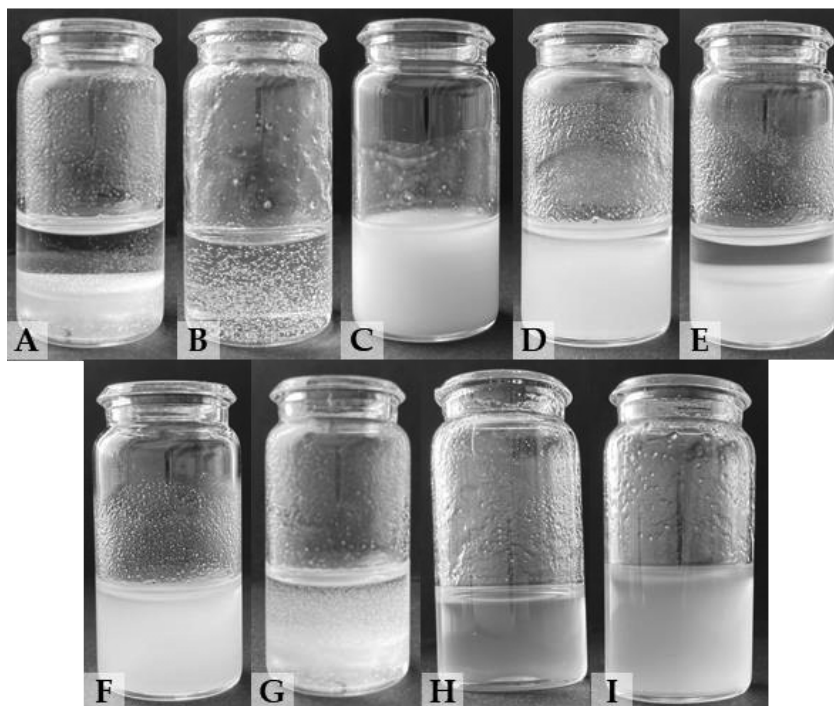


Figure 27. Appearance of the prepared DMSO – Excipient mixtures: **A** DMSO + Aeropearl® 300, **B** DMSO + Aerosil® 300, **C** DMSO + Florite® PS-10, **D** DMSO + Florite® PS-200, **E** DMSO + FujiSil™, **F** DMSO + Parateck® SLC 500, **G** DMSO + Neusilin®, **H** DMSO + Syloid® 244 FP, **I** DMSO + Syloid® AI-1FP

The next step was to investigate whether the remaining excipients affected, i.e., accelerated or slowed down the evaporation of DMSO. Therefore, pure DMSO and mixtures of DMSO with different amounts of excipients were dried at 40 °C without ventilation and monitored gravimetrically for three hours. **Figure 28** displays the results of pure DMSO compared to four blends of Aerosil® in DMSO, and three blends of Neusilin® in DMSO.

Within one hour, the loss on DMSO for all samples ranged between two and three percent and was therefore comparable. Significant differences occurred from two hours on, especially between pure DMSO and the Neusilin®-blends. Solvent evaporation was strongly increased for all concentrations (50 – 200 mg/g). In the case of pure DMSO, 71 % of the initial mass was still present after three hours, whereas the blends with Neusilin® offered only 58 – 66 %.

4. Results & Discussion

The observations for the Aerosil®-DMSO blends were quite promising. Especially for the blend with 25 mg/g, solvent evaporation was comparable to the values of the pure solvent throughout the entire test period. After three hours, the blends containing 5 and 10 mg/g offered comparable amounts of DMSO as well, but the mixture with 50 mg/g showed a significant difference. Based on these results, Aerosil® was chosen as stabilizing patch additive.

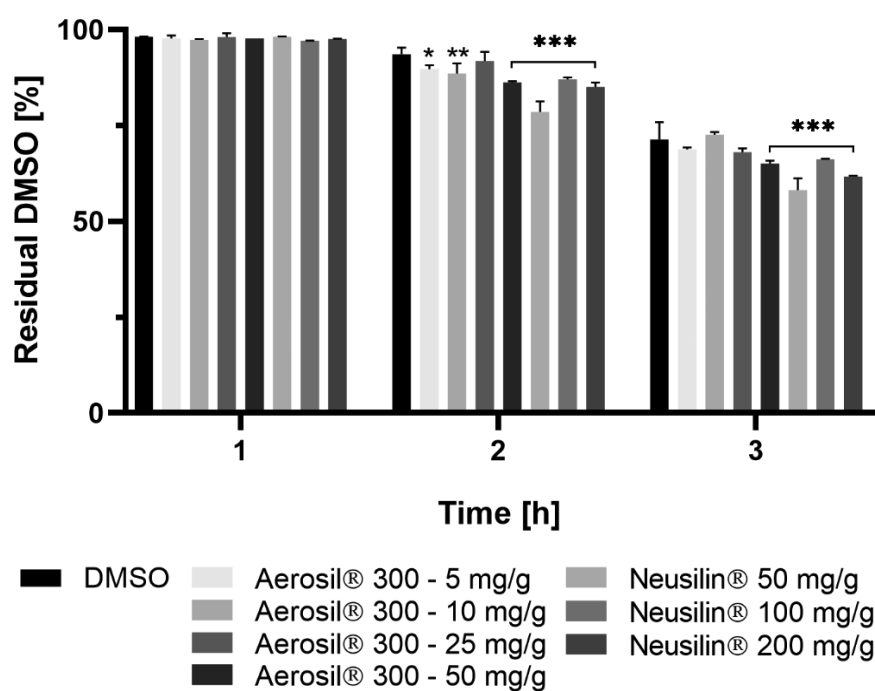


Figure 28. Comparison of the evaporation of pure DMSO and blends of DMSO and excipients. The resulting concentration is given in amount of excipient [mg] per DMSO [g]. Drying was performed at 40 °C and monitored gravimetrically. * Indicates significant differences ($p < 0.05$), ** indicates significant differences ($p < 0.01$) and *** indicates significant differences ($p < 0.001$) compared to DMSO.

4. Results & Discussion

4.3.2. Patch preparation and characterization

Following the preliminary experiments, DIA with increasing amounts of Aerosil were prepared according to chapter 4.1, whereby drying was performed at 35 °C for three hours. Subsequently, the patches were tested for the residual solvents EA and hexane, as well as the amount of DMSO. For all tested formulations, EA and hexane were not detectable via GC. The amount of DMSO after drying is displayed in **Figure 29**. Patches produced without Aerosil comprised about nine mg of DMSO/patch, the formulations prepared with silica in the range from five to 20 mg/g DMSO showed comparable residuals. Exceeding the limit of 20 mg/g DMSO led to a concentration-dependent decreased DMSO-value per patch, through to a value of < 5mg TC/patch from an amount of 25 mg Aerosil®/patch. All formulations were transparent, the microscopic investigation confirmed the absence of any droplets and crystals.

The formulation with the highest amount of silica that was incorporable without altering the amount of enhancer per patch, 20 mg/g DMSO, was chosen to be tested regarding permeation and stability. The resulting amount of DMSO/ patch was 9.8 mg.

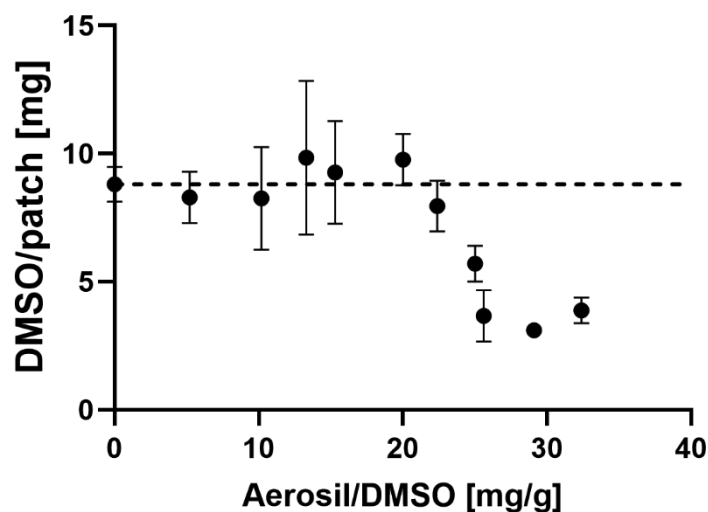


Figure 29. Influence of different amounts of Aerosil/DMSO in the initial mixture (0 - 32 mg/g) on the DMSO content after drying. Patches were dried at 35 °C for 3 h, monitoring was performed via GC.

4. Results & Discussion

4.3.3. Permeation studies & stability evaluation

Regarding drug permeation, the incorporation of silica particles surprisingly improved the transdermal transport. **Figure 30D** compares the resulting flux values of freshly prepared patches ($t = 0$) with and without Aerosil®, whereby the flux values of the silica patches ($J_{ss} = 4.8 \pm 0.9 \mu\text{g}\cdot\text{cm}^{-2}\cdot\text{h}^{-1}$) were significantly higher than those of the silica-free patches ($J_{ss} = 3.2 \pm 0.1 \mu\text{g}\cdot\text{cm}^{-2}\cdot\text{h}^{-1}$). This observation may be explained by the fact that silica particles were found to penetrate the upper layers of the SC [115]. It may be hypothesized that E2 could have been transported into the skin through adsorption onto the silica particles.

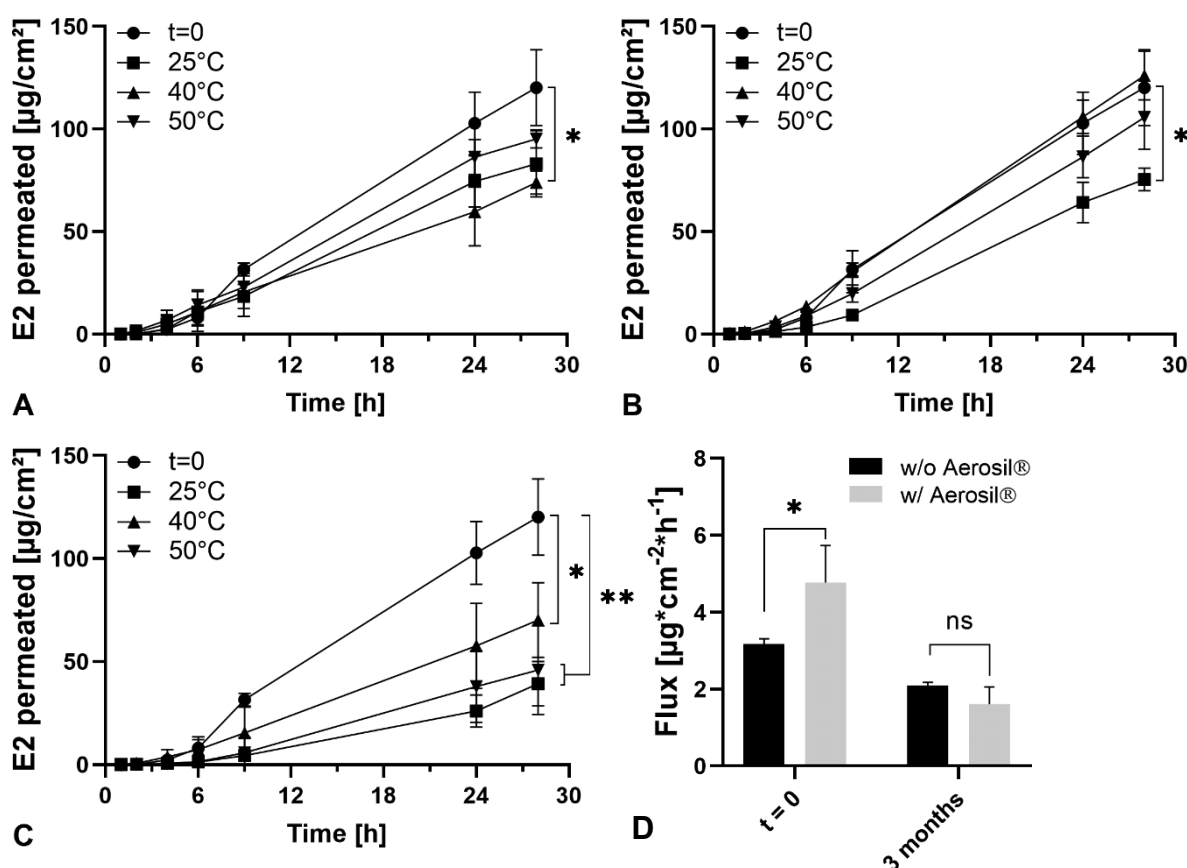


Figure 30. E2 permeation after one month (A), two months (B), and three months (C) of storage. The resulting curves were compared to the permeation of freshly prepared patches ($t = 0$). Samples were stored in sealed containers at 25 °C, 40 °C and 50 °C. (D) Flux-values of patches without (w/o) and with (w/) Aerosil® immediately after production ($t = 0$) and after three months of storage at 40 °C. * Indicates significant differences ($p < 0.05$) and ** indicates significant differences ($p < 0.01$) and “ns” indicates non-significant differences.

4. Results & Discussion

The permeation results of the patches stored for one month revealed significant differences for the accelerated storage conditions (40 °C/75% RH); after 28 hours, the permeated drug amounts of the other samples were statistically comparable to the values of the currently produced DIA (**Figure 30A**). Patches stored for two months offered drug values comparable to $t = 0$, except for the samples stored at long-term conditions (25 °C/60 % RH), where the permeation decreased significantly (**Figure 30B**). After three months of storage, the permeated amounts of E2 decreased for all formulations. According to **Figure 30C**, the lowest drug amounts permeated from the patches stored at 25 °C (45.9 $\mu\text{g}/\text{cm}^2$) and 50 °C (39.4 $\mu\text{g}/\text{cm}^2$). All values obtained were significantly lower than the initial value obtained subsequently after the production ($t = 0$, 120.1 $\mu\text{g}/\text{cm}^2$).

Initially, the transdermal transport of the patches containing Aerosil® was significantly enhanced, but after three months of storage, the flux values of the patches containing silica (1.6 \pm 0.4 $\mu\text{g}\cdot\text{cm}^{-2}\cdot\text{h}^{-1}$) aligned with the values of the silica-free formulations (2.1 \pm 0.1 $\mu\text{g}\cdot\text{cm}^{-2}\cdot\text{h}^{-1}$, **Figure 30D**). Hence, after storage in sealed containers at accelerated conditions, there was no longer any difference between the permeation behaviour of the formulations.

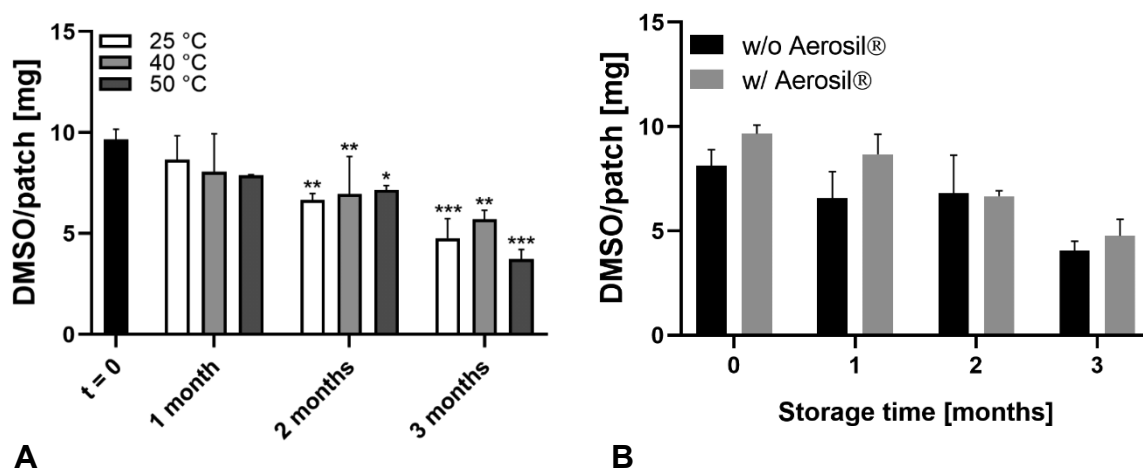


Figure 31. (A) DMSO-content of the silica patches at different storage conditions (25 °C, 40 °C and 50 °C) over a period of three months. * Indicates significant differences ($p < 0.05$), ** indicates significant differences ($p < 0.01$) and *** indicates significant differences ($p < 0.001$) compared to $t = 0$. (B) Comparison of patch stability after three months of storage at 25 °C.

4. Results & Discussion

Figure 31A displays the stability evaluation of the DMSO-content over a period of three months at different conditions (25 °C, 40 °C, 50 °C). The initial value was 9.9 mg DMSO/patch; comparable values were still detectable after one month of storage for the stabilized formulations. For the patches without Aerosil®, the initial value ($t=0$) was 8.13 mg DMSO/patch; therefore, the residual value after one month of storage was not significantly reduced. The first significant changes occurred after two months of storage, where the DMSO-content for all patches visibly decreased. After three months, the detected amount of enhancer sank further below half of the initial value for 25 °C (4.8 mg/patch) and 50 °C (3.7 mg/patch). The highest values were obtained for the samples stored at 40 °C, where 5.7 mg/patch were left. In summary, the patches stored at 40 °C offered the highest drug permeation values and the largest amounts of enhancer per patch after a storage time of three months. Although the amount of DMSO decreased significantly after the storage period, the corresponding transdermal drug transport was lower as well, but those values were not found to be statistically significant. Compared to the non-stabilized patches, the observed changes during storage were the same. Regarding the DMSO-loss during storage, the presence of Aerosil® resulted in a slightly increased remaining amount of DMSO compared to the stabilizer-free patches. The differences between the patches are displayed in **Figure 31B**. After a storage period of three months the stabilized patches still contained 4.8 mg, whereas the control (w/o Aerosil®) showed 4.1 mg, but the difference was not found to be statistically significant ($p > 0.05$). Therefore, the method of stabilization needs further improvement.

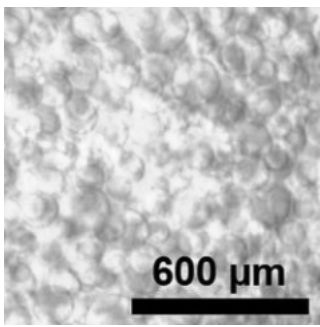
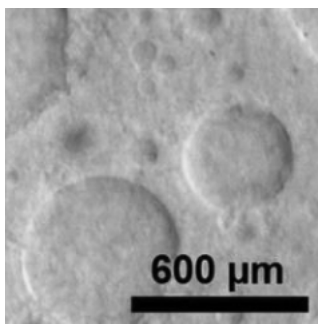
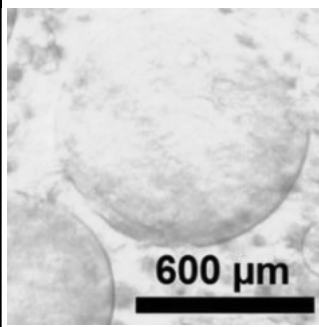
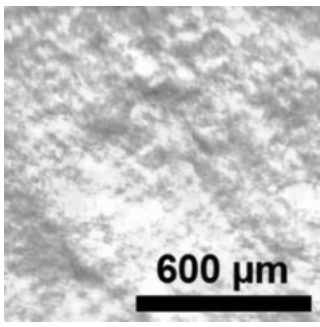
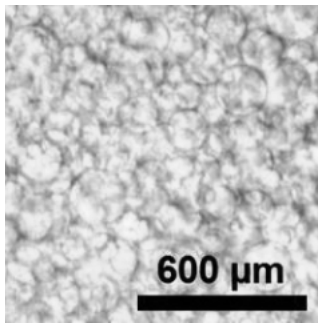
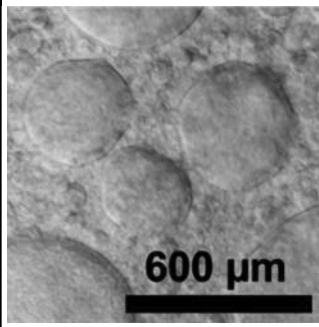
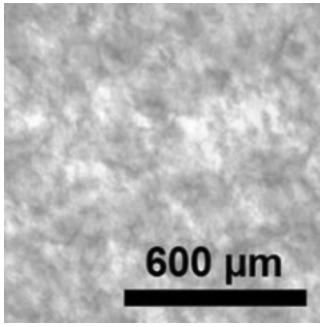
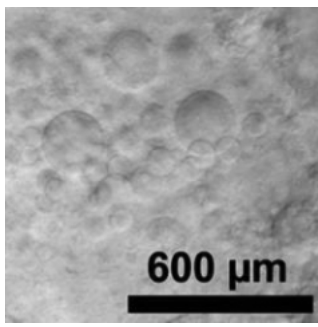
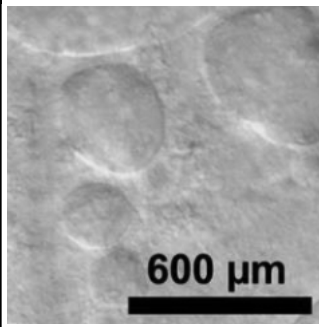
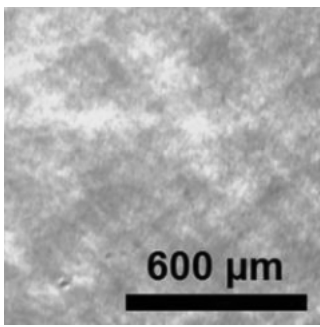
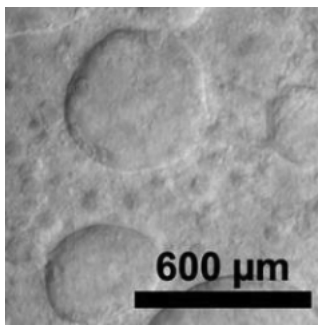
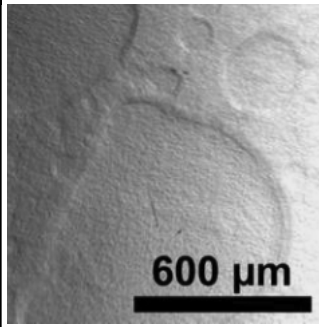
The results of the microscopic evaluation of the stability samples are displayed in **Table 10**. Patches prepared without Aerosil® displayed drop-formation after even one month of storage at 25 °C, whereas the patches containing silica as stabilizer were droplet-free after one month of storage at intermediate (25 °C), accelerated (40 °C) and stress test conditions (50 °C). The absence of crystals at this time was confirmed as well. Unfortunately, the formation of droplets was only delayed for the silica-patches and the formation of those structures was extended by one month. Hereby, the samples stored at 25 °C showed the smallest drop diameters over a period of three months. The samples stored at 40 °C and 50 °C displayed a stronger formation of drops, and the coalescence of small drops led to more prominent structures with diameters > 2 mm after three months of storage.

4. Results & Discussion

The silica-containing samples stored at 25 °C showed, in comparison to the silica-free patches, over the storage period a significantly smaller droplet size: after one month, the average diameter determined for the silica-free patches was $115.1 \pm 35 \mu\text{m}$, the silica patches were droplet-free. After two months of storage, the non-silica patches exhibited an average diameter of $205.1 \pm 171 \mu\text{m}$, whereas the patches containing stabilizer offered a diameter of $121.1 \pm 33 \mu\text{m}$. The standard deviation of the non-stabilized TTP was significantly higher, because the measured droplet sizes ranged between $53 \mu\text{m}$ and $540 \mu\text{m}$, while the measured values of the stabilized samples were between $55 \mu\text{m}$ and $198 \mu\text{m}$. After a storage period of three months, the non-stabilized TTP exhibited only a few (five), but large drops with diameters ranging between $83 \mu\text{m}$ and $904 \mu\text{m}$. On the contrary, the number of drops for the stabilized samples was larger (22), but the drops were smaller and ranged between $34 \mu\text{m}$ and $580 \mu\text{m}$.

4. Results & Discussion

Table 10. Microscopic evaluation of the stability samples stored for one, two, and three months. Patches without Aerosil® (storage at 25 °C) were compared to patches containing 20 mg Aerosil® as stabilizer stored at different conditions (25 °C, 40 °C, and 50 °C).

	1 Month	2 Months	3 Months
0 mg Aerosil, 25 °C			
20 mg Aerosil, 25 °C			
20 mg Aerosil, 40 °C			
20 mg Aerosil, 50 °C			

4. Results & Discussion

The physicochemical properties of Aerosil® 300 may explain the poor stabilizing performance of the chosen excipient. The powder with an average particle size of seven nm consists solely of silicon dioxide (> 99.8 %), is not chemically modified and therefore very hydrophilic [116]. According to Binks et al., it was not only important to create a rigid barrier with colloidal, solid particles to stabilize an emulsion against coalescence. Further, it was important that the solid particles at the oil-water interface were partially immersed in hydrophobic and hydrophilic phases. Due to their contact angle, hydrophilic particles (contact angle < 90 °) tend to align towards the hydrophilic phase of an emulsion, whereas hydrophobic substances (contact angle > 90 °) align towards the lipophilic components. The orientation of the particles caused, for hydrophilic particles, a larger fraction of the particle surface in the aqueous phase [117]. Imagining the particle barrier as a monolayer between the two immiscible phases, the monolayer would be curve-shaped due to the 'wettability' of the spherical particles and bend to surround a lipophilic droplet, forming an oil-in-water (o/w) emulsion [114]. But in the present study, the dispersed phase was the hydrophilic substance DMSO surrounded by a hydrophobic matrix. Thus, the dispersed system was a water-in-oil (w/o) emulsion. Therefore, the stability may be improved by replacing the hydrophilic Aerosil® with a hydrophobic equivalent.

Promising results were reported by Frelichowska et al., who successfully stabilized a w/o emulsion containing caffeine with hydrophobized silica. The substance was hydrophobized via surface modification with dimethyl silyl groups. Additionally, the research group examined the skin absorption of caffeine through full-thickness porcine skin and reported a faster absorption than a conventional emulsifier-stabilized emulsion by a factor of three. A candidate for further experiments may also be Aerosil® R 974. Here, the basic and hydrophilic fumed silica is treated with dimethyldichlorosilane, resulting in a hydrophobic surface and a contact angle of 134.7 ° (contact angle Aerosil® 300 < 90 °). Wu et al. recently found a method to stabilize w/o emulsions (water in silicone oil) by forming Pickering emulsions with this substance [112]. The good solubilizing properties of the used solvents (DMSO, EA, hexane) are a limiting factor for the choice of further stabilizing excipients with the capability to form stable, colloidal barriers to enhance the long-term stability of the patches.

4. Results & Discussion

An essentially aspect of the safety evaluation for drug products is the toxicologic profile of the used substances and the good tolerability of the product itself. Since the usage of silica particles in products for long-term transdermal application is relatively novel, studies regarding their safety evaluation are lacking. In cell-culture experiments the harmlessness of non-porous silica particles was proven, in contrast to porous particles neither cell-death nor oxidative stress was induced [118]. According to the supplier (Evonik), the usage of Aerosil® in both, membrane-controlled and matrix-controlled transdermal system is feasible at a concentration ranging from 1 – 5 % (w/w). From the regulatory point of view, the European Union has not limited the usage of silicon dioxide in cosmetics; a separate evaluation for drug products is not available. Since the concentration in the dried patch was below four percent (w/w), the formulation can be regarded as safe in this point [116].

4.4. Development and process optimization of a transdermal patch containing diethylene glycol monoethyl ether (Transcutol®) to enhance drug permeation and increase patch stability

4.4.1. Patch preparation and characterization

Replacing DMSO with TC required a new evaluation of the patch production process, because the evaporation behaviour of both enhancer substances was different (Figure 32). Patches containing TC were dried at 50 °C for half an hour and showed lower evaporation of the enhancer (62.5 %) than the patches with DMSO (94.1 %). After two hours at 50 °C, almost the total amount of DMSO (98.0 %) has evaporated, whereas it was merely 80 % for TC. In summary, the obtained drying kinetics showed faster evaporation for DMSO. Consequently, the drying of the TC patches was elevated to higher temperatures, which still allowed the proper monitoring of the process.

The drying process of the patches was monitored regarding the drying parameters that allowed the sufficient retention of TC and the elimination of the organic solvents, ethyl acetate, and n-hexane. The residual amount of both substances is due to their potential toxicity limited by Ph. Eur. and ICH guidelines [87], [119]. Transcutol® is a well-identified and safe excipient that conforms with the European and US pharmacopeia. The substance is well-tolerated, non-irritant, and non-sensitizing. Based on this profile, it is limited to a maximum amount of 430 mg per patch [120].

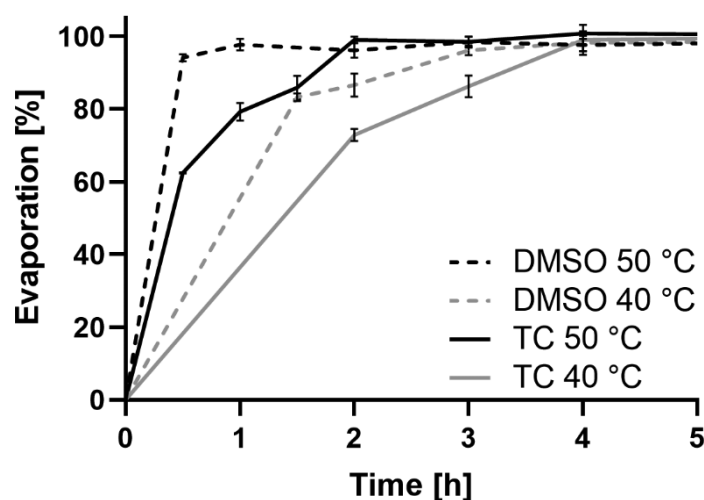


Figure 32. Residual amounts of DMSO and TC in matrix-type patches after the drying of the adhesive mass at 40 °C and 50 °C in a forced convection oven.

4. Results & Discussion

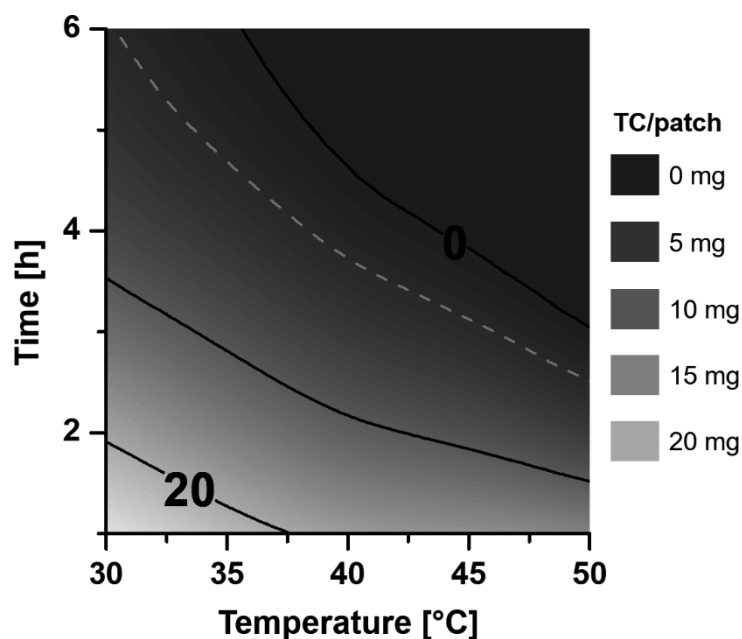


Figure 33. Effect of drying time and temperature on the residual amount of TC per patch. The red line displays the maximum amount of TC (2 mg) which can be incorporated to produce a suitable transdermal patch with sufficient adhesive properties.

According to **Figure 33**, approximately 2 mg per patch was the maximum incorporable amount of TC. Exceeding this limit led to a wet and unusable mass that was not further processable. Further, the regulatory limit was clearly not exceeded.

The production process of the patches should additionally be adjusted to ensure a short drying time. A shorter process saves time, which increases the economic efficiency of patch production. At a process temperature of 40 °C, the time required to achieve the targeted amount of enhancer (2 mg) was approximately four hours, while it took three hours at 45 °C. The obtained drying data demonstrated that higher drying temperatures led to shorter drying times; therefore, the temperature of the process was set to the oven maximum of 50 °C. The organic solvents EA and n-hexane were not detectable after 1 hour of drying at 50 °C (data not shown). Since the determined limits of detection were significantly below the prescribed values (PDE n-hexane: 2.9 mg/day, PDE EA: < 50 mg/day), any risk of toxicity was excluded.

4. Results & Discussion

The results of the drying process performed at 50 °C are displayed in **Figure 34**. As the image shows, drying for two, two and a half, three and six hours resulted in descending amounts of 1.9, 1.4, 0.1 and 0.0 mg TC per patch, respectively. Interestingly, the amount of enhancer per patch decreased non-linear. Drying for 2.5 h resulted in a TC reduction of 26 % compared to the patch dried for two hours, whereas it was reduced by 93 % from 2.5 h to three hours.

Those formulations (control, two, two and a half, three, and six hours) were chosen for further experiments. The control patch was prepared initially without TC. After the drying process, all patches were transparent and did not exhibit any crystallization (data not shown). As specified in chapter four, an excessively dried patch (six hours) was used to compare whether release and permeation behaviour differed from the resulting performance of the control patch.

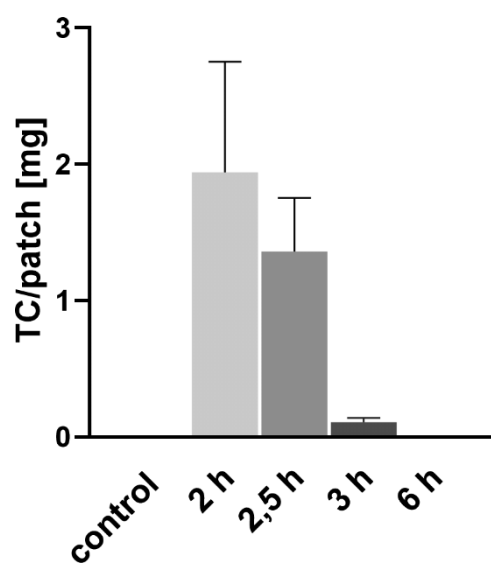


Figure 34. Resulting amount of TC per patch after drying at 50 °C for two, two and a half, three and six hours. The control patch was prepared without DMSO and dried for two hours at 50°C as well.

4. Results & Discussion

4.4.2. Release and permeation experiments

Although increasing amounts of Transcutol® were incorporated into the patches, the release curves did not differ considerably. Within 28 hours, 63 – 69 % of the total drug amount was released from all patches. Initially, the release rate was higher than at the end of the release experiment. After even one hour, the released amount was more than 30 %. During the following 27 hours, this value was merely doubled. The release modelling according to both, Weibull and Korsmeyer-Peppas, described the release profiles equally well, but the n -values for Korsmeyer-Peppas were below 0.5. Therefore, fitting was performed according to Weibull in **Figure 35A**. The resulting β -values ranged between 0.24 and 0.32. The shape parameter describes the slope of the release curve and indicates a steeper initial slope than exponential when $\beta < 1$. This may result from the reducing concentration gradient between vehicle and release medium during the experiment because the amount of drug within the vehicle decreased and the concentrations between patch and medium annealed. In summary, the presence of TC did not improve the release of E2.

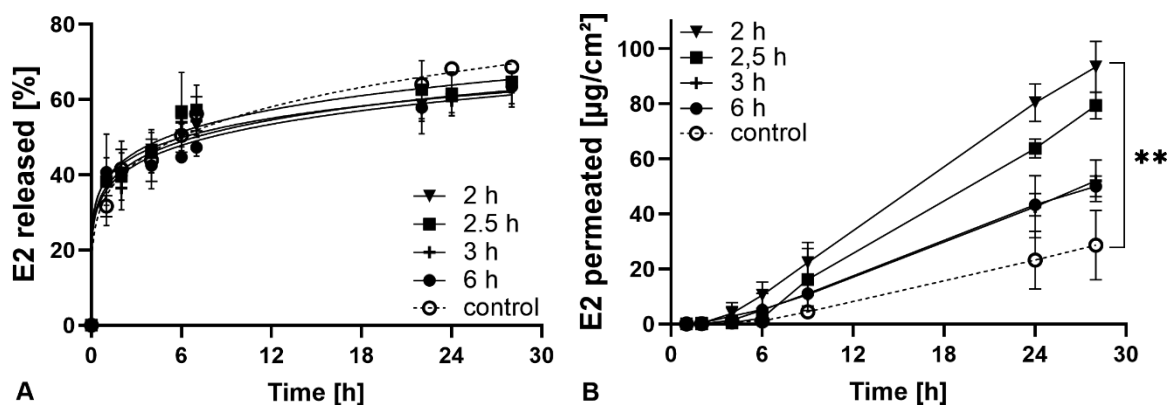


Figure 35. (A) In vitro release profiles in phosphate buffered saline (PBS, pH 7.4) at 32 °C. (B) Permeation profiles of E2 across pig skin at 32 °C over a period of 28 hours. The control patch was prepared without TC.

4. Results & Discussion

In contrast to the release experiments, the results of the permeation experiments displayed apparent differences between the formulations. As displayed in **Figure 35B** the amount of permeated drug increased significantly with increasing amounts of TC/patch. After 28 hours, the patch dried for two hours offered the highest amounts of permeated E2 ($80.0 \pm 6.5 \mu\text{g}/24 \text{ h}$), followed by two and a half hours ($68.0 \pm 3.4 \mu\text{g}/24 \text{ h}$), three hours ($44.6 \pm 5.3 \mu\text{g}/24 \text{ h}$), six hours ($40.9 \pm 2.6 \mu\text{g}/24 \text{ h}$) and the control patch ($24.6 \pm 8.8 \mu\text{g}/24 \text{ h}$) in descending order. Hence, the control patch without TC offered the lowest values of transdermal permeated E2. Interestingly, the values for the three hours and six hours patches were comparable, although the TC-amount of the patch dried for six hours was not detectable. Those results agree with recent studies from Javadzadeh et al., Puglia et al., and Degim et al., where the permeation of different drugs such as Finasteride, Lorazepam, Clonazepam and Bromocryptine was increased by TC as well [121]–[123].

The steady-state fluxes of Estradiol ($J_{\text{ss}} \text{ E2}$) were plotted against the corresponding release rates of Estradiol in **Figure 36A**. Because the correlation coefficient (R^2) of the linear regression was below 0.2, a correlation between release and permeation behaviour was negotiated. On the other hand, the relation between $J_{\text{ss}} \text{ E2}$ and the amount of TC/patch displayed in **Figure 36B** exhibited a high correlation ($R^2 \geq 0.8$). Thus, the permeation of E2 increased proportionally with rising amounts of enhancer substances. In general, the drug flux of the patches containing the highest TC-amount (two

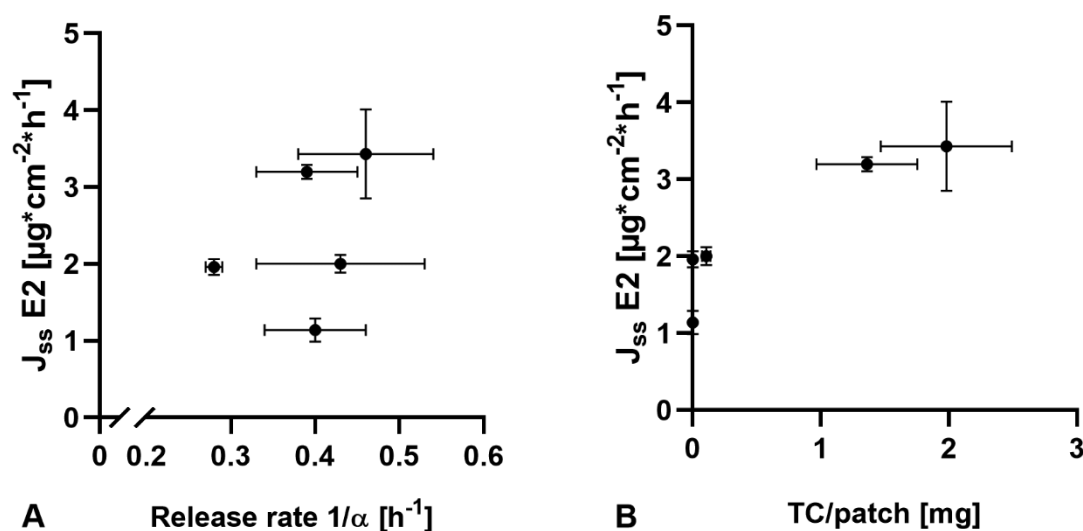


Figure 36. (A) Correlation between Weibull release rate of Estradiol ($1/\alpha$) and the steady-state flux of Estradiol ($J_{\text{ss}} \text{ E2}$) ($R^2 \leq 0.2$). (B) Correlation between the steady-state flux ($J_{\text{ss}} \text{ E2}$) of Estradiol and the amount of Transcutol® per patch ($R^2 \geq 0.8$).

4. Results & Discussion

hours) was trebled in comparison to the control patch. This result was supported by the findings of Shen et al. The researchers successfully developed a transdermal patch containing TC that significantly improved the permeation of Daphnetin through full-thickness excised rat skin. The molecule is a dihydroxy coumarin and offers hydroxylic functional groups as well as Estradiol. The interactions between drug, enhancer and PSA were investigated within this study via thermal analysis (DSC), molecular modelling, and Infrared-Spectrometry. The combination of the results led to the conclusion that both, TC and the drug, competitively interacted with the patch matrix. Thus, drug release was promoted due to the reduced interaction between drug and PSA [124]. This observation, in turn, was not confirmed since the drug release profiles of the patches without TC were comparable to the patches with increasing amounts of the enhancer. Shen et al. used an acrylic PSA with carboxylic groups, whereas the polymer used for the present study contains hydroxyl groups. The interaction between drug, TC, and PSA was therefore not comparable.

For the patches containing TC it was impossible to detect any amount of enhancer substance in the skin or in the acceptor compartment after the permeation experiments. Therefore, the determination of the flux values of TC ($J_{ss\ TC}$), according to $J_{ss\ DMSO}$ in chapter 4.1, was not feasible.

According to the distribution of E2 after the permeation experiments described in **Figure 37**, the permeated amount of drug did not exceed 14 % of the total amount per patch. This meant, in turn, that the major amount of drug remained in patch or skin. For the control patch, the non-permeated amount was mainly found in the patch (88 %) and a small portion in the skin (8 %). Hence, the percentage of drug in the skin was considerably larger than the permeated amount (3 %). This observation was found for all formulations, except for the 2 h patch, where as much drug permeated (13 %) as retained in the skin (13 %). In general, the amount of E2 found in the skin increased with the amount of permeated drug and, thus, the amount of enhancer through to a level of 2 mg TC/patch (2 h). The recovery rate of E2 ranged between 97 % and 101 %.

4. Results & Discussion

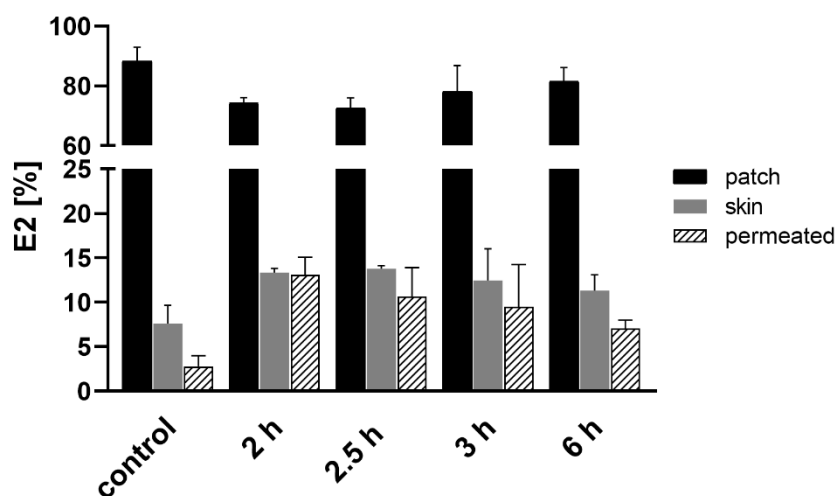


Figure 37. Distribution of E2 in skin, patch and permeated into the acceptor compartment of Franz cells after 28 h permeation experiments. The control patch was prepared without TC.

Interestingly, the amount of E2 in the skin did not exceed a value of 13 % for the patches with the second-largest amounts of TC, although the flux values increased further according to the enhancer load per patch. Compared to the E2 partitioning described in chapter four, where the highest values of drug detected in the skin were 15 %, one could assume that the skin got saturated with the drug. The ability of TC to facilitate an intracutaneous drug depot is well-known. Due to the unique solvent properties of the substance, the solubility of various drugs (Griseofulvin, Coumarin, Meperidine, Papaverine, Clobetasol) in the skin has been significantly increased [51]. The recent findings support the postulated formation of a depot within the skin, and the fact that the amount of drug increased to a certain extent could be an indicator for the saturation of the skin. Consequently, TC increased the solubility of drugs within the skin to a finite concentration.

4. Results & Discussion

4.4.3. Stability evaluation

The microscopic investigation of the freshly prepared patches confirmed the absence of Estradiol crystals for both, the TC-free control patch and the 2 h TC-patch (**Figure 38A, B**). For the patches containing TC dried for two and a half hours, three hours and six hours, the matrices were crystal-free as well (data not shown).

Figure 38C shows the drop-like structures that occurred for the DMSO-patches during storage. The goal of the approach to use TC instead of DMSO as an permeation enhancing substance was to inhibit the formation of those structures during storage. Fortunately, all patches were droplet-free after two months of storage at 40 °C. However, another major stability issue occurred because all patches exhibited crystals after two months. The control patch (without TC, **Figure 38D**) showed a crystal-structure similar to the 6 h, 3 h and 2.5 h TC-patches (data not shown). Here, the adhesive matrix was covered entirely with dendritic crystals. For the patches with the highest amount of TC (2 h), crystals within the matrix were also detectable (**Figure 38E**); however, unlike the other patches, the matrix was not completely littered with the fine structures described above. Here, crystals occurred to a lesser extent and amount and were found as single objects within the matrix. Therefore, the presence of TC may lead to a reduced crystal growth but did not inhibit drug recrystallization in general.

Compared to the patches containing DMSO, the feasible amount of TC was significantly lower: for DMSO, it was possible to incorporate a maximum amount of 9 mg/patch, whereas the limit for TC was 2 mg/patch. This amount was sufficiently low to prevent the coalescence of enhancer droplets within the matrix, but it was not enough to successfully inhibit the recrystallization of the drug. Here, the supersaturated state could not be maintained.

4. Results & Discussion

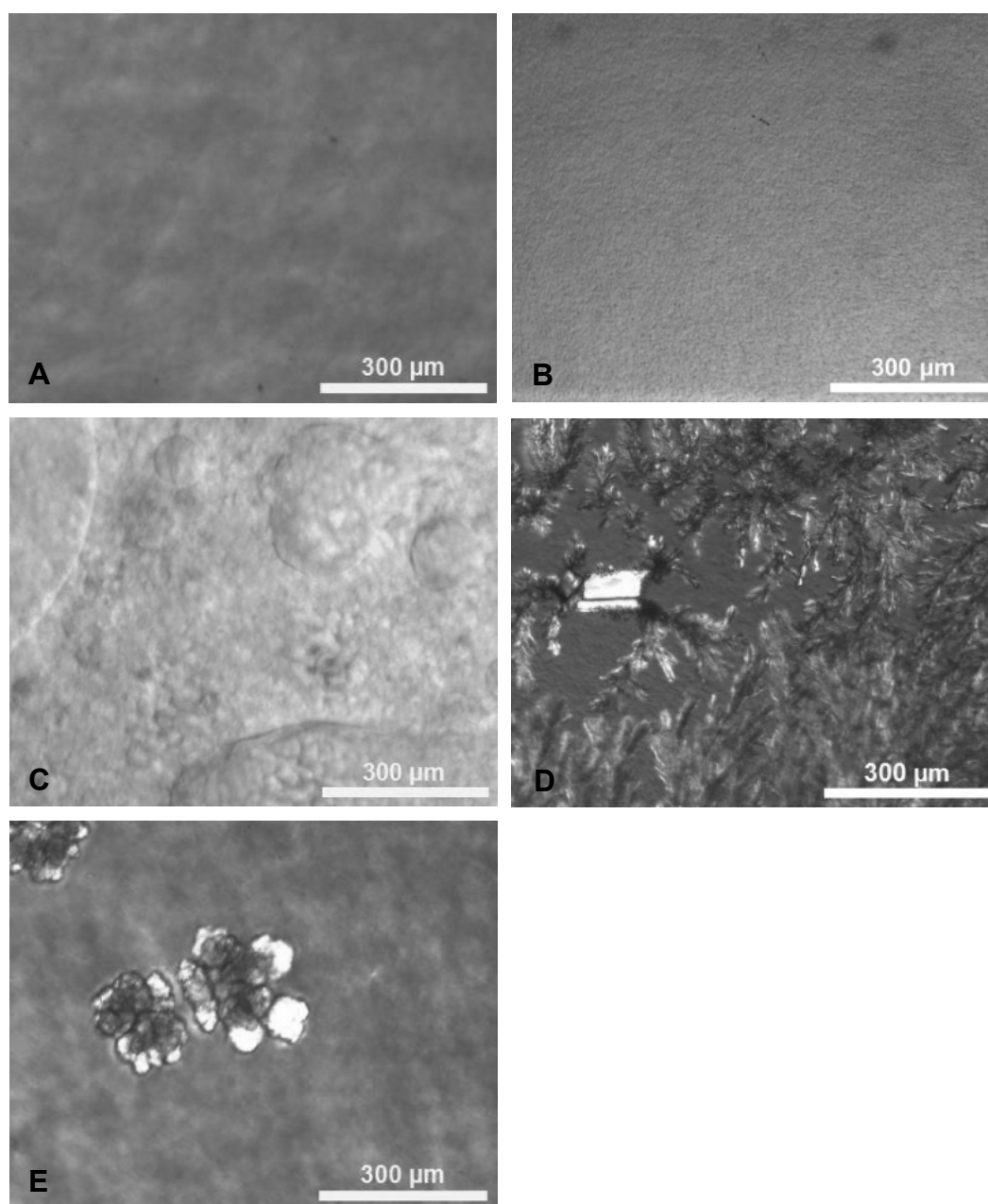


Figure 38. PLM pictures of the prepared E2 patches taken subsequently after production (A, B) and after two months of storage at 40 °C in sealed containers (C – E) (magnification = 10x). (A) TC-free control patch subsequently after production, (B) 2h-patch subsequently after production, (C) DMSO-patch (drying conditions: 36 °C, 3h) after two months of storage, (D) TC-free control patch after two months of storage, and (E) TC-patch (2h) after two months of storage.

4. Results & Discussion

Stability issues occurred for TC as well; the usage of a different penetration enhancer, or solubilizer, was therefore not the solution to overcome this quality affecting problem. A solution might be to evaluate further excipients with antinucleating properties. Kotiyan et al. reported on an effective way of stabilizing the supersaturated state of Estradiol within an acrylic PSA by adding Eudragit® E PO (cationic polymer based on dimethylaminoethyl methacrylate) to the transdermal system [125]. The resulting formulation was tested regarding skin permeation and compared to a marketed system. The permeation profile of the developed system showed a higher skin permeation and was still clear and free from crystals after six months of storage at room temperature. Additionally, Eudragit® E PO did not affect the adhesive properties of the transdermal system [126].

Further, the selection of excipients depends on the properties of the used drug substance. There may be substances, e.g., polyvinylpyrrolidone, that allows to incorporate and maintain higher concentrations of drugs but may affect their permeation. For PVP, it was shown that the substance affects the permeation behaviour of hydrophilic drugs: the delivered amount of Captopril was increased, whereas no effect was observed for the lipophilic drug Levonorgestrel [127]. PVP successfully acted as solubilizer for both substances but depending on their physicochemical properties the API flux values were different. This observation must be considered for the selection of further excipients because they may affect the release and/or transdermal permeation in a negative way as well.

5. General conclusion and outlook

5. General conclusion and outlook

The general attempt of retaining volatile excipients in therapeutic transdermal patches was successfully accomplished by using the solvent evaporation method. The results described within this work provide the opportunity to produce matrix-type patches containing volatile substances and opens new possibilities in transdermal patch design. Due to their volatility, they were excluded from the list of possible excipients so far. Therefore, the production process developed in this work is a novel and attractive process approach while handling volatiles. These substance class comprise various groups of excipients, ranging from permeation enhancers over recrystallization inhibitors through to stabilizing additives.

The integration of especially permeation enhancers into transdermal patches is a desirable feature to promote the drug transport through the skin. Within this work, the incorporated substances DMSO and Transcutol®, both are volatile permeation enhancers, successfully enhanced the transdermal permeation of the drugs Estradiol and Scopolamine. The chosen permeation enhancing substances used in this work both increased drug transport via the skin similarly, although for DMSO a significantly larger amount of substance was necessary. For the drugs Ibuprofen and Rotigotine, the presence of DMSO did not increase drug permeation. This observation underlines the critical role of the drug-matrix polymer interaction. For the drugs with an improved permeation behaviour, Estradiol and Scopolamine, DMSO reduced the drug-polymer interactions and facilitated a faster and enhanced drug permeation. The most probable root cause for this observation may be the polar surface area of the drug substances since the greatest improvement was observed for the substances with the lowest polar surface area. Thus, a higher polar surface area of the drug substance leads to stronger interactions with the polar matrix polymer. This relationship is a further, crucial factor for the future development of transdermal systems, especially when dealing with novel active pharmaceutical ingredients. The usage of tailor-made polymers will improve the development process: depending on the physicochemical properties of the drug, the release could be controlled by individually adjusting the surface properties of the pressure-sensitive adhesive.

This approach may also be used for controlled transdermal drug delivery to prolong the application period of rapid and easily permeable substances. For those patch systems that are changed daily, the residual drug amount after 24 h is usually too low to maintain the delivery rate or drug flow via the skin over a longer period. Thus, a new patch has to be applied every day. Higher drug loads per patch, in turn, could result in an overdosage because the increased concentration gradient between

5. General conclusion and outlook

patch and the skin leads to an increased drug delivery rate. In this case, the combination of higher drug load and custom-designed polymers could be used to decrease the drug delivery rate. The polymer should interact sufficiently with the drug substance and therefore chosen accordingly. The resulting polymer-drug interaction will reduce the drug release from the patch and consequently the transdermal permeation while concurrently prolonging the application intervals.

The long-term stability of a drug product (e.g., over a period of up to several years) is an essential and critical quality attribute. Since the described stabilization attempts did not result in a stable product, the formulation has to be further improved. Regarding this, using, e.g., hydrophobized instead of hydrophilic fumed silica particles as a stabilizer represents a promising approach. Nevertheless, the permeation-enhancing properties of the incorporated substances must be maintained in any case. Here, particular attention should be paid to the adsorption of the enhancer substance to the particles. Within this work, it was proven, especially for DMSO, that the substance permeates faster than the API and by this means the substance paves the way for a faster drug permeation. If DMSO would be adsorbed by an excipient within the DIA, it may be possible that the DMSO remains entirely within the vehicle, lacking any permeation enhancement. Therefore, the comprehensive effect of additional excipients must be evaluated carefully.

The described production process is suitable for lab-scale production, but the process has to be improved regarding efficiency, monitoring, and control mechanisms commercial for manufacturing purposes. First of all, the single steps, especially casting, drying, and laminating have to be transferred into a continuous process. Otherwise, the production would be time- and cost-consuming and, therefore, seen from an economic point of view, be non-profitable. The final determination of residual enhancer substance is a critical process parameter and must, compared to the step-wise production in lab-scale, occur in a continuously manufacturing process subsequently after the drying and prior to the lamination step. Additionally, in terms of process optimization, the determination should be performed without any process interruptions. To solve this problem, the manufacturing apparatus or rather the drying channel should be equipped with a weighing system that continuously determines the weight of the 'wet' laminate during drying. Within an initial calibration, the residual amounts of enhancer substance during drying should be closely monitored via GC and correlated with the continuously decreasing weight of the drying product. Thus, the weight of the product can be used as an in-process control (IPC) to monitor this critical part of the production process.

5. General conclusion and outlook

This, in turn, means that the weight of the drying DIA-layer decreases up to a predetermined value and achieving this specific value indicates the end of the drying process. The conveying system determines the process speed and the residence time of the wet laminate in the drying tunnel. By adjusting the speed, the residence time can be adjusted to a necessary value that ensures proper drying.

In general, the novel idea of retaining volatile substances via a modified drying process provides many new or rather now processable excipients for the development of transdermal drug products. When producing matrix-type patches, the initial goal of the drying step was hitherto to remove the used solvents completely from the final drug product. Therefore, an excessive drying was performed which led to the complete evaporation of every volatile substance, including organic solvents like substances as DMSO and Transcutol. Both examples are just two of other, innumerable substances, that can be from now on, based on the results described within this work, considered as new excipients for the development of transdermal drug delivery systems.

6. References

6. References

- [1] K. A. Walters, Ed., 'Chapter 1. The Structure and Function of Skin', in *Dermatological and Transdermal Formulations*, CRC Press, 2002, pp. 15–53. doi: 10.1201/9780824743239.
- [2] L. M. Milstone, 'Epidermal desquamation', *Journal of Dermatological Science*, vol. 36, no. 3, pp. 131–140, Dec. 2004, doi: 10.1016/j.jdermsci.2004.05.004.
- [3] J. Kielhorn and I. Mangelsdorf, 'Chapter 3. Skin Structure and Function', in *Dermal absorption*, Geneva: World Health Organization, 2006, pp. 10–22.
- [4] H. A. E. Benson, 'Chapter 1. Skin Structure, Function, and Permeation', in *Topical and Transdermal Drug Delivery: Principles and Practice*, A. C. Watkinson, Ed. Hoboken, NJ, USA: John Wiley & Sons, Inc., 2011, pp. 3–22. doi: 10.1002/9781118140505.
- [5] J. J. Berti and J. J. Lipsky, 'Transcutaneous Drug Delivery: A Practical Review', *Mayo Clinic Proceedings*, vol. 70, no. 6, pp. 581–586, Jun. 1995, doi: 10.4065/70.6.581.
- [6] Rote Liste® Service GmbH, 'Rote Liste', *Rote Liste*, Feb. 24, 2021. <https://www.rote-liste.de> (accessed Feb. 24, 2021).
- [7] M. R. Prausnitz and R. Langer, 'Transdermal drug delivery', *Nature Biotechnology*, vol. 26, no. 11, pp. 1261–1268, Nov. 2008, doi: 10.1038/nbt.1504.
- [8] M. N. Pastore, Y. N. Kalia, M. Horstmann, and M. S. Roberts, 'Transdermal patches: history, development and pharmacology', *British Journal of Pharmacology*, vol. 172, no. 9, pp. 2179–2209, 2015, doi: <https://doi.org/10.1111/bph.13059>.
- [9] R. J. Scheuplein and I. H. Blank, 'Permeability of the skin', vol. 51, p. 46, 1971.
- [10] G. L. Online, 'Fachinformation EVRA® 203/33,9 Mikrogramm/24 Stunden transdermales Pflaster | Gelbe Liste', *Gelbe Liste Online*. https://www.gelbe-liste.de/produkte/EVRA-203-33-9-Mikrogramm-24-Stunden-transdermales-Pflaster_367697/fachinformation (accessed Apr. 13, 2021).
- [11] G. L. Online, 'Fentanyl 12 µg/h Transdermales Pflaster (Transdermale Anwendung) | Gelbe Liste', *Gelbe Liste Online*. https://www.gelbe-liste.de/wirkstoffe/Fentanyl-12-g-h-Transdermales-Pflaster-Transdermale-Anwendung_514fde91-a149-46da-8111-6cf21fed0dd1?scope=activesubstance_1686 (accessed Apr. 13, 2021).
- [12] G. L. Online, 'Fachinformation Buprenorpharm 7 Tage 5 Mikrogramm/Stunde transdermales Pflaster | Gelbe Liste', *Gelbe Liste Online*. https://www.gelbe-liste.de/produkte/Buprenorpharm-7-Tage-5-Mikrogramm-Stunde-transdermales-Pflaster_971097/fachinformation (accessed Apr. 13, 2021).
- [13] G. L. Online, 'Fachinformation Neupro® 2 mg/24 h transdermales Pflaster | Gelbe Liste', *Gelbe Liste Online*. https://www.gelbe-liste.de/produkte/Neupro-2-mg-24-h-transdermales-Pflaster_482639/fachinformation (accessed Apr. 13, 2021).
- [14] K. A. Walters, Ed., 'Chapter 4. Skin Transport', in *Dermatological and transdermal formulations*, New York: M. Dekker, 2002, pp. 101–208.
- [15] M. E. Lane, 'Skin penetration enhancers', *International Journal of Pharmaceutics*, p. 10, 2013.
- [16] F. Cilurzo, C. G. M. Gennari, and P. Minghetti, 'Adhesive properties: a critical issue in transdermal patch development', *Expert Opinion on Drug Delivery*, vol. 9, no. 1, pp. 33–45, Jan. 2012, doi: 10.1517/17425247.2012.637107.

6. References

-
- [17] G. Oliveira, J. Hadgraft, and M. E. Lane, 'Toxicological implications of the delivery of fentanyl from gel extracted from a commercial transdermal reservoir patch', *Toxicology in Vitro*, vol. 26, no. 4, pp. 645–648, Jun. 2012, doi: 10.1016/j.tiv.2012.02.007.
- [18] H. Schaefer and T. E. Redelmeier, 'Chapter 5. Factors Effecting Percutaneous Absorption', in *Skin Barrier: Principles of Percutaneous Absorption*, S. Karger AG, 1996.
- [19] C. Yewale, H. Tandel, A. Patel, and A. Misra, 'Polymers in Transdermal Drug Delivery', in *Applications of Polymers in Drug Delivery*, Elsevier, 2021, pp. 131–158. doi: 10.1016/B978-0-12-819659-5.00005-7.
- [20] R. K. Subedi, J.-P. Ryoo, C. Moon, and H.-K. Choi, 'Influence of formulation variables in transdermal drug delivery system containing zolmitriptan', *International Journal of Pharmaceutics*, vol. 419, no. 1–2, pp. 209–214, Oct. 2011, doi: 10.1016/j.ijpharm.2011.08.002.
- [21] C. Liu, P. Quan, S. Li, Y. Zhao, and L. Fang, 'A systemic evaluation of drug in acrylic pressure sensitive adhesive patch in vitro and in vivo : The roles of intermolecular interaction and adhesive mobility variation in drug controlled release', *Journal of Controlled Release*, vol. 252, pp. 83–94, Apr. 2017, doi: 10.1016/j.jconrel.2017.03.003.
- [22] M. Yasunori, K. Takemasa, and S. Kenji, 'Diffusion of drugs in acrylic-type pressure-sensitive adhesive matrix. II. Influence of interaction', *Journal of Controlled Release*, vol. 18, no. 2, pp. 113–121, Feb. 1992, doi: 10.1016/0168-3659(92)90180-Y.
- [23] A. Couto, R. Fernandes, M. N. S. Cordeiro, S. S. Reis, R. T. Ribeiro, and A. M. Pessoa, 'Dermic diffusion and stratum corneum: A state of the art review of mathematical models', *Journal of Controlled Release*, vol. 177, pp. 74–83, Mar. 2014, doi: 10.1016/j.jconrel.2013.12.005.
- [24] T. Higuchi, 'Physical chemical analysis of percutaneous absorption process from creams and ointments', *J. Soc. Cosmet. Chem*, vol. 11, pp. 85–97, 1960.
- [25] J. Hadgraft and M. E. Lane, 'Drug crystallization – implications for topical and transdermal delivery', *Expert Opinion on Drug Delivery*, vol. 13, no. 6, pp. 817–830, Jun. 2016, doi: 10.1517/17425247.2016.1140146.
- [26] J.-H. Kim and H.-K. Choi, 'Effect of additives on the crystallization and the permeation of ketoprofen from adhesive matrix', *International Journal of Pharmaceutics*, vol. 236, no. 1–2, pp. 81–85, Apr. 2002, doi: 10.1016/S0378-5173(02)00017-0.
- [27] L. A. Mohamed *et al.*, 'Drug recrystallization in drug-in-adhesive transdermal delivery system: A case study of deteriorating the mechanical and rheological characteristics of testosterone TDS', *International Journal of Pharmaceutics*, vol. 578, p. 119132, Mar. 2020, doi: 10.1016/j.ijpharm.2020.119132.
- [28] R. Lipp, 'Pharmaceutics: Selection and Use of Crystallization Inhibitors for Matrix-type Transdermal Drug-delivery Systems Containing Sex Steroids*', *Journal of Pharmacy and Pharmacology*, vol. 50, no. 12, pp. 1343–1349, Dec. 1998, doi: 10.1111/j.2042-7158.1998.tb03357.x.
- [29] F. Cilurzo, P. Minghetti, A. Casiraghi, L. Tosi, S. Pagani, and L. Montanari, 'Polymethacrylates as crystallization inhibitors in monolayer transdermal patches containing ibuprofen', *European Journal of Pharmaceutics and Biopharmaceutics*, vol. 60, no. 1, pp. 61–66, May 2005, doi: 10.1016/j.ejpb.2005.02.001.

6. References

- [30] G. Van den Mooter *et al.*, 'Physical stabilisation of amorphous ketoconazole in solid dispersions with polyvinylpyrrolidone K25', *European Journal of Pharmaceutical Sciences*, vol. 12, no. 3, pp. 261–269, Jan. 2001, doi: 10.1016/S0928-0987(00)00173-1.
- [31] M. A. Tahir, M. E. Ali, and A. Lamprecht, 'Nanoparticle formulations as recrystallization inhibitors in transdermal patches', *International Journal of Pharmaceutics*, vol. 575, p. 118886, Feb. 2020, doi: 10.1016/j.ijpharm.2019.118886.
- [32] C. Liu, 'Investigation on the effect of deep eutectic formation on drug-polymer miscibility and skin permeability of rosiglitone drug-in-adhesive patch', p. 58.
- [33] H. A. E. Benson, *Chapter 15. Transdermal Product Formulation Development*. Hoboken, NJ, USA: John Wiley & Sons, Inc., 2011. doi: 10.1002/9781118140505.
- [34] G. A. Van Buskirk *et al.*, 'Passive Transdermal Systems Whitepaper Incorporating Current Chemistry, Manufacturing and Controls (CMC) Development Principles', *AAPS PharmSciTech*, vol. 13, no. 1, pp. 218–230, Mar. 2012, doi: 10.1208/s12249-011-9740-9.
- [35] European Medicines Agency and Committee for Medicinal Products for Human Use, 'Guideline on quality of transdermal patches', EMA/CHMP/QWP/608924/2014, 2014.
- [36] Gelbe Liste Pharmindex, 'Medizinische Medien Informations GmbH', 2022. <https://www.gelbe-liste.de/> (accessed Feb. 24, 2022).
- [37] G. Ma and C. Wu, 'Microneedle, bio-microneedle and bio-inspired microneedle: A review', *Journal of Controlled Release*, vol. 251, pp. 11–23, Apr. 2017, doi: 10.1016/j.jconrel.2017.02.011.
- [38] N. Hindiyeh, P. Schmidt, J. Engels, W. Halladay, and D. Kellerman, 'Effectiveness Of Qtrypta™ (Zolmitriptan Intracutaneous System) Before and After the Initiation of CGRP Antibody Therapy in Subjects With Migraine – A Preliminary Assessment', Jan. 21, 2022. https://www.zosanopharma.com/file.cfm/50/docs/CGRP_Concomitant_IHC_.pdf
- [39] M. B. Brown, G. P. Martin, S. A. Jones, and F. K. Akomeah, 'Dermal and Transdermal Drug Delivery Systems: Current and Future Prospects', *Drug Delivery*, vol. 13, no. 3, pp. 175–187, Jan. 2006, doi: 10.1080/10717540500455975.
- [40] M. R. Prausnitz and R. Langer, 'Transdermal drug delivery', *Nature Biotechnology*, vol. 26, no. 11, pp. 1261–1268, Nov. 2008, doi: 10.1038/nbt.1504.
- [41] B. W. Barry, 'Lipid-Protein-Partitioning theory of skin penetration enhancement', *Journal of Controlled Release*, vol. 15, no. 3, pp. 237–248, Jun. 1991, doi: 10.1016/0168-3659(91)90115-T.
- [42] N. Dragicevic and H. I. Maibach, Eds., '2: Chemical Penetration Enhancers: Classification and Mode of Action', in *Percutaneous Penetration Enhancers Chemical Methods in Penetration Enhancement*, Berlin, Heidelberg: Springer Berlin Heidelberg, 2015. doi: 10.1007/978-3-662-47039-8.
- [43] A. Allenby, J. Fletcher, C. Schock, and T. Tees, 'The effect of heat, pH and organic solvents on the electrical impedance and permeability of excised human skin', *British journal of dermatology*, vol. 81, pp. 31–39, 1969.
- [44] K. Marren, 'Dimethyl Sulfoxide: An Effective Penetration Enhancer for Topical Administration of NSAIDs', *The Physician and Sportsmedicine*, vol. 39, no. 3, pp. 75–82, Sep. 2011, doi: 10.3810/psm.2011.09.1923.
- [45] A. C. Williams and B. W. Barry, 'Penetration enhancers', *Advanced Drug Delivery Reviews*, vol. 56, no. 5, pp. 603–618, Mar. 2004, doi: 10.1016/j.addr.2003.10.025.

6. References

-
- [46] A. A. Gurtovenko and J. Anwar, 'Modulating the Structure and Properties of Cell Membranes: The Molecular Mechanism of Action of Dimethyl Sulfoxide', *The Journal of Physical Chemistry B*, vol. 111, no. 35, pp. 10453–10460, Sep. 2007, doi: 10.1021/jp073113e.
- [47] R. Strub and A. S. McKim, 'Advances in the Regulated Pharmaceutical Use of Dimethyl Sulfoxide USP, Ph.Eur.', *Pharmaceutical Technology*, vol. 40 (9), pp. 30–35, Sep. 2016.
- [48] D. W. Sullivan, S. C. Gad, and M. Julien, 'A review of the nonclinical safety of Transcutol®, a highly purified form of diethylene glycol monoethyl ether (DEGEE) used as a pharmaceutical excipient', *Food and Chemical Toxicology*, vol. 72, pp. 40–50, Oct. 2014, doi: 10.1016/j.fct.2014.06.028.
- [49] D. W. Osborne, 'Diethylene glycol monoethyl ether: an emerging solvent in topical dermatology products', *Journal of Cosmetic Dermatology*, vol. 10, no. 4, pp. 324–329, 2011, doi: <https://doi.org/10.1111/j.1473-2165.2011.00590.x>.
- [50] M. Špaglová *et al.*, 'Possibilities of the microemulsion use as indomethacin solubilizer and its effect on *in vitro* and *ex vivo* drug permeation from dermal gels in comparison with transcutol®', *Drug Development and Industrial Pharmacy*, vol. 46, no. 9, pp. 1468–1476, Sep. 2020, doi: 10.1080/03639045.2020.1802483.
- [51] D. W. Osborne and J. Musakhanian, 'Skin Penetration and Permeation Properties of Transcutol®—Neat or Diluted Mixtures', *AAPS PharmSciTech*, vol. 19, no. 8, pp. 3512–3533, Nov. 2018, doi: 10.1208/s12249-018-1196-8.
- [52] Y. Koyama, H. Bando, F. Yamashita, Y. Takakura, H. Sezaki, and M. Hashida, 'Comparative Analysis of Percutaneous Absorption Enhancement by d-Limonene and Oleic Acid Based on a Skin Diffusion Model', *Pharm Res*, vol. 11, no. 3, pp. 377–383, Mar. 1994, doi: 10.1023/A:1018904802566.
- [53] A. F. Davis and J. Hadgraft, 'Effect of supersaturation on membrane transport: 1. Hydrocortisone acetate', *International Journal of Pharmaceutics*, vol. 76, no. 1–2, pp. 1–8, Sep. 1991, doi: 10.1016/0378-5173(91)90337-N.
- [54] A. M. Kligman, 'Chapter 8 Hydration Injury to Human Skin: A View from the Horny Layer', in *Handbook of Occupational Dermatology*, L. Kanerva, J. E. Wahlberg, P. Elsner, and H. I. Maibach, Eds. Berlin, Heidelberg: Springer, 2000, pp. 76–80. doi: 10.1007/978-3-662-07677-4_8.
- [55] M. Prausnitz *et al.*, 'Skin barrier and transdermal drug delivery', *Dermatology* 3, pp. 2065–2073, 2012.
- [56] T. L. G. Andersson, B. Stehle, B. Davidsson, and P. Höglund, 'Bioavailability of estradiol from two matrix transdermal delivery systems: Menorest® and Climara®', *Maturitas*, vol. 34, no. 1, pp. 57–64, Jan. 2000, doi: 10.1016/S0378-5122(99)00088-2.
- [57] H. D. Nelson, M. Walker, B. Zakher, and J. Mitchell, *Menopausal Hormone Therapy for the Primary Prevention of Chronic Conditions: Systematic Review to Update the 2002 and 2005 U.S. Preventive Services Task Force Recommendations*. Rockville (MD): Agency for Healthcare Research and Quality (US), 2012. Accessed: Mar. 31, 2020. [Online]. Available: <http://www.ncbi.nlm.nih.gov/books/NBK97827/>
- [58] W. Weng, P. Quan, C. Liu, H. Zhao, and L. Fang, 'Design of a Drug-in-Adhesive Transdermal Patch for Risperidone: Effect of Drug-Additive Interactions on the Crystallization Inhibition

6. References

- and In Vitro / In Vivo Correlation Study', *Journal of Pharmaceutical Sciences*, vol. 105, no. 10, pp. 3153–3161, Oct. 2016, doi: 10.1016/j.xphs.2016.07.003.
- [59] C.-W. Park *et al.*, 'Investigation of formulation factors affecting in vitro and in vivo characteristics of a galantamine transdermal system', *International Journal of Pharmaceutics*, vol. 436, no. 1–2, pp. 32–40, Oct. 2012, doi: 10.1016/j.ijpharm.2012.06.057.
- [60] Tomita Pharmaceutical Co., Ltd., 'FLORITE® - New Technology for Innovative Formulation Design', Dec. 18, 2021. <http://www.tomitaph.co.jp/english/data/FLORITE.pdf> (accessed Dec. 18, 2021).
- [61] ©2010 Fuji Chemical Industries Co., Ltd, 'FujiSil™ | Application to Bitterness Masking Drug product utilizing Adsorption Capacity', *FujiSil™ | Application to Bitterness Masking Drug product utilizing Adsorption Capacity*. <https://tech-en.fujichemical.co.jp/fujisil-info/> (accessed Dec. 18, 2021).
- [62] Fuji Chemical Industries Co., Ltd., 'Neusilin® - The specialty excipient', *Neusilin® - The specialty excipient*, Sep. 2015. https://www.fujichemical.co.jp/english/medical/medicine/neusilin/neusilin_brochure.pdf (accessed Dec. 18, 2021).
- [63] Merck KGaA, Darmstadt, 'Parteck® SLC 500 Analysenzertifikate', 2021. https://www.merck-millipore.com/DE/de/product/Parteck-SLC-500,MDA_CHEM-120091?RefererURL=https%3A%2F%2Fwww.google.com%2F#anchor_COA (accessed Jan. 22, 2022).
- [64] W. R. Grace & Co.-Conn., 'Syloid Silicas - Pharmaceutical Excipient. Technical Note', *Syloid Silicas - Pharmaceutical Excipient. Technical Note*, Sep. 2015. <https://pdf4pro.com/amp/view/syloid-silicas-grace-19a641.html> (accessed Dec. 18, 2021).
- [65] L. J. Waters *et al.*, 'Enhancing the dissolution of phenylbutazone using Syloid® based mesoporous silicas for oral equine applications', *Journal of Pharmaceutical Analysis*, vol. 8, no. 3, pp. 181–186, Jun. 2018, doi: 10.1016/j.jpha.2018.01.004.
- [66] Evonik Resource Efficiency GmbH, 'AEROSIL and AEROPERL Colloidal Silicon Dioxide for Pharmaceuticals. Technical Information TI 1281', Jul. 2015. <https://silo.tips/download/aerosil-and-aeroperl-colloidal-silicon-dioxide-for-pharmaceuticals-technical-inf> (accessed Aug. 31, 2021).
- [67] J. Sclafani, P. Liu, E. Hansen, M. G. Cettina, and J. Nightingale, 'A protocol for the assessment of receiver solution additive-induced skin permeability changes. An example with γ -cyclodextrin', *International Journal of Pharmaceutics*, vol. 124, no. 2, pp. 213–217, Oct. 1995, doi: 10.1016/0378-5173(95)00091-V.
- [68] Y. Zhang *et al.*, 'DDSolver: An Add-In Program for Modeling and Comparison of Drug Dissolution Profiles', *AAPS J*, vol. 12, no. 3, pp. 263–271, Sep. 2010, doi: 10.1208/s12248-010-9185-1.
- [69] P. Costa and J. M. Sousa Lobo, 'Evaluation of Mathematical Models Describing Drug Release from Estradiol Transdermal Systems', *Drug Development and Industrial Pharmacy*, vol. 29, no. 1, pp. 89–97, Jan. 2003, doi: 10.1081/DDC-120016687.
- [70] T. Higuchi, 'Rate of release of medicaments from ointment bases containing drugs in suspension', p. 2.
- [71] T. Higuchi, 'Mechanism of sustained-action medication. Theoretical analysis of rate of release of solid drugs dispersed in solid matrices', *Journal of Pharmaceutical Sciences*, vol. 52, no. 12, pp. 1145–1149, Dec. 1963, doi: 10.1002/jps.2600521210.

6. References

-
- [72] J. Siepmann and N. A. Peppas, 'Modeling of drug release from delivery systems based on hydroxypropyl methylcellulose (HPMC)', *Advanced Drug Delivery Reviews*, vol. 64, pp. 163–174, Dec. 2012, doi: 10.1016/j.addr.2012.09.028.
- [73] R. W. Korsmeyer and N. A. Peppas, 'Effect of the morphology of hydrophilic polymeric matrices on the diffusion and release of water soluble drugs', *Journal of Membrane Science*, vol. 9, no. 3, pp. 211–227, Jan. 1981, doi: 10.1016/S0376-7388(00)80265-3.
- [74] R. W. Korsmeyer, R. Gurny, E. Doelker, P. Buri, and N. A. Peppas, 'Mechanisms of solute release from porous hydrophilic polymers', *International Journal of Pharmaceutics*, vol. 15, no. 1, pp. 25–35, May 1983, doi: 10.1016/0378-5173(83)90064-9.
- [75] J. A. Goldsmith, N. Randall, and S. D. Ross, 'On methods of expressing dissolution rate data', *Journal of Pharmacy and Pharmacology*, vol. 30, no. 1, pp. 347–349, Apr. 2011, doi: 10.1111/j.2042-7158.1978.tb13253.x.
- [76] F. Langenbucher, 'Letters to the Editor: Linearization of dissolution rate curves by the Weibull distribution', *Journal of Pharmacy and Pharmacology*, vol. 24, no. 12, pp. 979–981, 1972, doi: <https://doi.org/10.1111/j.2042-7158.1972.tb08930.x>.
- [77] W. Weibull, 'A Statistical Distribution Function of Wide Applicability', *Journal of Applied Mechanics*, vol. 18, no. 3, pp. 293–297, Sep. 1951, doi: 10.1115/1.4010337.
- [78] Y. Kalia, 'Modeling transdermal drug release', *Advanced Drug Delivery Reviews*, vol. 48, no. 2–3, pp. 159–172, Jun. 2001, doi: 10.1016/S0169-409X(01)00113-2.
- [79] A. M. Barbero and H. F. Frasch, 'Pig and guinea pig skin as surrogates for human in vitro penetration studies: A quantitative review', *Toxicology in Vitro*, vol. 23, no. 1, pp. 1–13, Feb. 2009, doi: 10.1016/j.tiv.2008.10.008.
- [80] K. A. Walters, Ed., *Dermatological and transdermal formulations*. New York: M. Dekker, 2002.
- [81] OECD, *Test No. 428: Skin Absorption: In Vitro Method*. Paris, France: OECD, 2004. doi: 10.1787/9789264071087-en.
- [82] T. J. Franz, 'Percutaneous Absorption. On the Relevance of in Vitro Data', *Journal of Investigative Dermatology*, vol. 64, no. 3, pp. 190–195, Mar. 1975, doi: 10.1111/1523-1747.ep12533356.
- [83] The council of europe, 'Estradiol hemihydrate', in *European Pharmacopoeia (Ph. Eur.)*, vol. 9th edition, Directorate for the Quality of Medicines and Healthcare, Ed. Strasbourg, France, 2017, pp. 2406–2407.
- [84] H. Farrar, L. Letzig, and M. Gill, 'Validation of a liquid chromatographic method for the determination of ibuprofen in human plasma', *Journal of Chromatography B*, vol. 780, no. 2, pp. 341–348, Nov. 2002, doi: 10.1016/S1570-0232(02)00543-3.
- [85] The council of europe, 'Scopolamine', in *European Pharmacopoeia (Ph. Eur.)*, vol. 9th edition, Directorate for the Quality of Medicines and Healthcare, Ed. Strasbourg, France, 2017, pp. 5624–5626.
- [86] The council of europe, 'Rotigotine', in *European Pharmacopoeia (Ph. Eur.)*, vol. 9th edition, Directorate for the Quality of Medicines and Healthcare, Ed. Strasbourg, France, 2017, pp. 5577–5579.

6. References

- [87] The council of europe, '2.4.24 "Identification and control of residual solvents', in *European Pharmacopoeia (Ph. Eur.)*, vol. 9th edition, Directorate for the Quality of Medicines and Healthcare, Ed. Strasbourg, France, 2017, pp. 123–124.
- [88] E. Gutschke, S. Bracht, S. Nagel, and W. Weitschies, 'Adhesion testing of transdermal matrix patches with a probe tack test – In vitro and in vivo evaluation', *European Journal of Pharmaceutics and Biopharmaceutics*, vol. 75, no. 3, pp. 399–404, Aug. 2010, doi: 10.1016/j.ejpb.2010.03.016.
- [89] 'Q 1 A (R2) Stability Testing of new Drug Substances and Products', p. 20, 2006.
- [90] E.-S. Park, S.-J. Chang, Y.-S. Rhee, and S.-C. Chi, 'Effects of Adhesives and Permeation Enhancers on the Skin Permeation of Captopril', *Drug Development and Industrial Pharmacy*, vol. 27, no. 9, pp. 975–980, Jan. 2001, doi: 10.1081/DDC-100107679.
- [91] A. H. Elshafeey, Y. E. Hamza, S. Y. Amin, and H. Zia, 'In vitro transdermal permeation of fenoterol hydrobromide', *Journal of Advanced Research*, vol. 3, no. 2, pp. 125–132, Apr. 2012, doi: 10.1016/j.jare.2011.05.009.
- [92] C. Amrish and S. P. Kumar, 'Transdermal Delivery of Ketorolac', *YAKUGAKU ZASSHI*, vol. 129, no. 3, pp. 373–379, Mar. 2009, doi: 10.1248/yakushi.129.373.
- [93] I. S. Özgüney, H. Y. Karasulu, G. Kantarci, S. Sözer, T. Güneri, and G. Ertan, 'Transdermal delivery of diclofenac sodium through rat skin from various formulations', *AAPS PharmSciTech*, vol. 7, no. 4, pp. E39–E45, Dec. 2006, doi: 10.1208/pt070488.
- [94] R. Kadir, D. Stempler, Z. Liron, and S. Cohen, 'Delivery of Theophylline into Excised Human Skin from Alkanoic Acid Solutions: A "Push-Pull" Mechanism', *Journal of Pharmaceutical Sciences*, vol. 76, no. 10, pp. 774–779, Oct. 1987, doi: 10.1002/jps.2600761004.
- [95] T. M. Greve, K. B. Andersen, and O. F. Nielsen, 'Penetration mechanism of dimethyl sulfoxide in human and pig ear skin: An ATR–FTIR and near-FT Raman spectroscopic *in vivo* and *in vitro* study', *Spectroscopy*, vol. 22, no. 5, pp. 405–417, 2008, doi: 10.1155/2008/109782.
- [96] A. N. C. Anigbogu, A. C. Williams, B. W. Barry, and H. G. M. Edwards, 'Fourier transform raman spectroscopy of interactions between the penetration enhancer dimethyl sulfoxide and human stratum corneum', *International Journal of Pharmaceutics*, vol. 125, no. 2, pp. 265–282, Oct. 1995, doi: 10.1016/0378-5173(95)00141-5.
- [97] J. Z. Shainhouse, L. M. Grierson, and Z. Naseer, 'A Long-Term, Open-Label Study to Confirm the Safety of Topical Diclofenac Solution Containing Dimethyl Sulfoxide in the Treatment of the Osteoarthritic Knee', *American Journal of Therapeutics*, vol. 17, no. 6, pp. 566–576, Dec. 2010, doi: 10.1097/MJT.0b013e3181d169b5.
- [98] U. T. Lashmar, J. Hadgraft, and N. Thomas, 'Topical Application of Penetration Enhancers to the Skin of Nude Mice: a Histopathological Study', *Journal of Pharmacy and Pharmacology*, vol. 41, no. 2, pp. 118–121, Feb. 1989, doi: 10.1111/j.2042-7158.1989.tb06405.x.
- [99] X. Ma, J. Taw, and C.-M. Chiang, 'Control of drug crystallization in transdermal matrix system', *International Journal of Pharmaceutics*, vol. 142, no. 1, pp. 115–119, Sep. 1996, doi: 10.1016/0378-5173(96)04647-9.
- [100] W. Song *et al.*, 'Probing the role of chemical enhancers in facilitating drug release from patches: Mechanistic insights based on FT-IR spectroscopy, molecular modeling and thermal analysis', *Journal of Controlled Release*, vol. 227, pp. 13–22, Apr. 2016, doi: 10.1016/j.jconrel.2016.02.027.

6. References

-
- [101] M. Fujita, M. Kajiyama, A. Takemura, H. Ono, H. Mizumachi, and S. Hayashi, 'Effects of miscibility on probe tack of natural-rubber-based pressure-sensitive adhesives', *Journal of Applied Polymer Science*, vol. 70, no. 4, pp. 771–776, 1998, doi: 10.1002/(SICI)1097-4628(19981024)70:4<771::AID-APP17>3.0.CO;2-#.
- [102] A. Naik, Y. N. Kalia, and R. H. Guy, 'Transdermal drug delivery: overcoming the skin's barrier function', *Pharmaceutical Science & Technology Today*, vol. 3, no. 9, pp. 318–326, Sep. 2000, doi: 10.1016/S1461-5347(00)00295-9.
- [103] D. E. Clark, 'Rapid calculation of polar molecular surface area and its application to the prediction of transport phenomena. 1. Prediction of intestinal absorption', *Journal of Pharmaceutical Sciences*, vol. 88, no. 8, pp. 807–814, Aug. 1999, doi: 10.1021/js9804011.
- [104] P. L. Ritger and N. A. Peppas, 'A simple equation for description of solute release I. Fickian and non-fickian release from non-swellable devices in the form of slabs, spheres, cylinders or discs', *Journal of Controlled Release*, vol. 5, no. 1, pp. 23–36, Jun. 1987, doi: 10.1016/0168-3659(87)90034-4.
- [105] P. L. Ritger and N. A. Peppas, 'A simple equation for description of solute release II. Fickian and anomalous release from swellable devices', *Journal of Controlled Release*, vol. 5, no. 1, pp. 37–42, Jun. 1987, doi: 10.1016/0168-3659(87)90035-6.
- [106] R. S. Harland, A. Gazzaniga, M. E. Sangalli, P. Colombo, and N. A. Peppas, 'Drug/Polymer Matrix Swelling and Dissolution', *Pharm Res*, vol. 5, no. 8, pp. 488–494, Aug. 1988, doi: 10.1023/A:1015913207052.
- [107] T. G. Mason, J. N. Wilking, K. Meleson, C. B. Chang, and S. M. Graves, 'Nanoemulsions: formation, structure, and physical properties', *J. Phys.: Condens. Matter*, vol. 18, no. 41, pp. R635–R666, Oct. 2006, doi: 10.1088/0953-8984/18/41/R01.
- [108] V. F. Patel and N. M. Patel, 'Statistical evaluation of influence of viscosity and content of polymer on dipyridamole release from floating matrix tablets: A technical note', *AAPS PharmSciTech*, vol. 8, no. 3, pp. E140–E144, Sep. 2007, doi: 10.1208/pt0803069.
- [109] S. U. Pickering, 'CXCVI. — Emulsions', *J. Chem. Soc., Trans.*, vol. 91, no. 0, pp. 2001–2021, 1907, doi: 10.1039/CT9079102001.
- [110] J. Frelichowska, M.-A. Bolzinger, and Y. Chevalier, 'Pickering emulsions with bare silica', *Colloids and Surfaces A: Physicochemical and Engineering Aspects*, vol. 343, no. 1–3, pp. 70–74, Jul. 2009, doi: 10.1016/j.colsurfa.2009.01.031.
- [111] F. Macedo Fernandes Barros, C. Chassenieux, T. Nicolai, M. M. de Souza Lima, and L. Benyahia, 'Effect of the hydrophobicity of fumed silica particles and the nature of oil on the structure and rheological behavior of Pickering emulsions', *null*, vol. 40, no. 8, pp. 1169–1178, Aug. 2019, doi: 10.1080/01932691.2018.1500480.
- [112] F. Wu *et al.*, 'Investigation of the stability in Pickering emulsions preparation with commercial cosmetic ingredients', *Colloids and Surfaces A: Physicochemical and Engineering Aspects*, vol. 602, p. 125082, Oct. 2020, doi: 10.1016/j.colsurfa.2020.125082.
- [113] S. Wang, Y. He, and Y. Zou, 'Study of Pickering emulsions stabilized by mixed particles of silica and calcite', *Particuology*, vol. 8, no. 4, pp. 390–393, Aug. 2010, doi: 10.1016/j.partic.2010.05.002.

6. References

- [114] R. Aveyard, B. P. Binks, and J. H. Clint, 'Emulsions stabilised solely by colloidal particles', *Advances in Colloid and Interface Science*, vol. 100–102, pp. 503–546, Feb. 2003, doi: 10.1016/S0001-8686(02)00069-6.
- [115] J. Frelichowska, M.-A. Bolzinger, J.-P. Valour, H. Mouaziz, J. Pelletier, and Y. Chevalier, 'Pickering w/o emulsions: Drug release and topical delivery', *International Journal of Pharmaceutics*, vol. 368, no. 1–2, pp. 7–15, Feb. 2009, doi: 10.1016/j.ijpharm.2008.09.057.
- [116] Evonik Operations GmbH, 'Produktinformation Aerosil 300', *Produktinformation Aerosil 300*, Aug. 28, 2021. <https://products-re.evonik.com/www2/uploads/productfinder/AEROSIL-300-DE.pdf>
- [117] B. P. Binks, 'Particles as surfactants – similarities and differences', *Interface Science*, p. 21, 2002.
- [118] H. Kettiger, D. Sen Karaman, L. Schiesser, J. M. Rosenholm, and J. Huwyler, 'Comparative safety evaluation of silica-based particles', *Toxicology in Vitro*, vol. 30, no. 1, pp. 355–363, Dec. 2015, doi: 10.1016/j.tiv.2015.09.030.
- [119] J. Connelly, 'ICH Q3C Impurities: Guideline for Residual Solvents', in *ICH Quality Guidelines*, A. Teasdale, D. Elder, and R. W. Nims, Eds. Hoboken, NJ, USA: John Wiley & Sons, Inc., 2017, pp. 199–232. doi: 10.1002/9781118971147.ch7.
- [120] Gattefosse, 'Transcutol-P-Brochure.pdf', *Transcutol-P-Brochure.pdf*, 2020. <https://www.pharmaexcipients.com/wp-content/uploads/2021/01/Transcutol-P-Brochure.pdf> (accessed Sep. 02, 2021).
- [121] Y. Javadzadeh, J. Shokri, S. Hallaj-Nezhadi, H. Hamishehkar, and A. Nokhodchi, 'Enhancement of percutaneous absorption of Finasteride by cosolvents, cosurfactant and surfactants', *Pharmaceutical Development and Technology*, vol. 15, no. 6, pp. 619–625, Dec. 2010, doi: 10.3109/10837450903397610.
- [122] C. Puglia, F. Bonina, G. Trapani, M. Franco, and M. Ricci, 'Evaluation of in vitro percutaneous absorption of lorazepam and clonazepam from hydro-alcoholic gel formulations', *International Journal of Pharmaceutics*, vol. 228, no. 1, pp. 79–87, Oct. 2001, doi: 10.1016/S0378-5173(01)00806-7.
- [123] I. T. Degim, F. Acartürk, D. Erdogan, and N. Demirez Lortlar, 'Transdermal Administration of Bromocriptine.', *Biological & Pharmaceutical Bulletin*, vol. 26, no. 4, pp. 501–505, 2003, doi: 10.1248/bpb.26.501.
- [124] M. Shen, C. Liu, X. Wan, N. Farah, and L. Fang, 'Development of a daphnetin transdermal patch using chemical enhancer strategy: insights of the enhancement effect of Transcutol P and the assessment of pharmacodynamics', *Drug Development and Industrial Pharmacy*, vol. 44, no. 10, pp. 1642–1649, Oct. 2018, doi: 10.1080/03639045.2018.1483391.
- [125] Evonik Nutrition & Care GmbH, 'Technical Information EUDRAGIT® E 100, EUDRAGIT® E PO and EUDRAGIT® E 12,5'. <https://www.pharmaexcipients.com/wp-content/uploads/attachments/TI-EUDRAGIT-E-100-E-PO-E-12-5-EN.pdf?t=1508413942> (accessed Sep. 06, 2021).
- [126] P. Kotiyan, 'Eudragits: Role as crystallization inhibitors in drug-in-adhesive transdermal systems of estradiol', *European Journal of Pharmaceutics and Biopharmaceutics*, vol. 52, no. 2, pp. 173–180, Sep. 2001, doi: 10.1016/S0939-6411(01)00174-6.

6. References

-
- [127] P. Jain and A. K. Banga, 'Inhibition of crystallization in drug-in-adhesive-type transdermal patches', *International Journal of Pharmaceutics*, vol. 394, no. 1, pp. 68–74, Jul. 2010, doi: 10.1016/j.ijpharm.2010.04.042.

7. Appendix

7. Appendix

7.1. Publications

In scientific journals:

A. Otterbach and A. Lamprecht, 'Enhanced Skin Permeation of Estradiol by Dimethyl Sulfoxide Containing Transdermal Patches', *Pharmaceutics*, vol. 13, no. 3, Art. no. 3, Mar. 2021, doi: 10.3390/pharmaceutics13030320.

Conference participations:

A. Otterbach and A. Lamprecht, "Stabilization of therapeutic transdermal patches," PBP world meeting in: Granada, Spain, Mar. 2018.

7.2. List of abbreviations

α	Weibull release constant/scale parameter [h]
API	active pharmaceutical ingredient
β	shape parameter (Weibull)
cm ²	square centimetre
CPE	chemical penetration enhancer
CPP	critical process parameter
d	day
DIA	drug-in-adhesive
DMI	1.3-dimethyl-2-imidazolidinone
DMSO	dimethyl sulfoxide
DT	Duro-Tak®
E2	Estradiol
EA	ethyl acetate
EU	European Union
FDA	Food and Drug Administration
g	gram
GC	gas chromatography
h	hour
H ₃ PO ₄	phosphoric acid
HPLC	high performance liquid chromatography
IBU	Ibuprofen
IPC	in-process controls
J _{ss}	steady-state flux [$\mu\text{g}\cdot\text{cm}^{-2}\cdot\text{h}^{-1}$]
kg	kilogram
K _{KP}	Korsmeyer-Peppas-constant, kinetic release rate
mg	milligram
mL	millilitre

7. Appendix

M _v	molecular volume [cm ³]
n	Korsmeier-Peppas release exponent
N	Newton
N/A	not applicable
NMP	N-Methyl pyrrolidinone
PBS	phosphate buffered saline
Ph. Eur.	Pharmacopoeia European
PIB	polyisobutylene
PLM	polarized-light microscopy
PSA	pressure-sensitive adhesive
PVP	polyvinylpyrrolidone
R ²	correlation coefficient
RH	relative humidity
ROT	Rotigotine
σ	tensile stress [N/mm ²]
SC	stratum corneum
SCO	Scopolamine
SD	standard deviation
SLC	silica
SLS	sodium lauryl sulphate
t	time [h]
TC	Transcutol®
T _g	glass-transition temperature
T _M	melting point
TTP	transdermal therapeutic patch
USA	United States of America

7.3. List of figures

- Figure 1.** Schematic structure of the skin. 4
- Figure 2.** Layers of a monolithic DIA. The release liner is part of the drug product, although it has to be removed before usage. 7
- Figure 3.** Process steps for manufacturing of DIA: Overview of coating, drying and lamination. Image by courtesy of LTS Lohmann Therapie-Systeme AG. 13
- Figure 4.** Process steps for manufacturing of DIA: (A) Slitting apparatus, (B) overview of slitting, (C) overview of pouching. Image by courtesy of LTS Lohmann Therapie-Systeme AG. 14
- Figure 5.** Structural formulae of the used model drugs. 26
- Figure 6.** (A) Schematic overview of the patch production process, (B) dried and covered adhesive laminate and (C) final dosage form: circular drug-in-adhesive patches. 29
- Figure 7.** (A) Franz diffusion cell stirrer system: six franz cells are installed next to each other and connected to a heater/circulator system. The six cells can be used simultaneously. (B) Franz-diffusion cell scheme of the experimental set up for drug release experiments. 30
- Figure 8.** Franz diffusion cell (A) scheme of the experimental set up for permeation experiments, (B) Franz-diffusion cell – experimental set up in lab scale. 34
- Figure 9.** Chromatogram obtained from a mixture of 0.50 $\mu\text{L/mL}$ n-hexan, 0.05 $\mu\text{L/mL}$ EA, 5.00 $\mu\text{L/mL}$ DMSO and 5.00 $\mu\text{L/mL}$ TC dissolved in DMI and analysed via headspace-GC. 1 = n-hexane ($t_{\text{R}} = 1.73$), 2 = ethyl acetate ($t_{\text{R}} = 1.89$), 3 = dimethylsulfoxide ($t_{\text{R}} = 3.26$), 4 = Transcutol® ($t_{\text{R}} = 6.38$), 5 = DMI ($t_{\text{R}} = 4.42$). 37
- Figure 10.** Exemplary stress-time curve of the probe-tack test. The bonding phase describes the contact of the probe with the specimen. During the debonding phase, the probe was retracted at a defined speed. 39
- Figure 11.** Contour plot of the effect of drying time and temperature on the residual amount of DMSO/patch. The line with the value 9 displays the maximum amount of DMSO (9 mg) which can be incorporated to produce a suitable transdermal patch. 44

7. Appendix

Figure 12. XRD patterns of pure E2 and the prepared patches. The placebo patch was prepared without DMSO and E2 (consisting of DT), and the control patch was prepared without DMSO (consisting of E2 + DT). 45

Figure 13. In vitro release profile in phosphate buffered saline (PBS, pH 7.4) at 32 °C. 46

Figure 14. Permeation profiles of E2 (A) and DMSO (B) across pig skin at 32 °C. Percental permeated amount of DMSO: 35 °C, 4 h: 11.5 ± 0.7 ; 40 °C, 2 h: 21.8 ± 1.9 ; 35 °C, 3 h: 65.4 ± 3.1 (mean \pm SD). *** Indicates significant differences ($p < 0.001$). 48

Figure 15. (A) Correlation between steady-state flux (J_{ss} E2) of Estradiol and DMSO per patch ($R^2 = 0,972$). (B) Correlation between steady-state flux of DMSO (J_{ss} DMSO) and DMSO per patch ($R^2 = 0,924$). (C) Correlation between steady-state flux of Estradiol (J_{ss} E2) and steady-state flux of DMSO (J_{ss} DMSO) ($R^2 = 0.884$). (D) Correlation between kinetic release rate of Estradiol (J_{ss} E2) and steady-state flux of Estradiol (J_{ss} E2) ($R^2 \leq 0.5$). * Indicates significant differences ($p < 0.05$), ** indicates significant differences ($p < 0.01$) and *** indicates significant differences ($p < 0.001$). 49

Figure 16. Distribution of E2 after 28 h permeation experiments in skin and patch and through permeation into the acceptor compartment of Franz cells. 50

Figure 17. DMSO/patch at different storage conditions over a period of six months. (A) 2–8 °C (sealed), (B) 25 °C/60% RH (sealed), (C) 25 °C/60% RH (unsealed). Residual amounts after one, two, three and six months were compared to the initial amount at $t = 0$. * Indicates significant differences ($p < 0.05$), ** indicates significant differences ($p < 0.01$) and *** indicates significant differences ($p < 0.001$). 53

Figure 18. E2 permeation of 35 °C, 3h after three (A) and six months (B), 40 °C, 2h after three (C) and six months (D), and of 35 °C, 4h after three (E) and six months (F) of storage. Flux values after three and six months were compared to the initial value at $t = 0$. * Indicates significant differences ($p < 0.05$), ** indicates significant differences ($p < 0.01$) and *** indicates significant differences ($p < 0.001$). 54

Figure 19. Comparison of DMSO-amount/ patch of test patches with E2-patches, chapter 4 (see 4.1, p. 41). Test formulations (IBU, SCO, ROT) were produced analogous to the beforementioned E2-patches, drying was performed at 35 °C for 3 h. "ns" indicates non-significant differences. 55

7. Appendix

Figure 20. (A) XRD patterns of pure SCO and the prepared patches. The placebo patch was prepared without DMSO and drug-free (consisting of DT). (B) PLM pictures of the DMSO-free SCO control patch, (C) the IBU test patch and (D) the IBU control patch (magnification = 10x). 57

Figure 21. Probe tack results of the prepared DIA (test: with DMSO, control: without DMSO) compared to the adhesive properties of a placebo patch consisting solely of DT. * Indicates significant differences ($p < 0.05$) and ** indicates significant differences ($p < 0.01$) in comparison with the placebo patch. 59

Figure 22. In vitro release profiles of (A) Ibuprofen, (B) Scopolamine and (C) Rotigotine in phosphate buffered saline (PBS, pH 7.4) at 32 °C. (D) Relationship between drug release constant (K_{KP}) and polar surface area ($R^2 > 0.9$). Filled symbols with solid line represent test patches (with DMSO), unfilled symbols with dotted line label control patches (without DMSO). ** indicates significant differences ($p < 0.01$). 62

Figure 23. (A) Permeation of Ibuprofen from patches containing IBU prepared without DMSO (control) and with DMSO (test). (B) Distribution of Ibuprofen after 28 h permeation experiments in skin and patch and through permeation into the acceptor compartment of Franz cells. "ns" indicates non-significant differences. 64

Figure 24. (A) Permeation of SCO from patches prepared without DMSO (control) and with DMSO (test). (B) Distribution of SCO after 28 h permeation experiments in skin and patch and through permeation into the acceptor compartment of Franz cells. *** Indicates significant differences ($p < 0.001$), "ns" indicates non-significant differences. 65

Figure 25. (A) Permeation of ROT from patches prepared without DMSO (control) and with DMSO (test). (B) Distribution of ROT after 28 h permeation experiments in skin and patch and through permeation into the acceptor compartment of Franz cells. "ns" indicates non-significant differences. 66

Figure 26. PLM-pictures of the patches containing DMSO (A) subsequently after drying at 35 °C, 3 h (B) after two months and (C) after three months of storage at 40 °C. 69

Figure 27. Appearance of the prepared DMSO – Excipient mixtures: A DMSO + Aeropearl® 300, B DMSO + Aerosil® 300, C DMSO + Florite® PS-10, D DMSO + Florite® PS-200, E DMSO + FujiSilTM, F DMSO + Parteck® SLC 500, G DMSO + Neusilin®, H DMSO + Syloid® 244 FP, I DMSO + Syloid® AI-1FP 73

7. Appendix

Figure 28. Comparison of the evaporation of pure DMSO and blends of DMSO and excipients. The resulting concentration is given in amount of excipient [mg] per DMSO [g]. Drying was performed at 40 °C and monitored gravimetrically. * Indicates significant differences ($p < 0.05$), ** indicates significant differences ($p < 0.01$) and *** indicates significant differences ($p < 0.001$) compared to DMSO. 74

Figure 29. Influence of different amounts of Aerosil/DMSO in the initial mixture (0 - 32 mg/g) on the DMSO content after drying. Patches were dried at 35 °C for 3 h, monitoring was performed via GC. 75

Figure 30. E2 permeation after one month (A), two months (B), and three months (C) of storage. The resulting curves were compared to the permeation of freshly prepared patches ($t = 0$). Samples were stored in sealed containers at 25 °C, 40 °C and 50 °C. (D) Flux-values of patches without (w/o) and with (w/) Aerosil® immediately after production ($t = 0$) and after three months of storage at 40 °C. * Indicates significant differences ($p < 0.05$) and ** indicates significant differences ($p < 0.01$) and “ns” indicates non-significant differences. 76

Figure 31. (A) DMSO-content of the silica patches at different storage conditions (25 °C, 40 °C and 50 °C) over a period of three months. * Indicates significant differences ($p < 0.05$), ** indicates significant differences ($p < 0.01$) and *** indicates significant differences ($p < 0.001$) compared to $t = 0$. (B) Comparison of patch stability after three months of storage at 25 °C. 77

Figure 32. Residual amounts of DMSO and TC in matrix-type patches after the drying of the adhesive mass at 40 °C and 50 °C in a forced convection oven. 83

Figure 33. Effect of drying time and temperature on the residual amount of TC per patch. The red line displays the maximum amount of TC (2 mg) which can be incorporated to produce a suitable transdermal patch with sufficient adhesive properties. 84

Figure 34. Resulting amount of TC per patch after drying at 50 °C for two, two and a half, three and six hours. The control patch was prepared without DMSO and dried for two hours at 50°C as well. 85

Figure 35. (A) In vitro release profiles in phosphate buffered saline (PBS, pH 7.4) at 32 °C. (B) Permeation profiles of E2 across pig skin at 32 °C over a period of 28 hours. The control patch was prepared without TC. 86

Figure 36. (A) Correlation between Weibull release rate of Estradiol ($1/\alpha$) and the steady-state flux of Estradiol (J_{ss} E2) ($R^2 \leq 0.2$). **(B)** Correlation between the steady-state flux (J_{ss} E2) of Estradiol and the amount of Transcutol® per patch ($R^2 \geq 0.8$). 87

Figure 37. Distribution of E2 in skin, patch and permeated into the acceptor compartment of franz cells after 28 h permeation experiments. The control patch was prepared without TC. 89

Figure 38. PLM pictures of the prepared E2 patches taken subsequently after production **(A, B)** and after two months of storage at 40 °C in sealed containers **(C – E)** (magnification = 10x). **(A)** TC-free control patch subsequently after production, **(B)** 2h-patch subsequently after production, **(C)** DMSO-patch (drying conditions: 36 °C, 3h) after two months of storage, **(D)** TC-free control patch after two months of storage, and **(E)** TC-patch (2h) after two months of storage. 91

7. Appendix

7.4. List of tables

Table 1. Licensed transdermal drug products in 2021. The listed drug products represent the original preparations approved in the EU; generic drug products were excluded. h = hour, d = day. **Fehler! Textmarke nicht definiert.**

Table 2. Indication and physicochemical properties of the used APIs. Substance information were obtained from (1) the European chemicals agency (ECHA), (2) PubChem, (3) S. K. Chandrasekaran et al. or McAfee et al. [57] – [60], (4) predicted using advanced chemistry development (ACD/Labs) software V11.02. 26

Table 3. Equilibrium drug solubility in the acceptor medium of release and permeation experiments after 28 hours at 32 °C. 40

Table 4. Exemplary compositions of the adhesive mass at different production times. From an initially (t = 0 h) viscous and liquid mixture to a homogeneous drug-in-adhesive layer (per DIA). Control was prepared without dimethyl sulfoxide (DMSO) (mean ± SD; n.d. = not detected). 45

Table 5. Flux values, lag- time, mean delivered dose and kinetic release rate of the prepared patches. 47

Table 6. Composition and appearance of the prepared patches dried at 35 °C for three hours. Control patches were prepared without dimethyl sulfoxide (DMSO). Values indicate mean ± SD; n.d. = not detected. 56

Table 7. DSC results of pure APIs, drug-free matrix, and the drug-containing control patches. Mean values ± standard deviation. 58

Table 8. Model fitting parameters of the release profiles. * Due to the limited applicability of Korsmeyer-Peppas, the corresponding release profiles were fitted for the initial 60 % of fractional drug release. 61

Table 9. Flux values, lag- time, mean permeated dose, and fractional rate control of the prepared patches. Values represent mean ± SD. 67

Table 10. Evaluation of the physical mixtures of excipients and DMSO. C_{max} describes the maximum amount of excipient/1g DMSO that led to a liquid suspension with appropriate fluid properties for

further processing. Sedimentation was affirmed when the particles deposited within five minutes.

72

Table 11. Microscopic evaluation of the stability samples stored for one, two, and three months. Patches without Aerosil® (storage at 25 °C) were compared to patches containing 20 mg Aerosil® as stabilizer stored at different conditions (25 °C, 40 °C, and 50 °C).

80